## SCMS SCHOOL OF ENGINEERING AND TECHNOLOGY,KARUKUTTY
## BOOKS/CONFERENCE INDEX 2022-2023

*3.3.2 Number of books and chapters in edited volumes/books published and papers published in national/ international conference proceedings per teacher during 2022-2023*

| Sl. No. | Name of the teacher | Title of the book/chapters published | Title of the paper | Title of the proceedings of the conference | Name of the conference | National / International | Calendar Year of publication | ISBN number of the proceeding | Affiliating Institute at the time of publication | Name of the publisher |
|---|---|---|---|---|---|---|---|---|---|---|
| 1 | Vinoj P G | 2022 Smart Technologies, Communication and Robotics (STCR) | | Wearable Fabric Tactile Sensors for Robotic Elderly Assistance | 2022 Smart Technologies, Communication & Robotics (STCR) 10 – 11 December 2022 SathyamangalaM | International | Dec 2022 | 978-1-6654-6047-7 | SCMS School of Engineering and Technology, Ernakulam, India | IEEE |
| 2 | Anandhi V | 2023 International Conference on Advances in Intelligent Computing and Applications (AICAPS) | | Malware detection using dynamic analysis | International Conference on Advances in Intelligent Computing and Applications (AICAPS), | International | Feb 2023 | 979-8-3503-3381-7 | SCMS School of Engineering and Technology, Ernakulam, India | IEEE |
| 3 | Beena Puthillath | Life Skills in Contemporary Education System: Critical Perspectives; Chapter No 10:Self-Awakening: An Important Life Skill | | | | | 2023 | ISBN: 979-8-88697-704-2 | SCMS School of Engineering and Technology, Ernakulam, India | novapublishers |
| 4 | Dr.Nithya Mohan | Copper(II) Based Potential Pharamaceutical Drugs Against Cancer | | International Conference on Materials for the Millennium, MatCon-2023 | International Conference on Materials for the Millennium | International | Jan 2023 | 978-81-954804-8-7 | SCMS School of Engineering and Technology, Ernakulam, India | Directorate of Public Relations and Publications |

| | | | | | | | | | | |
|---|---|---|---|---|---|---|---|---|---|---|
| 5 | Dr.Raghav G R | Lecture Notes in Mechanical Engineering book series (LNME) | A Review on Computational Techniques for Nanostructured Polymer Composite Materials | Applications of Computation in Mechanical Engineering | | | Nov, 2022 | ISBN:978-981-19-6032-1 | SCMS School of Engineering and Technology, Ernakulam, India | Springer Link |
| 6 | Dr Sam Joshy | Applications of Computation in Mechanical Engineering | Optimisation of Parameters in Numerical Simulation of Hot Forging Using Taguchi Approach | | Lecture Notes in Mechanical Engineering book series (LNME) | International | Nov, 2022 | ISBN:978-981-19-6032-1 | SCMS School of Engineering and Technology, Ernakulam, India | Springer Link |
| 7 | Dr.Vidhya Chandran | Applications of Computation in Mechanical Engineering | Aerodynamic analysis of deployable wing arrangement for space shuttle | | Lecture Notes in Mechanical Engineering book series (LNME) | International | Nov, 2022 | ISBN:978-981-19-6032-1 | SCMS School of Engineering and Technology, Ernakulam, India | Springer Link |
| 8 | N. Nikhil Asok | Applications of Computation in Mechanical Engineering | Optimization of Geometrical Parameters in Magnetorheological Dampers Using Finite Element Modeling | | Lecture Notes in Mechanical Engineering book series (LNME) | International | Nov, 2022 | ISBN:978-981-19-6032-1 | SCMS School of Engineering and Technology, Ernakulam, India | Springer Link |
| 9 | Dr Rag R L | IEEE Xplore: | Comparative performance Evaluation of wire-bonded Micro Heat pipes with Acetone and water as working fluid | | 2022 International Conference on Innovations in Science and Technology for Sustainable Development (ICISTSD) | International | Aug, 2022 | 978-1-6654-9936-1 | SCMS School of Engineering and Technology, Ernakulam, India | IEEE Xplore |

| | | | | | | | | | | |
|---|---|---|---|---|---|---|---|---|---|---|
| 10 | Dr. Manish T I | | Deep learning architectures for Brain Tumor detection: A Survey . | IEEE Xplore | 2023 Advanced Computing and Communication Technologies for High Performance Applications (ACCTHPA) | | April, 2023 | 979-8-3503-9844-1 | SCMS School of Engineering and Technology, Ernakulam, India | IEEE |
| 11 | Dr. Varun G Menon | | Towards energy-efficient UAV-assisted 5G internet of underwater things | ACM MobiCom '22: The 28th Annual International Conference on Mobile Computing and Networking | DroneCom '22: Proceedings of the 5th International ACM Mobicom Workshop on Drone Assisted Wireless Communications for 5G and Beyond | International | Oct,2022 | 978-1-4503-9514-4 | SCMS School of Engineering and Technology, Ernakulam, India | Association for Computing MachineryNew YorkNYUnited States |
| 12 | Susmi Jacob | | Context-aware gender and age recognition from smartphone sensors | Context-aware gender and age recognition from smartphone sensors | 2022 International Conference on Computing, Communication, Security and Intelligent Systems (IC3SIS) | International | September,2022 | 978-1-6654-6883-1 | SCMS School of Engineering and Technology, Ernakulam, India | IEEE |
| 13 | Dr. Varun G Menon | | | Performance of hybrid satellite-UAV NOMA systems | ICC 2022 - IEEE International Conference on Communications | International | August,2022 | 1938-1883 | SCMS School of Engineering and Technology, Ernakulam, India | IEEE |

| | | | | | | | | | | |
|---|---|---|---|---|---|---|---|---|---|---|
| 14 | Josna Philomina | | Multi-Domain Network Traffic Analysis using Machine Learning and Deep Learning Techniques | | IC3-2022: Proceedings of the 2022 Fourteenth International Conference on Contemporary Computing | International | October, 2022 | 978-1-4503-9675-2 | SCMS School of Engineering and Technology, Ernakulam, India | ACM Digital Library |
| 15 | Ms. Josna Philomina | | A comparitative study of machine learning models for the detection of Phishing Websites | IEEE Xplore | 2022 International Conference on Computing, Communication, Security and Intelligent Systems (IC3SIS) | International | September,2022 | 978-1-6654-6883-1 | SCMS School of Engineering and Technology, Ernakulam, India | IEEE |
| 16 | Bini Omman | | Speech Emotion Recognition Using Bagged Support Vector Machines | IEEE Xplore | 2022 International Conference on Computing, Communication, Security and Intelligent Systems (IC3SIS) | International | September,2022 | 978-1-6654-6883-1 | SCMS School of Engineering and Technology, Ernakulam, India | IEEE |
| 17 | Sindhya K Nambiar | | Sentence Similarity- A state of art approaches | IEEE Xplore | 2022 International Conference on Computing, Communication, Security and Intelligent Systems (IC3SIS) | International | September,2022 | 978-1-6654-6883-1 | SCMS School of Engineering and Technology, Ernakulam, India | IEEE |
| 18 | Neenu Sebastian | | Personality Prediction using Machine Learning | IEEE Xplore | 2022 International Conference on Computing, Communication, Security and Intelligent Systems (IC3SIS) | International | September,2022 | 978-1-6654-6883-1 | SCMS School of Engineering and Technology, Ernakulam, India | IEEE |

| | | | | | | | | | | |
|---|---|---|---|---|---|---|---|---|---|---|
| 19 | Athira Manikuttan | | Attendance Management System Using Facial Recognition | IEEE Xplore | 2022 International Conference on Computing, Communicatio n, Security and Intelligent Systems (IC3SIS) | International | September,2022 | 978-1-6654-6883-1 | SCMS School of Engineering and Technology, Ernakulam, India | IEEE |
| 20 | Deepa K | | Malware Image Classification using VGG16 | IEEE Xplore | 2022 International Conference on Computing, Communicatio n, Security and Intelligent Systems (IC3SIS) | International | September,2022 | 978-1-6654-6883-1 | SCMS School of Engineering and Technology, Ernakulam, India | IEEE |
| 21 | Rosebell Paul | | A Swarm-based AI Aided Wheel Bot System to Detect Cracks in Railway Tracks | IEEE Xplore | 2022 Sixth International Conference on I-SMAC (IoT in Social, Mobile, Analytics and Cloud) (I-SMAC) | International | December,2022 | 978-1-6654-6941-8 | SCMS School of Engineering and Technology, Ernakulam, India | IEEE |
| 22 | Rosebell Paul | Intelligent Communicatio n Technologies and Virtual Mobile Networks | Li-Fi: A Novel Stand-In for Connectivity and Data Transmission in Toll System | | Lecture Notes on Data Engineering and Communicatio ns Technologies | International | July ,2022 | 978-981-19-1843-8 | SCMS School of Engineering and Technology, Ernakulam, India | Springer Link |
| 23 | Koshy P Joseph | | Simulation of Graphene Battery and other Battery Technologies in an EV Powertrain | IEEE Xplore | 2021 IEEE Transportation Electrification Conference (ITEC-India) | International | Nov,2022 | Electronic ISBN: 978-1-6654-2146-1 | SCMS School of Engineering and Technology, Ernakulam, India | IEEE |

**Total number of books and chapters in edited volumes/books published and papers published in national/ international conference proceedings per teacher during 2022-2023** — 23

PRINCIPAL
SCMS SCHOOL OF ENGINEERING & TECHNOLOGY
VIDYANAGAR, PALLISSERY, KARUKUTTY
ERNAKULAM, KERALA-683 576

IEEE *Xplore*®    Browse ∨    My Settings ∨    Help ∨    **Institutional Sign In**    ◆IEEE

All ▼    [search]    🔍

ADVANCED SEARCH

Conferences > 2021 IEEE Transportation Elec... ❓    Back to Results

# Simulation of Graphene Battery and other Battery Technologies in an EV Powertrain

**Publisher: IEEE**    Cite This    📄 PDF

Anubhav S ; Tony Sabu ; Madhav Hari ; Joemon CT ; Koshy P Joseph    **All Authors**

Department of Automobile Engineering,
SCMS School of Engineering and
Technology, Ernakulam, India

**247**
Full
Text Views

Ⓡ  ⮜  ©  🗁  🔔

created in Simulink using MATLAB software. The constructed model is based on the existing electric car TATA Nexon EV. Also, unlike the real car the model presented has a different battery pack and the battery parameters such as SOC, current, voltage, distance, velocity, and weight are changed to carry out the comparison between different battery technologies. The model will be simulated to obtain data regarding vehicle performance, energy consumption and range on the new FTP75 test cycle. The obtained know-how will help on later improvements of the electric model regarding methods to improve the vehicle performance and the simulation helps to choose the right powertrain for the vehicle without carrying out any real-life experiments.

II. Overview of Battery Technologies

III. Study and Analysis of the Simulated Model

IV. Simulation and Analysis of Batteries in the Simulated Model

V. Conclusion

Authors

Figures

References

Keywords

**Published in:** 2021 IEEE Transportation Electrification Conference (ITEC-India)

**Date of Conference:** 16-19 December 2021    **DOI:** 10.1109/ITEC-India53713.2021.9932539

**Date Added to IEEE *Xplore*:** 09 November 2022    **Publisher:** IEEE

**Conference Location:** New Delhi, India

▼ **ISBN Information:**

Electronic ISBN:978-1-6654-2146-1

Print on Demand(PoD)
ISBN:978-1-6654-2147-8

# Li-Fi: A novel stand-in for Connectivity and Data Transmission in Toll System

Rosebell Paul

Assistant Professor
Department of Computer Science and Engineering
SCMS School of Engineering and Technology
Karukutty, India
rosebell@scmsgroup.org

Neeraj M

[2]Department of Computer Science and Engineering
SCMS School of Engineering and Technology
Karukutty, India
neerajmallisseri07@ieee.org

Yadukrishnan P S

Department of Computer Science and Engineering
SCMS School of Engineering and Technology
Karukutty, India
yedhups@ieee.org

**Abstract.** This paper describes an application framework which uses Li-Fi (Light fidelity) technology to reduce the time delay and congestion caused at the toll system. The Li-Fi is a disruptive technology driven by the visible light spectrum that makes the data transmission process much faster and enhances the system efficiency. In Li-Fi there is no interference as in radio waves and it provides higher bandwidth. It is a bidirectional wireless data carrier medium that uses only visible light and photodiodes. Everything happens very fast in this world, including transportation. In the present scenario spending a long time in traffic is irritating. Even after the introduction of Fastag, there is not much change in toll booth queues. It is at this point where we start to think about a different plan to avoid unwanted blocks at toll booths. Hence we introduce the concept of Li-Fi where vehicles can move through the toll booths without any pause. All that we are using here is DRL (Daytime Running lights). This will have a corresponding receiver section which will accept the signals from the DRL. This method also has certain extra perks which will provide an interdisciplinary help to many major fields.

## 1. Introduction

Li-Fi (Light Fidelity) which was developed by Professor Harald Haas a German physicist is now an emerging technology for establishing hazard free fast connection and data transmission in denser networks. [1] Wi-Fi uses high and low pulses of electromagnetic waves to send data from the internet to the end devices. Similarly, Li-Fi uses fluctuations in the intensity of light to transmit data to the end devices.[12] So where there is light, there is Li-Fi. Li-Fi can clock about 224Gbps in lab conditions and in real life simulations about 1Gbps which is much faster considering the fastest Wi-Fi speed which is approximately 30Mbps.[5] The Li-Fi transmits data via LED bulb which is quite cheaper when compared to the expense of the Wi-Fi router. The security aspect of Li-Fi makes it safer to use as light rays do not penetrate through the opaque objects like walls hence eliminating all chances of intrusion. [6]

In the next section the basic principle of Li-Fi is explained followed by a briefing on the state of art of Li-Fi with several examples where it has already been implemented. In section 4, a comparative study is made with different existing connection technologies. The conventional toll plaza system is described in section 5.We have discussed the system requirements and system design in the following section. Finally, this paper is a journey through the developments made so far using Li-Fi and the authenticity of it is studied with the prototype model.

## 2. Principle of LI FI

In Li-Fi light plays the dominant role. It becomes the data carrier. A study of analog and digital data transmission using Li-Fi is illustrated in [17]. When an electric current is applied to an electric light bulb, a constant stream of light is emitted from the bulb which we see as illumination. Since the LED bulbs are electronic devices the current and therefore the light can be modulated at extremely high speed. This can be detected by a photo detector and converted back to electric current therefore carrying data.[32] The high frequency of 'ON' and 'OFF' of the LED bulb is so fast that human eyes cannot see it in any way. [22] The ''ON' and

'OFF' signifies binary 1 and 0. [14] The data from the internet is sent to the server via Ethernet connection and this data is transferred from the servers to the lamp drivers which has a software module to convert the data from the internet into binary. It is then used to flicker the LED bulb. The LED bulb flickers in a particular pattern for a certain piece of data. The photo detector receives these light rays and amplifies them before sending them to the computer or other devices. [8]
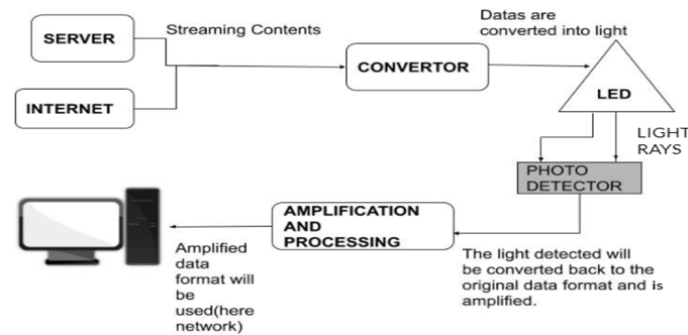


Fig1. Conversion of data into light for Li-fi data transmission

## 3. State of art of Li-Fi

Industry 4.0 which aims at automation in all phases of life with increased digitization has tapped Li-Fi for a revolutionary change. Several companies like PureLiFi, Oledcomm, LightBee, Velmenni, Firefly, Lucibel, Lightbee,LVX System, Signify, Vlncomm, LIFX, Luciom, Acuity brands lighting etc. are investing on Li-Fi technology as it is a hazard free solution to several problems like security and provides higher data density without any interference. According to the statistical prediction made by Vertical industry, the Li-Fi market is expected to reach 9.6 billion in revenue by 2025. [23] The plot below shows the global LiFi revenue growth and future prediction. Lifi is going to spread its wings in several sectors like warehousing, smart offices, buildings, healthcare, education, aviation, maritime and government sectors. This wireless bidirectional system is disruptive in nature. [28]
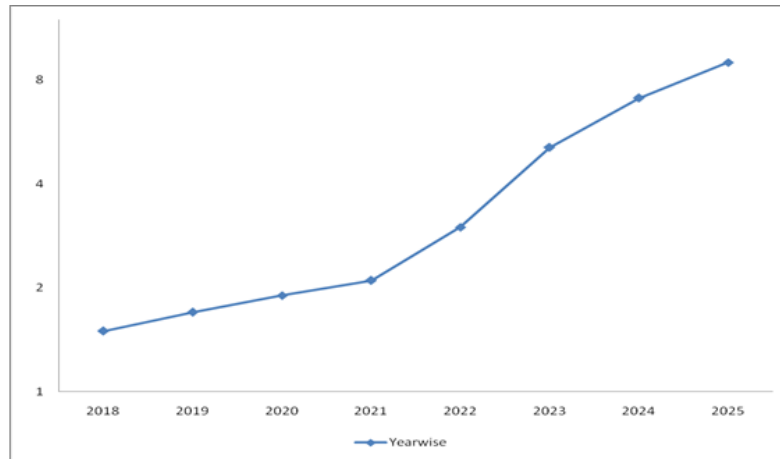
Fig2. Expected use of Li-Fi in near future

## 3.1. Li-Fi Products

Several LiFi products that are already in demand are:

1. LiFi enabled phone: This idea has been launched by Pure LiFi in 2021. LiFi enabled phones allow transfer of data with much ease and low latency by just pointing the device towards the target device. Screen sharing features are also enabled using Li-Fi. It is of great demand in scenarios where users can transfer images or videos in a very short span of time. The Getac technology has joined hands with pure LiFi to offer UX10 fully rugged Lifi based tablet.[30]

2. LiFi Router Mount for TPLink Deco M5/P7 - Wall Mount for TPLink M5,P7  Mesh Router

3. LiFi Nano V2 Visible Light Communication:Li Fi Transmitter +Li Fi Receiver + LED Light+LED Driver+FT232RL Breakout Board-2+USB Cable-2+Jumper Wires.

4. PureLiFi's LiFi-XC. : Li-Fi dongle. [10]

### 3.2. Li-Fi based smart cities

Two Gujarat villages in India named Akrund and Navanagar got Li-Fi based internet from the electricity lines. The startup Nav wireless Technologies have implemented the li-fi based systems in the educational institutions, government offices and hospitals successfully and are planning to extend the project to almost 6000 villages in Gujarat by the end of 2022.[18] A huge amount of funding has been sanctioned for the same which is a green signal of acceptance of this new technology for faster connectivity.[7] Remote places where the conventional connectivity technologies fail can be made smarter using LiFi technology.[27] Rural areas of Himachal Pradesh and Uttarakhand are soon going to get faster network connectivity as several startups have it in their agenda.[4]

## 4. Comparison of Different Existing Connection Technologies

| FEATURE | Wi-Fi | BLUETOOTH | ZigBee |
|---|---|---|---|
| Mode of operation | Using radio waves | Using short wavelength radio waves | Using radio waves |

| Coverage distance | 32m | 10m, 100m | 10-100m |
|---|---|---|---|
| Frequency of operation | 2.4GHz, 4.9GHz and 5GHz | 2.4 – 2.485 GHz | 2.4GHz |
| Speed of transmission | 150Mbps | 25Mbps | 250 Kbits/s |

Table 1: Comparison of existing connection technologies

## 5. Comparison of Existing Connection Technologies as an Alternative for Conventional Toll-System

### 5.1. Wi-Fi

In the current world of technology we can see Wi-Fi everywhere. It is the most used connection technology due to its easy availability. It requires a router for its complete working. It's an efficient mode of data transmission and data handling as they can be used to control and monitor the smart devices from anywhere in the world with the help of smartphones and other devices. One of the disadvantages of Wi-Fi is the unwanted leakage of data which paves way for data security issues. When we try to introduce Wi-Fi as a mode of toll system management, it may face certain difficulties. There are chances of signal interruption between the signals of

different vehicles. Every vehicle contains an infotainment system with Bluetooth, and there are chances for interference with the Wi-Fi signal. Wi-Fi signals are always relied upon by a router, which should be mounted outside the car (preferably at the front). When we connect a router on the car, the heat from the car and the heat from the sun can damage the router which eventually leads to signal loss. Network speed of Wi-Fi is good, but with the above conditions it will not be a good alternative for managing the toll system.[20][29]

### 5.2 Bluetooth

Bluetooth is one of the most established modes of connection technology. Since it is available within smartphones and devices, it doesn't require extra expense for the router. Currently every device has Bluetooth compatibility. When we considered Bluetooth for our toll system, it should be considered that the bandwidth is very low when compared. Transmission speed of Bluetooth will be very low and hence it is not preferable to manage a toll booth, as it requires instant data transfer and data recording.

### 5.3 Zigbee

It is considered to be one of the basic requirements for a smart home. Not all connection technologies require a router like wifi but a smart hub is always necessary [15]. While considering Zigbee, it should be noted that it is not managed through smartphones. It has a customized controller for its management. When we consider Zigbee for our toll management, then it is going to be a prolonged task. Since the maximum speed of Zigbee is even less than the least transfer speed of Wi-fi. To be precise, with a data transfer speed of 250 kb/s, the proposed task of managing a busy toll system is impossible. Advantages of Zigbee include low power consuming and efficient battery life. For economy, it's hard to beat Bluetooth. [13,24]

## 6. Conventional Toll System

The current toll system creates great fuss in case of heavy traffic as all the vehicles have to spend a lot of time waiting for their turn. A gate will be used which is automatically or manually controlled to restrict the entry for the toll collection. A

ticket or token is given which has to be kept carefully for two ways if necessary. The electronic fast tag is based on RFID (Radio frequency Identification Technology) which consists of a stamp size tag which is placed on the car and scanned when the car crosses the toll but this system also requires the barricade to monitor the process. The light being much faster than radio waves can be used here and the system becomes more sustainable as it only uses the head and tail light of the vehicles crossing the toll for the toll collection. [3]

## 7. Prototype Description

In the present scenario where people run behind time, long queues at the Toll Plaza`s is one among time wasting factors. Through this project, we design an automatic money collecting Toll system through Li-Fi. Nowadays the daytime running light (DRL) of the car is used to reduce accidents. Most of the latest vehicles are equipped with this DRL setup which is purely automatic. This DRL can be used as a transmission medium to transmit the Li-Fi modulated signals to the receivers. The receivers are present at the toll center at specific lanes positioned in such a manner that they maintain a straight contact. [3]
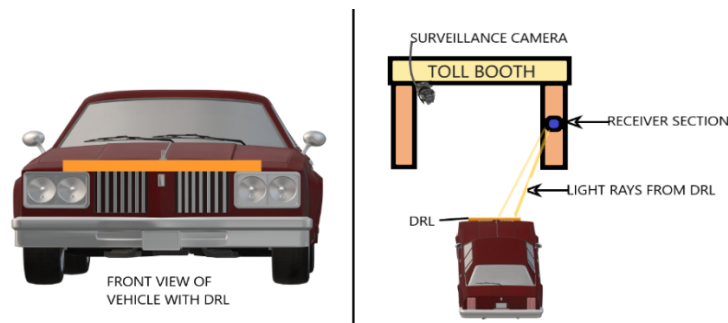


Fig3: Front view and pictorial representation of Li-fi based Toll System

Through the proposed idea the data of the vehicle which includes the vehicle number, owner name and phone number will be added to the database. The data received through the receiver section will be instantly processed and accessed through the serial ports of the system. [9] This system can bring a huge difference in the maintenance of data of the vehicle passing through certain tolls. Identity of

each car will be unique as each vehicle will have a specified modulated signal of light rays from DRL. If a vehicle doesn't have a DRL system, then they can install a DRL feature with a modulated light signal.

Since this system deducts toll money using the Li-fi signal, if the driver doesn't have enough balance to pay the toll then the surveillance camera will click the picture of the car which includes the registration number of the car. This will be an extra feature as details regarding the driver and the car will be automatically stored when the Li-fi signal is received.

# 8. System Requirements

## 8.1. Hardware Requirements

### Arduino UNO

The Arduino Uno is a microcontroller board based on the Microchip ATmega328P microcontroller and it can be programmed with the help of an open source Arduino software. It acts as an Integrated Development Environment which helps to do the required coding on the computer side and then upload it to the physical Arduino board. The hardware section of the board comprises digital and analog input/output (I/O) pins that can be interfaced to required circuits. This Arduino UNO is essential for the data transfer from one device to another.

### LED

LEDs are used in Li-Fi as visible light transmitters. Li-Fi data is transmitted through the LEDs and received by photo diodes. The LED is connected to one of the digital pins. The LED blinks according to the binary logic received from the processing software. [26] (Here DRL:-Daytime Running Light)

**LDR**

An LDR is a component with variable resistance that changes with the intensity of light that falls upon it. It uses the concept of photoconductivity and it has a resistor whose resistance value decreases when the intensity of light decreases. It is an optoelectronic device mostly used in light varying sensor circuits. The light from the LED is identified by using LDR and the data is transmitted to the Arduino.

## 8.2. Software Requirements

### Arduino programming language

Arduino is an open-source platform used for programming. Arduino consists of both a physical programmable circuit board (often referred to as a microcontroller) and IDE that acts as the software compartment that runs in the computer. Computer codes and the writing are done using this IDE (Integrated Development Environment). It supports C and C++, and includes libraries for various hardware components, such as LEDs and switches. It can be run and will remain in memory until it is replaced.

### Python Idle

It is an integrated development environment for Python programming. IDLE can be used to create, modify, and execute Python scripts and also execute a single statement.

### XAMPP

XAMPP is a free and open-source cross-platform web server solution stack package. It consists mainly of the Apache HTTP Server, MariaDB database, and interpreters for scripts written in the PHP and Perl programming languages. Here, we have used XAMPP for creating a local server to work on.

**PhpMyAdmin**

It is a portable web application and is primarily written in Php. It is one of the efficient MySQL administration tools and is basically used for web hosting services. This software is relevant in our system to maintain the whole database.

**Tinkercad**

Tinkercad is a free, online 3D modeling program that runs in a web browser, known for its simplicity and ease of use. We have used it to stimulate circuits and to generate Arduino codes.

## 9. System Design

The system design is represented in the block diagram below:
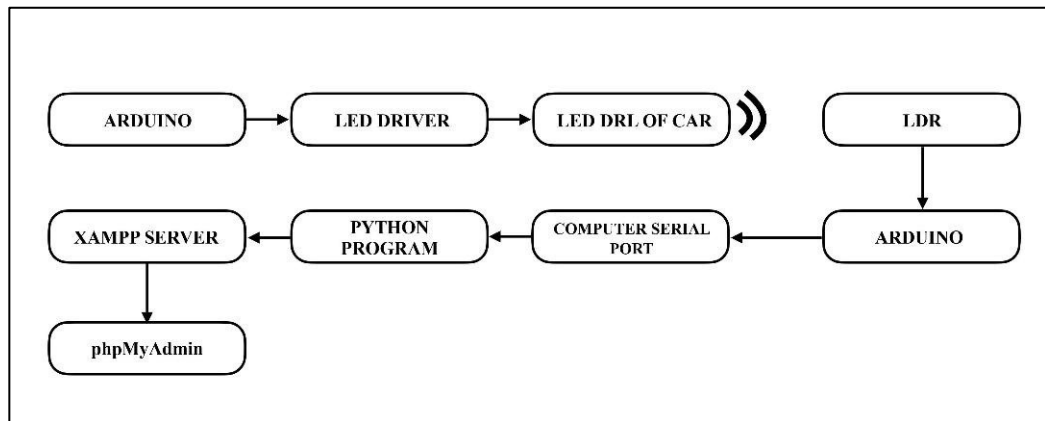
Fig4. Receiver section of Toll booth

## The flowchart explains the basic working of the system:

According to the flowchart below, the light from the DRL that falls on the LDR is responsible for the binary string that is produced from the arduino at the receiver end. The binary string generated will be the primary key that is also called the LiFi id. This primary key belongs to the database named Car details and further query based operations take place at this database table. Once the car details are verified, check whether the vehicle contains a sufficient amount of balance. Deduct the toll amount from the balance. If the balance is less than the toll amount, the details about the vehicle will be collected and a fine will be imposed.
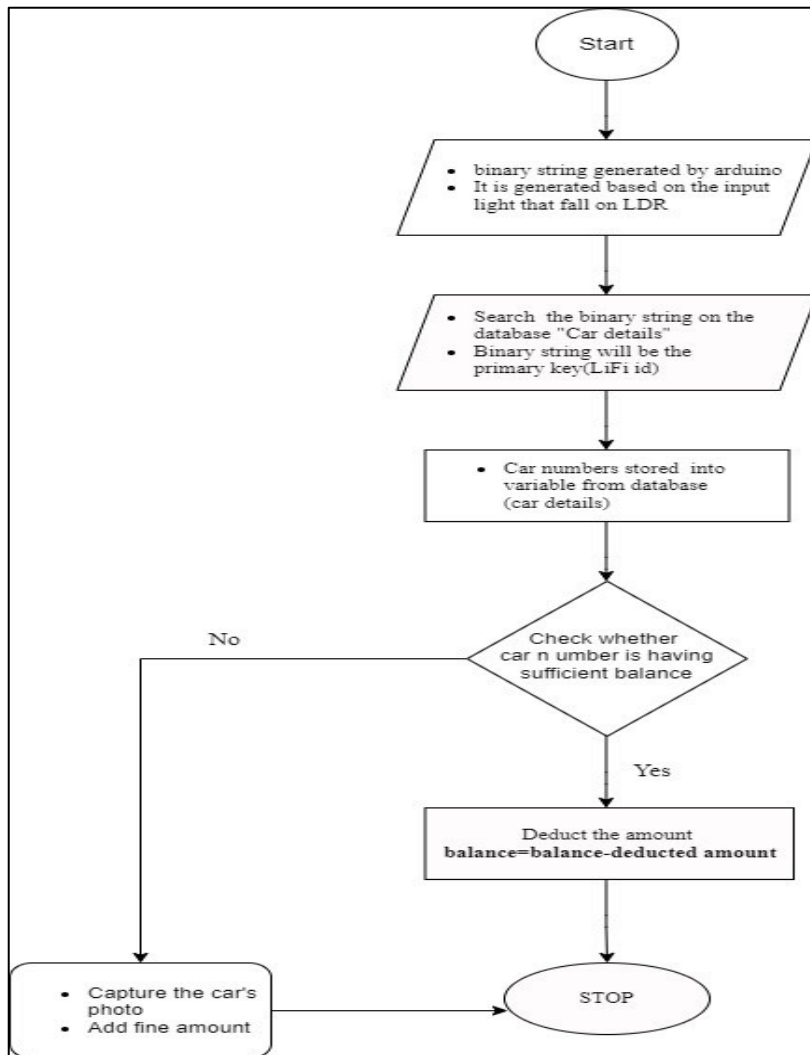
Fig 5. Flowchart explaining the working of system

the system setup can be depicted using 2 sections: Transmitter section and Receiver section:

## 9.1. Transmitter Section

14

We use visible light for this means of transmission of data.[26] The vehicle will be the carrier of the transmitter section whereas the receiver section will be positioned at a small portion of the post at the right side of each lane where the entire toll system is situated. When a vehicle passes through the lane, the details of the driver and vehicle from the individually modulated DRL (Daytime running Light) will be captured by the receiver section. [7]
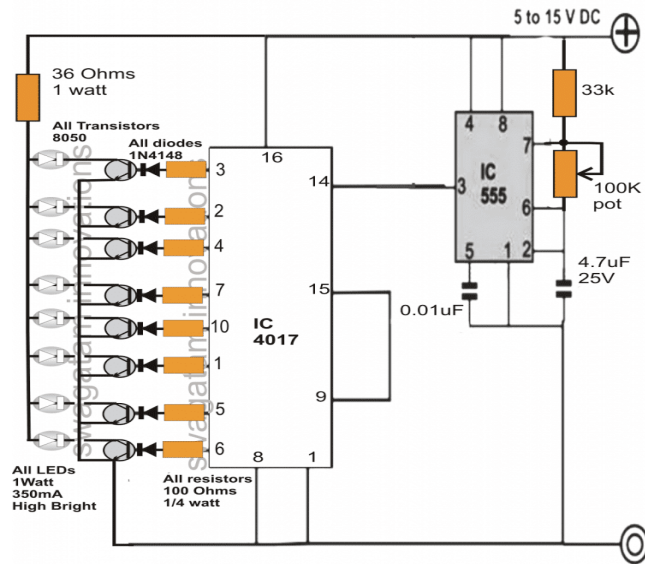
Fig 6: Transmitter section (DRL of a normal vehicle) [9]

Fig 7: DRL setup which are currently available in vehicles [11]

Transmitter section will be always on as the supply of light is through DRL. The receiver section will have an LDR module to receive the required signal from the DRL emitter. This light signal will transfer the details for transfer of required amount for the corresponding toll booth. [11, 26]
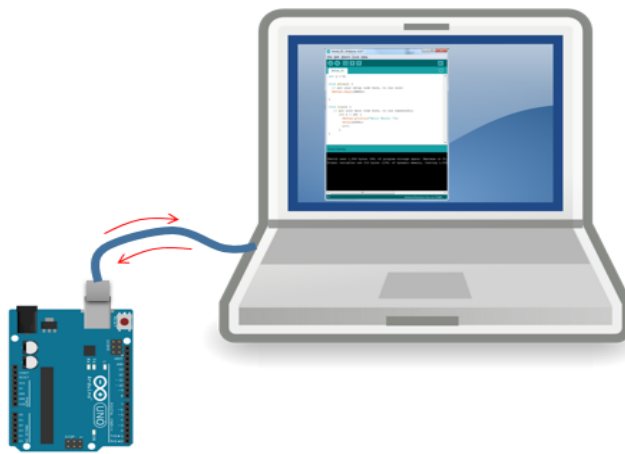


Fig 8: Data is transferred to the system through serial port (RX/TX) from Arduino which process the data from LDR [38]

## 9.2. Receiver Section

This data will be taken into the serial port of the computer at the toll center. By using the python Idle we will be collecting those data from the serial port of the computer by means of Pi- serial. By using XAMPP we create a local server in our system. With the help of phpMyAdmin we will add these data to the database. Since tolls are maintained by the NHAI (National Highway Authority of India), we have to integrate their database with our data for a full flourished maintenance.
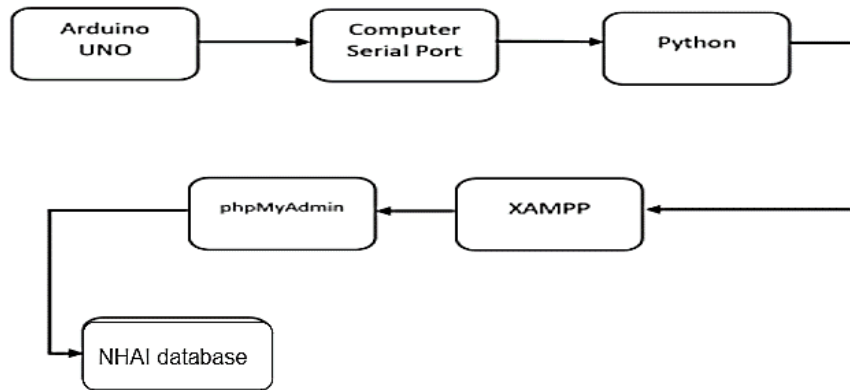
Fig 9. Receiver Block Diagram

## 10. Results

The whole idea of introducing a Li-fi based toll system was to reduce unwanted queues and rush at the toll centers. With this development in the toll system, we can get instantaneous data collecting techniques. These data are easily accessed through the modulated signal of Light from each vehicle which provides the identity of the vehicle which ensures the reliability of this system. Even if the toll amount is not deducted, the details of the car and the owner will be saved which will help to track the vehicle and impose fine. The data transmission using LiFi based system was initially tested using the arduino. The receiver section of the toll system used here is LDR. Any photoresistive device can be used. If a solar panel is used instead of LDR, then the output from the graph can be plotted as below.
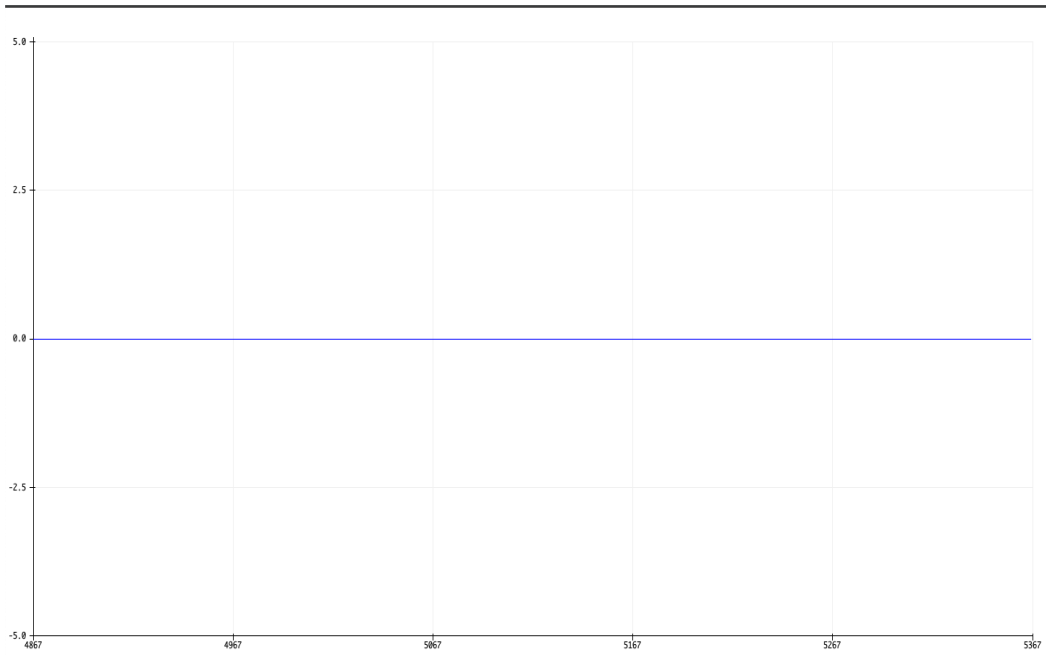
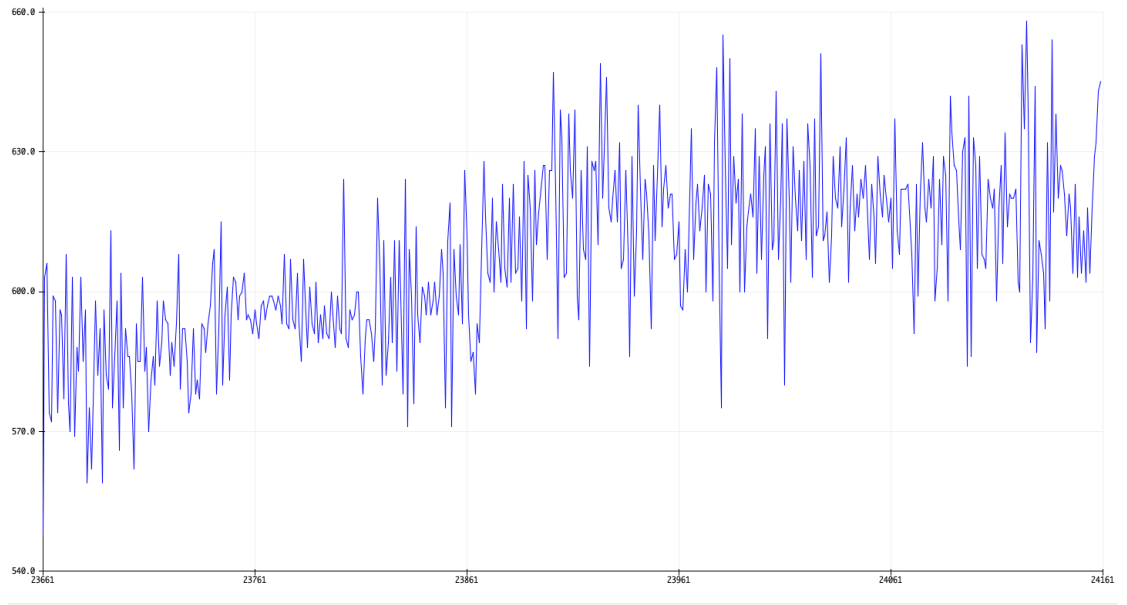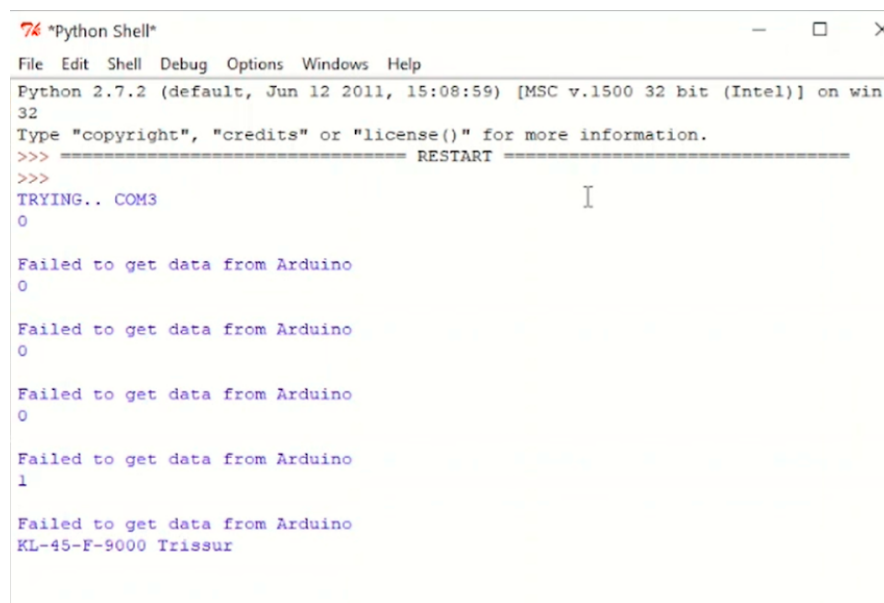Fig 10: Graph plotted when no light is detected by Solar panel

Fig 11: Graph plotted when the data in the form of light falls on solar panel

**Output obtained when vehicles pass through the toll booth is as follows:**



Fig 12: Data of vehicles recorded in the server

**Method of analyzing the input from modulated li-fi signals of the DRL**



Fig 13: Input from a vehicle is analyzed to produce the output

From the figure we can understand that, the Li-Fi id in binary formats is received at the receiving end and the receiver section decodes it and records all the details of the vehicle which primarily includes the vehicle number and the destination to where it is heading to. For each vehicle this li-fi id will differ and assures the iden-

tity of each vehicle. From Fig 7 the vehicle li-fi id is obtained as 1-0-0-0-1 which is instantly decrypted to its raw data.

Details including the Li-Fi id, registration number, destination towards and the time of passing the toll will also be recorded along with the cash withdrawal. This will help the NHAI and the toll management to easily store the data. With the inclusion of destination and time, it would be easy for investigators to track the vehicle if the vehicle is involved in any crime. Thus reducing the risk of crimes in the city.[31]

## 11. Challenges in the Implementation of Li-Fi

Li Fi is a new generation method of connectivity which is to be completely explored. The initial setup might be costly compared to the conventional and RFID methods of toll collection. There are no existing systems to use as reference for this study. Implementation of LiFi based systems under daylight should be monitored perfectly. The proposed system is based on certain ideal conditions i.e, all cars should have DRL. Large scale implementations using Li Fi with the existing studies and researches are challenging. Since LiFi uses visible light and light cannot penetrate through walls, the signal's range is limited by physical barriers. Sunlight being one of the potential threats to Li Fi technology, it may interrupt the working of the system. [21, 25]

## 12. Conclusion and Future Works

In the system we make use of Li-Fi signals thus it completely digitalizes the process reducing all the hazards and delays caused at the toll system. No need for barricades to restrict entry and it helps to speed up the process thereby making time management much efficient at toll booths. Efficient method of transportation through the hectic toll traffic will help vehicles like ambulances which should be given at most priority to move forward with ease. [2] Even after the intervention of fast tag, manual barricade management is a tedious task and causes unwanted struggle at the toll system surroundings which ultimately questions the cause of its use. It is at this situation we are introducing this concept of Li-fi based toll system where the vehicle users can move through the toll booth as simply as moving through a normal highway. This can further be modified and even used to detect

fake vehicles that are crossing the toll by checking the vehicle number identified by the LiFi system with the original registered number in the vehicle department. Lifi will definitely be a promising solution to converge with advanced technologies that will pave the way to an intelligent transportation system that aims at faster, safer and efficient driving minimising vehicle collision. [16,19] Li-Fi technology being in its infancy stage of development has to compete with several issues like line of sight, initial deployment cost and coalescence with the original equipment manufacturer(OEM) outside the LiFi based industry.

## 13. References

1. George, Rahul & Vaidyanathan, Srikumar & Rajput, Amandeep & Kaliyaperumal, Deepa. (2019). LiFi for Vehicle to Vehicle Communication – A Review. Procedia Computer Science. 165. 25-31. 10.1016/j.procs.2020.01.066.

2. L. E. M. Matheus, A. B. Vieira, L. F. M. Vieira, M. A. M. Vieira and O. Gnawali, "Visible Light Communication: Concepts, Applications and Challenges," in IEEE Communications Surveys & Tutorials, vol. 21, no. 4, pp. 3204-3237, Fourth Quarter 2019, doi: 10.1109/COMST.2019.2913348.

3. D. Singh, A. Sood, G. Thakur, N. Arora and A. Kumar, "Design and implementation of wireless communication system for toll collection using LIFI," 2017 4th International Conference on Signal Processing, Computing and Control (ISPCC), Solan, 2017, pp. 510-515, doi: 10.1109/ISPCC.2017.8269732.

4. M. Leba, S. Riurean and A. Lonica, "LiFi — The path to a new way of communication," 2017 12th Iberian Conference on Information Systems and Technologies (CISTI), Lisbon, 2017, pp. 1-6, doi: 10.23919/CISTI.2017.7975997.

5. "Visible-light communication: Tripping the light fantastic: A fast and cheap optical version of Wi-Fi is coming". The Economist. 28 January 2012.

6. Haas, Harald (July 2011). "Wireless data from every light bulb". TED Global. Edinburgh, Scotland.

7. IEEE Std., IEEE Std. 802.15.7-2011, "IEEE Standard for Local and Metropolitan Area Networks, Part 15.7: Short-Range Wireless Optical Communication Using Visible Light", 2011.

8. A.V.N. Jalajakumari, E. Xie, J. McKendry, E. Gu, M.D. Dawson, H. Haas, et al., "High speed integrated digital to light converter for short range visible light communication", IEEE Photonics Technology Letters, 10 2016.

9. A. Vega, "Li-fi record data transmission of 10Gbps set using LED lights", Engineering and Technology Magazine, November 2015.

10. O.D. Alao, J.V Joshua, A.S Franklyn and O. Komolafe, "Light Fidelity (LiFi): An Emerging Technology for The Future", IOSR Journal of Mobile Computing & Application (IOSR-JMCA), vol. 3, no. 3, pp. 18-28, May.–Jun. 2016, ISSN 2394-0050.

11. R. Sharma, A. Sanganal and S. Pati, "Implementation of A Simple Li-Fi Based System", IJCAT - International Journal of Computing and Technology, vol. 1, no. 9, October 2014.

12. Haas H, Yin L, Wang Y, and Chen C 2016 What is LiFi? J. Light. Technol. 34 pp 1533–44.

13. Ayyash M et al 2016 Coexistence of WiFi and LiFi toward 5G: Concepts, opportunities, and challenges IEEE Commun. Mag. 54(2) pp 64–71.

14. Singh P Y P and Bijnor U P 2013 A comparative and critical technical study of the Li-Fi (A Future Communication) V / S Wi-Fi 2(4) pp 2011–3.

15. Lee S J and Jung S Y 2012 A SNR analysis of the visible light channel environment for visible light communication APCC 2012 - 18th Asia-Pacific Conf. Commun. "Green Smart Commun. IT Innov." pp 709–12

16. Philip, A. Oommen and Saravanaguru, RA K. "Secure Incident & Evidence Management Framework (SIEMF) for Internet of Vehicles using Deep Learning and Blockchain" Open Computer Science, vol. 10, no. 1, 2020, pp. 408-421,https://doi.org/10.1515/comp-2019-0022

17. Paul R., Sebastian N., Yadukrishnan P.S., Vinod P. (2021) Study on Data Transmission Using Li-Fi in Vehicle to Vehicle Anti-Collision System. In: Pandian A., Fernando X., Islam S.M.S. (eds) Computer Networks, Big Data and IoT. Lecture Notes on Data Engineering and Communications Technologies, vol 66. Springer, Singapore. https://doi.org/10.1007/978-981-16-0965-7_41

18.http://timesofindia.indiatimes.com/articleshow/81080015.cms?utm_source=con tentofinterest&utm_medium=text&utm_campaign=cppst

19. Abin Oommen Philip and Dr. Saravanaguru RA.K, A Vision of Connected and Intelligent Transportation Systems. International Journal of Civil Engineering and Technology, 9(2), 2018, pp. 873-882

20. Wu, X., Soltani, M. D., Zhou, L., Safari, M., & Haas, H. (2021). Hybrid LiFi and WiFi networks: A survey. IEEE Communications Surveys & Tutorials, 23(2), 1398-1420.

21. Haas, H., Yin, L., Chen, C., Videv, S., Parol, D., Poves, E., ... & Islim, M. S. (2020). Introduction to indoor networking concepts and challenges in LiFi. Journal of Optical Communications and Networking, 12(2), A190-A203.

22. Ramadhani, E., & Mahardika, G. P. (2018, March). The technology of li fi: A brief introduction. In IOP conference series: materials science and engineering (Vol. 325, No. 1, p. 012013). IOP Publishing.

23. Leba, M., Riurean, S., & Lonica, A. (2017, June). LiFi—The path to a new way of communication. In 2017 12th Iberian Conference on Information Systems and Technologies (CISTI) (pp. 1-6). IEEE.

24. Haas, H. (2018). LiFi is a paradigm-shifting 5G technology. Reviews in Physics, 3, 26-31.

27. Haas, H., & Cogalan, T. (2019, August). LiFi opportunities and challenges. In 2019 16th International Symposium on Wireless Communication Systems (ISWCS) (pp. 361-366). IEEE.

26. Lee, C., Islim, M. S., Videv, S., Sparks, A., Shah, B., Rudy, P., ... & Raring, J. (2020, February). Advanced LiFi technology: Laser light. In Light-Emitting Devices, Materials, and Applications XXIV (Vol. 11302, p. 1130213). International Society for Optics and Photonics.

27. Mukku, V. D., Lang, S., & Reggelin, T. (2019). Integration of LiFi technology in an industry 4.0 learning factory. Procedia Manufacturing, 31, 232-238.

28. Goswami, P., & Shukla, M. K. (2017). Design of a li-fi transceiver. Wireless Engineering and Technology, 8(04), 71.

29. Wu, X., O'Brien, D. C., Deng, X., & Linnartz, J. P. M. (2020). Smart handover for hybrid LiFi and WiFi networks. IEEE Transactions on Wireless Communications, 19(12), 8211-8219.

30. Jungnickel, V., Berenguer, P. W., Mana, S. M., Hinrichs, M., Kouhini, S. M., Bober, K. L., & Kottke, C. (2020, March). LiFi for industrial wireless applications. In 2020 Optical Fiber Communications Conference and Exhibition (OFC) (pp. 1-3). IEEE.

31. R. Paul and M. P. Selvan, "A Study On Naming and Caching in Named Data Networking," 2021 Fifth International Conference on I-SMAC (IoT in Social, Mobile, Analytics and Cloud) (I-SMAC), 2021, pp. 1387-1395, doi: 10.1109/I-SMAC52330.2021.9640947.

32. Paul, Rosebell & Sebastian, Neenu & Yadukrishnan, P. & Vinod, Parvathy. (2021). Study on Data Transmission Using Li-Fi in Vehicle to Vehicle Anti-Collision System. 10.1007/978-981-16-0965-7_41.

33. Smys, S., and Mr C. Vijesh Joe. "Metric Routing Protocol for Detecting Untrustworthy Nodes for Packet Transmission." Journal of Information Technology 3, no. 02 (2021): 67-76.

34. Chen, Joy Iong Zong, and Lu-Tsou Yeh. "Graphene based Web Framework for Energy Efficient IoT Applications." Journal of Information Technology 3, no. 01 (2021): 18- 28.

35. Bashar, Abul. "AGRICULTURAL MACHINE AUTOMATION USING IOT THROUGH ANDROID." Journal of Electrical Engineering and Automation 1, no. 2 (2019): 83-92.

36. Raj, Jennifer S. "Optimized Mobile Edge Computing Framework for IoT based Medical Sensor Network

# A Swarm-Based AI Aided Wheel Bot System to Detect Cracks in Railway Tracks

Rosebell Paul
Department of Computer Science and Engineering
SCMS School of Engineering and Technology
rosebell@scmsgroup.org

Neeraj M
Department of Computer Science and Engineering
SCMS School of Engineering and Technology
neerajmallisseri@gmail.com

Neeraj Sagar
Department of Computer Science and Engineering
SCMS School of Engineering and Technology
neerajsagar1998@gmail.com

Vaibhav Nair
Department of Computer Science and Engineering
SCMS School of Engineering and Technology
vaibhavnair008@gmail.com

Yadukrishnan PS
Department of Computer Science and Engineering
SCMS School of Engineering and Technology
yedhups@yahoo.com

*Abstract*—Railway is one of our country's most important sources of transit, yet it is a source of great concern since our railway tracks are vulnerable to damage/cracks. The major causes of railway accidents are railway track crossings and unseen faults in railway tracks. Due to such primitive conditions a numerous number of accidents are seen every year with heavy tolls to human life and infrastructure. The aim of this project is to develop a swarm robotic system to provide a real-time solution to crack detection and danger mitigation. Crack detection has been manual which is time-consuming and tedious, until recently, when the crack detection system started to become automated. But the system still has major flaws such as inability in identifying the different types of cracks, distinguishing between intentional and actual cracks, and providing a real-time solution to the identified problem. The proposed system is aimed towards efficient detection of not just cracks, but obstacles and animal detection along with fault detection in case of agent failure. A swarm robotic approach is implemented where the agents are deployed on the tracks and they are able to communicate among themselves as well as the base station in real-time. The system is integrated with an android application which updates the status of the agents of the assigned cluster in real-time. The agent also has the mechanism of detaching itself off the tracks when a train approaches to avoid collisions.

*Keywords—Swarm Robotics;Crack detection;Railway tracks;Animal Detection*

## I. INTRODUCTION

Indian Railway is one of the largest transportation networks in the world. It has a daily passenger count of 24 million passengers.For such a vast network the possibilities of lapses in safety is alarmingly high [10].

One of the major causes of hazard would be disruption in locomotive movement. Cracks in railway tracks have been identified as one of the major causes of railway accidents.Currently there isn't a fail proof system to detect and fix cracks on railway tracks. The system still follows the primitive methods of manual checking and solving [9].The project focuses on providing a real-time solution to the identified cracks on railway tracks. Once identifying a crack as a threat the agent aims at alerting the nearby agents as well as a base station by an active communication channel that updates the status in real-time. The project implements a wheel-bot (UGV) which is able to differentiate between cracks and intentional gaps(thermal expansion). The Robots Dynamically communicate with other agents ( Swarm Robotics approach ) and the main workstation to relay information regarding the problems identified [1].Once the agent has identified a crack, it is intimated to the nearest base station for the track engineer to address the issue at the earliest.It also communicates to its nearest agents and alerts them regarding the identified setback. The system also tries to provide a safe environment for the locomotive system in the regions of animal crossing.

## II. LITERATURE REVIEW

Extensive research was carried out during the idea phase of the project. This was done to acquire sufficient knowledge in the fields of infrastructure of railways, swarm robotics and image processing algorithms. Over the course of development of the project, a number of existing research papers were studied in order to plan and achieve modules of the project in an efficient manner. [1] explains the dilemma in the exploration and exploitation in the movement of multi-agent swarm systems.Provides valuable information on FIFO-list, which helps maintaining a dynamic list for recently visited states.This provided a baseline for implementing the pipeline communication system for the communicating between the robots. [4], on the basis of various baseline methods contributes to various cross lingual image annotation and retrieval.The COCO library is highly suitable for annotating images with Chinese language as it provides over 20,000 images with Chinese labeling. [2] displays a comprehensive study on the substructure of railway tracks which includes ballast, sub-ballast, subgrade and drainage. It also provides great insight on the basic layout and structure of the railway tracks which provides great insights on railway track characteristics. This helps us with major understanding about the infrastructures and function with respect to the project.

Micro-robotics has provided game changing innovation in the field of medicine through minimally invasive medicine. A single micro robot has limited volume and surface area which leads to high orders of inefficiency. The coordinated feature of swarm robots prioritizes on modeling ,simulation and hive control of the swarm robots.This f eature can solve numerous issues put forward by the medical community. [5] provides a fine overlay and detailed understanding about the aforementioned.

## III. GENERAL BACKGROUND

### A. Objective

The project focuses on providing a real-time solution to the identified cracks on railway tracks. Once identifying a crack as a threat the agent aims at alerting the nearby agents as well as a base station by an active communication channel that updates the status in real-time [2]. In conclusion, the study's primary contributions might be stated as follows:

1. Implementation of wheel-bot (UGV) which is able to differentiate between cracks and intentional gaps(thermal expansion).

2. The Robots Dynamically communicate with other agents ( Swarm Robotics approach ) and the main workstation to relay information regarding the problems identified

3. Once the agent has identified a crack, it is intimated to the nearest base station for the track engineer to address the issue at the earliest

4. It also communicates to its nearest agents and alerts them regarding the identified setback

### B. Scope

The scope of the project stretches as far as the entirety of the Indian Railway Catering and Tourism Corporation(IRCTC). The system works with a fixed number of agents reporting to a common base station. This makes the project vastly extendable as we can set up as many base stations as required want and since the project follows a swarm robotic approach, we can deploy agents for each and every railway track in India [15].Also by linking the system with the main database of IRCTC, communication and performance units' performance can be ramped up, with the agents being able to send/receive data with greater efficiency. This can help us mitigate any kind of danger due to cracks on railway tracks at the largest scale possible.

## IV. IMPLEMENTATION

### A. Infrastructure

The system is divided into clusters. Each cluster has a base station and a fixed number of agents. These agents follow swarm robotic architecture. The agents are deployed on the tracks. The number of agents in a cluster is determined by the maximum communication range of an NRF module which is the communication unit used in the product [5]. The aforementioned can be extended up to 3 km [7]. The cluster also has a fixed number of free robots that replace the working agents in case of a fault or low battery. The designed UGV is a four-wheeled bot that is deployed directly onto the railway tracks.
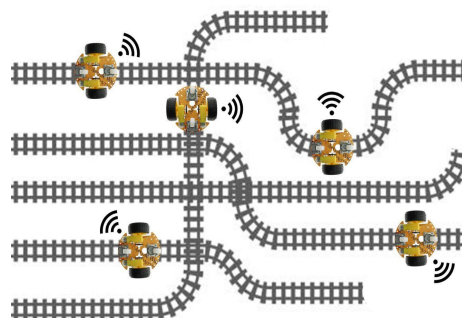


Fig.1.  Basic deployment pattern of the bots

## B. Architecture

The system mainly comprises the communication unit and the sensor data processing unit [6]. Communication is responsible for the efficient exchange of data between the agents as well as the base station. The agents communicate to the nearest bots and base station in the case of any kind of hindrance identified by the sensor data processing unit. The Arduino is used for capturing the data from the sensor and encoding it into a suitable packet format for the smooth transmission of data through the network using the NRF24L01 module connected to the Arduino.The model uses an NRF24L01 module for communication. The sensor data processing unit is responsible for the perception of various kinds of cracks, obstacles, and faults in the agent itself. Various sensors are integrated and implemented for fault detection [8]. The data is fed to the Arduino board which handles the communication and sensor data processing tasks. The raspberry module is integrated in the system for image processing.A Raspberry Pi model 4b with 4GB of RAM is selected for this project.The image detection process requires ample amount of processing power for stutter-less output.Raspberry Pi with less RAM was seen to provide low FPS video output. The project aims toward efficient animal crossing detection which is common on the Indian railway tracks due to the terrains it passes through. The agents will be equipped with an FPV camera, which captures images when it encounters live object detection [12]. Then running efficient image processing algorithms it identifies the subject in front of it and starts over only when the path is clear. The model is also equipped with a GPS module which helps the other agents know its current location when it sends out data in case of fault detection. This helps other agents to reach that specific location and aid it. It also helps the base station to know the location of the fault.
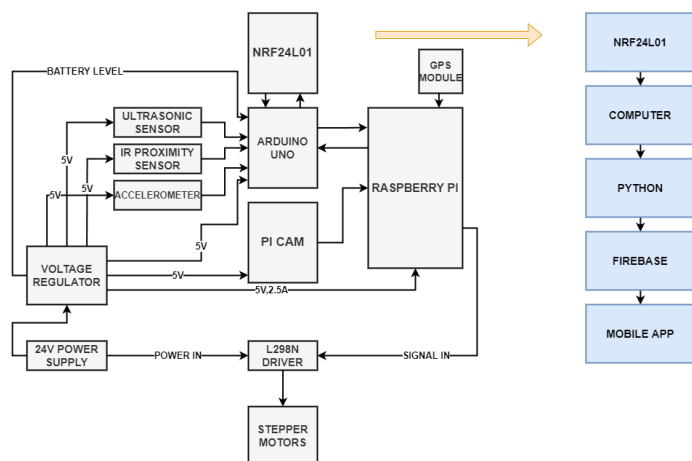
assignments for this NRF24L01 module is done using Arduino.. That is, this module runs according to the program which is burned in the Arduino. This module employs GFSK modulation to transmit data and is meant to operate in the 2.4 GHz global ISM frequency band.. The transmission rate can be 250kbps, 1Mbpz or 2Mbps. The voltage range of this NRF24L01 module is between 1.9V-3.6V, we will be using a level shifter for this module in order to maintain the correct voltage for the module [14].

## B. RF channel configuration

Two or more NRF24L01 modules must be on the same channel in order to communicate. Any frequency in the 2.4 GHz ISM band may be used for this channel. We have 125 potential channels with a 1Mhz spacing because each channel uses less than 1Mhz of bandwidth. Here we will be again splitting these channels into different logical channels, that is we will be splitting our physical channels into many logical channels for the communication between each agent in the network. This opens a way for the One-to-One and One-to-Many communication in the network. The One-to-One generally happens in the communication between agents to agents and Agent to Server. Many-to-Many configuration happens in the communication between the server and all the clients in the network [13].

As shown in Figure 3, there will be a broadcast channel, which is used by the server for sending data or alerts to all other agents in the system. Each client in the network receives the same. There will be another logical channel for each client to communicate with the server. If a client wants to communicate to another client in the network, that message will be first sent to the server then broadcasts the message and the client which is meant to receive that message will accept it and others will reject it. If it is a common message then, every client in the network will accept the message. This acceptance and rejection of messages is done with the help of packet format in Figure 4.
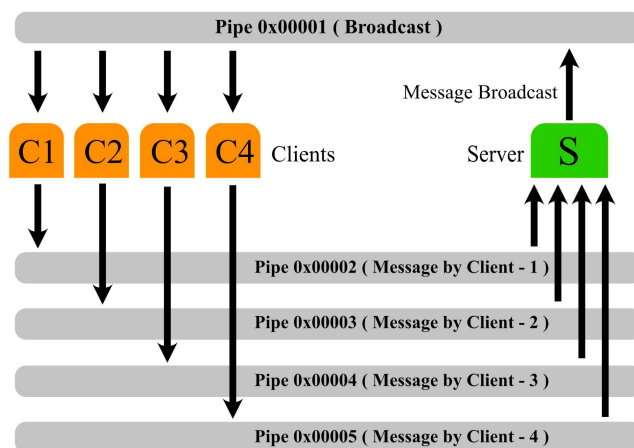


Fig.2. System Architecture

## V. COMMUNICATION UNIT

### A. Overview

The Communication between the agents and the server is done using NRF24L01 modules, which is a wireless transceiver module capable of listening to 6 other modules at the same time. The channel configuration, address



Fig.3. Broadcast pipeline

## C. Packets

The data is transmitted between the agents in the form of packets. In figure 4 we can see the packet format of the data which is transmitted and received on each agent in the network. The data from the sensors are first given to the Arduino board, then the Arduino creates the packet of data which will be then transmitted through the network using NRF24L01. The first part of the packet is used for an identification number. Each agent in the network will have an unique identification number and this will be the first parameter checked when another agent receives this data, to confirm whether this data is meant to be received or not by that agent. Next is ACK CLIENT, which is used for verifying the data has been successfully received on the other agent by acknowledgement status bit. ACK SERVER is used for the acknowledgement by the server. Then comes the ADDRESS, which is used for retransmission and replying or sending back the acknowledgement. In the DATA part we will be sending the sensor data. That is X and Y axis of the accelerometer (MPU6050), Temperature of the battery and the internal components, Proximity value from the proximity sensor (HC-SR04) which works by ultrasonic sounds, IR_1 and IR_2 are two Infrared based proximity sensors for the detection of the crack and finally the Latitude and Longitude from the GPS module (NEO 6M) [17].
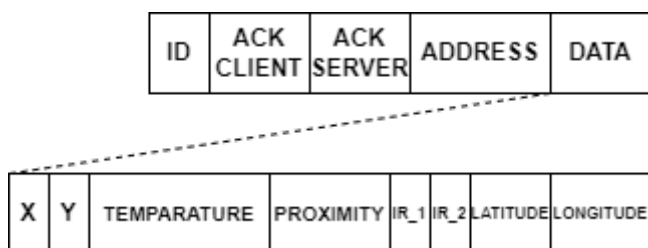


Fig.4. Packet Format

## D. Retransmission

The wireless communication module we are using here is NFR24L01 and its range can be extended only to a maximum of 2Km. For sending data and alerts to the base station which is located more than 2Km from the agent is done by retransmitting the data packets to the nearest agent like a chain mechanism. The agent which is far away from the base station initially will try to send the data packets to the base station and waits for the acknowledgement from the base station. After a limiting time the agent confirms that the base station is no longer on its range limit. So that agent will send this packets to its nearest agent which is in the range of 2Km radius with base station and so on

## VI. GPS MODULE

### A. Sensor module

The project utilizes the GPS module Neo-6m for calculation of the live GPS coordinates of the agents. The immediate geo-location is instantaneously delivered to the android application, which can be viewed by the user in the UI. The neo-6m model was chosen for the project, as it is low-powered, which means it is highly suitable for battery-operated devices, and is cost efficient as well. The chosen GPS module can perform up to 5 location updates within a second, which makes it optimum for the proposed project, which involves continuous movements of the agents throughout [11]. The continuous location-output delivered by the sensor helps with keeping track of the agent status effectively.

### B. Haversine formula

The geo-location of all the agents is relayed to the android application held in their respective base station. Now with the immediate latitude and longitude of any two robots respective to that base station, we can successfully compute the effective distance between the two agents. This has the use case, whenever an agent has encountered a hindrance, may it be an obstacle or fault. The agent communicates regarding it to the nearest available agents at that moment. Also, if the agent has encountered a fault, where it might have faced a circuit problem or de-railed the track, the agent uses the geo-locations to find the nearest free-agent to replace it. The android app also displays the distance between any two tops within a base station. The calculation is done using the Haversine formula. The haversine formula is used to calculate the distance between any two objects on the sphere using the radius of the earth.

$$\text{haversine}(\theta) = \sin^2(\theta/2) \tag{1}$$

$$a = \sin^2(\varphi B - \varphi A/2) + \cos \varphi A * \cos \varphi B * \sin^2(\lambda B - \lambda A/2) \tag{2}$$

$$c = 2*\text{atan2}(\sqrt{a}, \sqrt{(1-a)}) \tag{3}$$

$$d = R \cdot c \tag{4}$$

where $\varphi$ is the latitude, $\lambda$ is the longitude and R is the radius of the circle.

## VII. ANIMAL DETECTION UNIT

### A. Animal detection unit

The pathways of the crack detection robots are medalled with a plethora of obstacles and dangers. The bot actively responds against non-living obstacles using its array of proximity sensors. The next challenge are the living obstacles and dangers caused in specific locations like animal crossings and wildlife sensitive areas. Elephant crossings along various railway tracks can cause untimely disruptions in the proper movement of the robot. An efficient way to tackle this problem is a real-time animal detection system that takes in live camera feed and detects elephant crossings present in the frame. On the detection of an elephant the robot is signaled to halt its movement and wait for a safer environment to continue

its movement by analyzing the live camera feed.The process of animal detection is carried out on a Raspberry Pi module attached onto the robot. Upon detection the Raspberry Pi is programmed to provide a motor signal to the required L298N motor driver module.Detecting an item includes both expressing the presence of an object of a specific class and localizing it in the picture. A bounding box is commonly used to depict an object's position.

### B. Requirements

- Raspberry Pi 3 Model b-1GB RAM
- Raspberry Pi High Quality (HQ) camera

This image detection process utilizes both machine learning and open-source software like Open-CV in a Raspberry Pi ecosystem. The library used for image detection is called a COCO (Common Objects Context) library, which is a pre-trained library of objects and common images [4]. COCO provides a large-scale object detection and segmenting dataset that allows accurate image segmentation and recognition. It contains over 333,000 images which gives 91 object categories. This dataset was created in collaboration with Microsoft, Facebook and CVDF.

### C. OpenCV and COCO Library

OpenCV (Open Source Computer Vision Library) is used to tackle all kinds of real time image processing problems by using the vast resource of imaging functionalities. It establishes a standard architecture upon which computer vision applications may be conducted and accelerated to achieve optimum accuracy. OpenCV contains a collection of both cutting-edge and conventional machine learning methods that may be used for a variety of image processing applications.

COCO library is consistently used for computer vision applications due to its large set of annotated object sets that can be easily used for object detection purposes.The COCO dataset on testing showed an average precision(AP) of 56.8.While detecting almost 18 object categories the model showed an average reaction time of 8.6 milliseconds. COCO library provides exact resources for animal detection. A weightspath and configpath file are retrieved from the model which provides us with a frozen instance of the model to work with.

The object detection system is implemented on the Raspberry Pi Buster OS by importing several OpenCV functionalities. The python program invokes pre-trained graph models and the required config files from the COCO library. These attributes are later crosschecked with the real-time image frames from the Raspberry Pi camera. The image frames characteristics like scale, size and RGB values are modulated to fit the desired model. A Threshold number (nms percentage)is pre-set to narrow down the detecting window and selective recognition of elephants is implemented by specifying the object category available in the dataset. The COCO library dataset is highly useful in such a situation.It already contains 91 object categories including elephants. Thus by specifying the label name "Elephant" in the object fetching method we can focus detection only towards elephants.The detected object is seen inside a coloured box enclosing the perimeter of the detected object with corresponding label and confidence percentage [16].
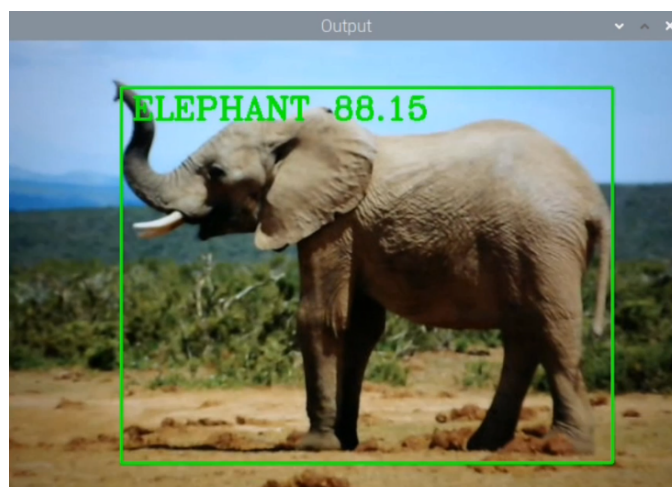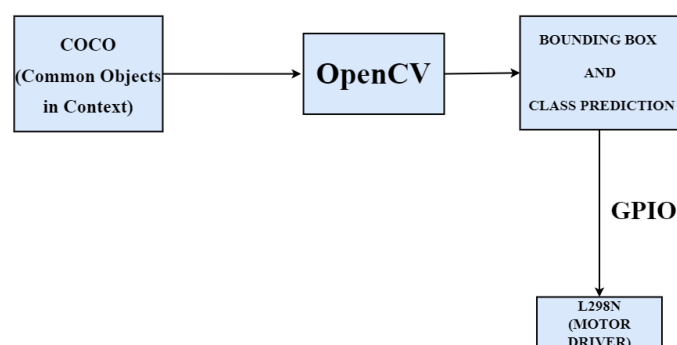


Fig.6. Detected Animal as seen in Raspberry

### D. GPIO control

The output from the image detection is linked to the hardware using GPIO control [3].GPIO(General Purpose input/output) .It is an uncommitted digital pin available in the Raspberry Pi board that can be programmed by the user for specific purposes. Here we utilize this pin to send a motor signal to the motor driver to stop the robot on detection of an elephant.This signal provides the the robot with instructions to stop until further commands are received.When the surroundings are deemed clear through the camera the robot is given a green signal to continue its subsequent movement.

## VIII. App Development

As an added feature an android application was developed to assist and enhance the performance of the proposed system. The android application provides adequate details regarding



Fig.5. Animal Detection flowchart

the cracks found and also lists the various factors that are found during its routine travel through the rails. Some of the major features which judge the crack and the protection of the track include proximity, IR value,Temperature around and the change in the accelerometer values.Software used in the process was Android Studio and Realtime Firebase was also used for database management.
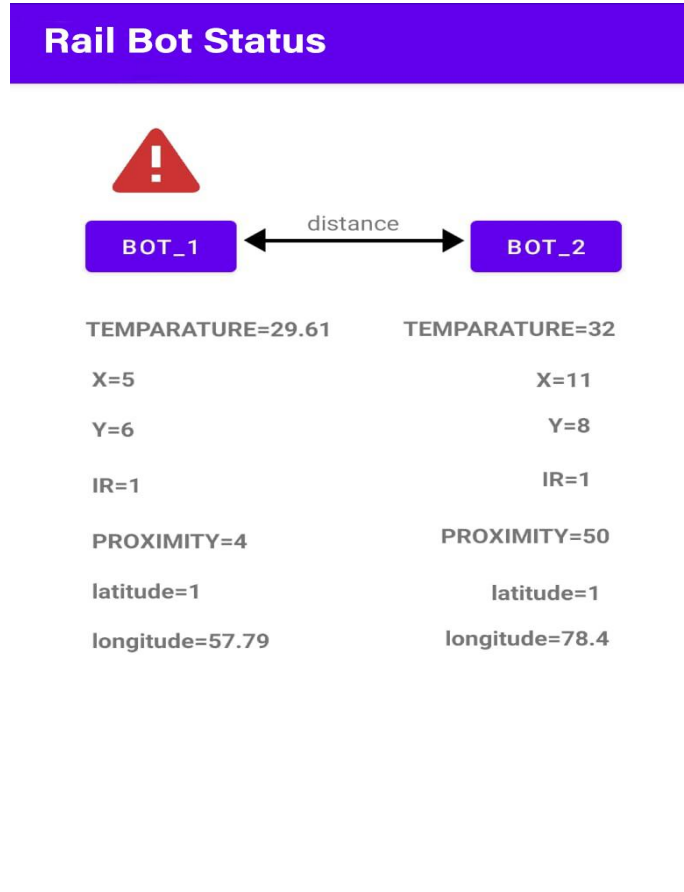
## Rail Bot Status



Fig.7. Mobile application indicating detected crack

An Android application is developed to alert the officials and the concerned individuals regarding the emergency condition that has to be addressed fast. The developed app gives the provision to know the different values of the sensors which include an IR sensor, a combined sensor module of Temperature and Accelerometer called MPU 6050, and a GPS module. The app gives an alert alarm and a warning image as the sudden response to cracks or any other obstacle encountered by the bot during their routine crack detection check-up. It consists of a parallel display providing a side-by-side view of the status of each bot. The app also consists of the two buttons named BOT_1 and BOT_2 which once clicked will lead to the live location of the robot where they are present. The approximate distance between the two

robots will be displayed between the two buttons. This app is basically an interface that helps the authorities to know when to start the accident prevention steps. Basically, this app provides full-fledged access to know all the details regarding the robot including their nearest distance. The alarm system in the application causes a sudden alert throughout and constantly rings until an immediate step is taken. This app will be provided only to the Railway Authority officers as there are high chances of this app getting misused. The distance between the coordinates namely Latitude and the Longitudes are calculated using the Haversine formula. When one robot is getting tampered with or derailed, then the nearest robot will come to assist the damaged robot. The nearest distance is hence calculated with the help of the haversine formula.
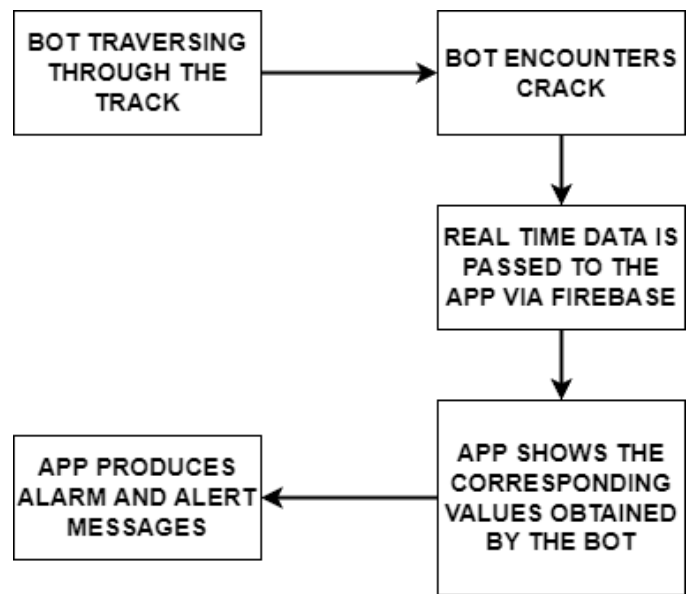


Fig.8. Mobile app dataflow

## IX. RETRACTION MECHANISM

Since our agents are moving on the tracks, when a train comes there will be a feasibility issue. To overcome this we will be placing a NRF24L01 module in the train with a low power mode configuration through Arduino Nano board. Which will be powered through the batteries of the train itself. It will generate a signal of radius 1Km, and whenever this signal comes in the proximity range of our agents, our agents are equipped with a retraction mechanism on its wheels to go under the cavity present in between the track. It is a Servo controlled mechanism and it will be triggered whenever a train comes into the proximity range of our agents which is 2Km, and resets itself when the train leaves its proximity range.
As shown in the figures 2.1 and 2.2, each wheel in our agents is connected through a hinge which is capable of retracting the wheels off from the track and leaving space for the train to cross above its current position.

## X. RESULT

The proposed model was successfully integrated and the prototype was tested on a simulated environment of railway tracks. The components in the bot are HC-SR04 Ultrasonic Sensor having a maximum range of 10 meters, IR Proximity sensor having a range of 5cm, Arduino Uno, BO2 Motors for wheel and for controlling the motors L298D is used, MPU6050 is used as accelerometer as well as temperature sensor, lithium-ion battery is used for powering the bot.The data was successfully transmitted to nearby agents, base stations and the android application whenever an agent detected an anomaly.The animal detection system showed satisfactory response to vulnerable conditions by promptly stopping the robot in its tracks.
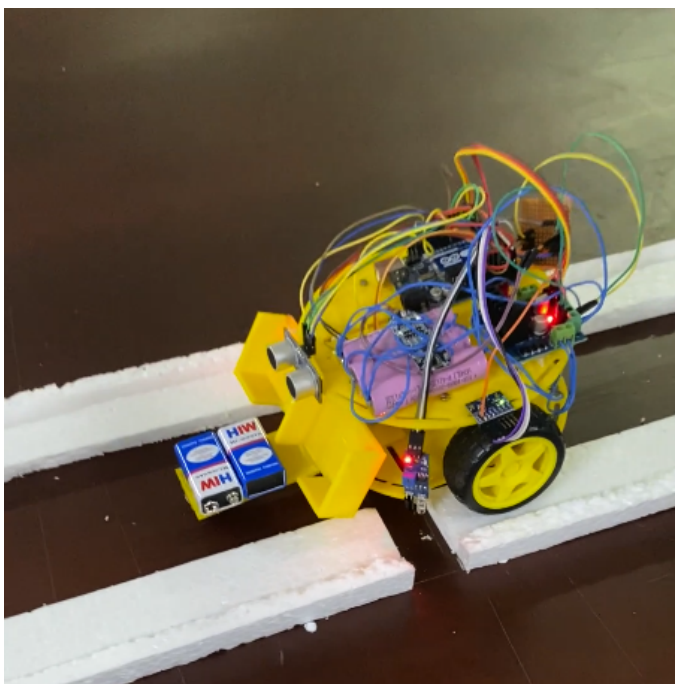


Fig.9. Prototype model on model tracks

## XI. CONCLUSION AND FUTURE SCOPE

The prototype was successfully run on the simulated railway tracks and the results suggest that the final model can be successfully run on the actual railway track along with the implementation of auto-detachment feature from the track feature. The trains will be set up with proximity sensors and using the geo-location of the trains, when the train is within a proximity threshold distance, the agent proceeds to detach itself off the tracks onto the surface of the tracks. The agent uses actuators to lift itself off the track, then scissor hinges flips the wheels inside the tracks and the actuator proceeds to

rest the agent onto the base of the tracks. The agent then lifts back up and places itself back onto the track when the train leaves the proximity threshold region. The integration of the Indian railway database with the model can make the project extendable across the railway network of the country. With access to geo-location of trains and the thermal expansion tracks along with the train timings and delays, the efficiency of the model can be increased exponentially.The communication among the entities can be made more safe and secure using Named Data Networking as traditional IP Architecture faces several challenges to maintain stable connection in dynamic environment.[20]

## REFERENCES

[1] M. Yogeswaran, S. G. Ponnambalam and G. Kanagaraj, "Reinforcement learning in swarm-robotics for multi-agent foraging-task domain," 2013 IEEE Symposium on Swarm Intelligence (SIS), 2013, pp. 15-21, doi: 10.1109/SIS.2013.6615154.

[2] Dingqing Li, Stephen Wilk, Recent studies on railway-track substructure at TTCI, Transportation Safety and Environment, Volume 3, Issue 1, April 2021, Pages 36–49, https://doi.org/10.1093/tse/tdaa031

[3] Sun, Jiankun & Yang, Jun & Zheng, Wei Xing & Li, Shihua. (2016). GPIO-Based Robust Control of Nonlinear Uncertain Systems under Time-Varying Disturbance with Application to DC-DC Converter. IEEE Transactions on Circuits and Systems II: Express Briefs. 63. 1-1. 10.1109/TCSII.2016.2548298.

[4] X. Li et al., "COCO-CN for Cross-Lingual Image Tagging, Captioning, and Retrieval," in IEEE Transactions on Multimedia, vol. 21, no. 9, pp. 2347-2360, Sept. 2019, doi: 10.1109/TMM.2019.2896494

[5] L. Yang, J. Yu, S. Yang, B. Wang, B. J. Nelson and L. Zhang, "A Survey on Swarm Microrobotics," in IEEE Transactions on Robotics, vol. 38, no. 3, pp. 1531-1551, June 2022, doi: 10.1109/TRO.2021.3111788.

[6] Guo, Hongliang and Yan Meng. "Dynamic correlation matrix based multi-Q learning for a multi-robot system." 2008 IEEE/RSJ International Conference on Intelligent Robots and Systems (2008): 840-845.

[7] X. Jiang and S. Wang, "Railway Panorama: A Fast Inspection Method for High-Speed Railway Infrastructure Monitoring," in IEEE Access, vol. 9, pp. 150889-150902, 2021, doi: 10.1109/ACCESS.2021.3125645.

[8] M. Molodova, Z. Li, A. Núñez and R. Dollevoet, "Automatic Detection of Squats in Railway Infrastructure," in IEEE Transactions on Intelligent Transportation Systems, vol. 15, no. 5, pp. 1980-1990, Oct. 2014, doi: 10.1109/TITS.2014.2307955.

[9] Y. Sun, Q. Zhang, Z. Yuan, Y. Gao and S. Ding, "Quantitative Analysis of Human Error Probability in High-Speed Railway Dispatching Tasks," in IEEE Access, vol. 8, pp. 56253-56266, 2020, doi: 10.1109/ACCESS.2020.2981763.

[10] H. Alawad, S. Kaewunruen and M. An, "Learning From Accidents: Machine Learning for Safety at Railway Stations," in IEEE Access, vol. 8, pp. 633-648, 2020, doi: 10.1109/ACCESS.2019.2962072

[11] D. Turner, A. Lucieer and L. Wallace, "Direct Georeferencing of Ultrahigh-Resolution UAV Imagery," in IEEE Transactions on Geoscience and Remote Sensing, vol. 52, no. 5, pp. 2738-2745, May 2014, doi: 10.1109/TGRS.2013.2265295.

[12] Y. Wu, H. Zhang, Y. Li, Y. Yang and D. Yuan, "Video Object Detection Guided by Object Blur Evaluation," in IEEE Access, vol. 8, pp. 208554-208565, 2020, doi: 10.1109/ACCESS.2020.3038913.

[13] A. Karra, B. Kondi and R. Jayaraman, "Implementation of Wireless Communication to Transfer Temperature and Humidity Monitoring Data using Arduino Uno," 2020 International Conference on Communication and Signal Processing (ICCSP), 2020, pp. 1101-1105, doi: 10.1109/ICCSP48568.2020.9182139.

[14] P. Christ, B. Neuwinger, F. Werner and U. Rückert, "Performance analysis of the nRF24L01 ultra-low-power transceiver in a

multi-transmitter and multi-receiver scenario," *SENSORS, 2011 IEEE,* 2011, pp. 1205-1208, doi: 10.1109/ICSENS.2011.6127100.

[15] J. K. Suhr, J. Jang, D. Min and H. G. Jung, "Sensor Fusion-Based Low-Cost Vehicle Localization System for Complex Urban Environments," in IEEE Transactions on Intelligent Transportation Systems, vol. 18, no. 5, pp. 1078-1086, May 2017, doi: 10.1109/TITS.2016.2595618.

[16] P. Tang, C. Wang, X. Wang, W. Liu, W. Zeng and J. Wang, "Object Detection in Videos by High Quality Object Linking," in IEEE Transactions on Pattern Analysis and Machine Intelligence, vol. 42, no. 5, pp. 1272-1278, 1 May 2020, doi: 10.1109/TPAMI.2019.2910529.

[17] X. Chen and P. Yu, "Research on hierarchical mobile wireless sensor network architecture with mobile sensor nodes," 2010 3rd International Conference on Biomedical Engineering and Informatics, 2010, pp. 2863-2867, doi: 10.1109/BMEI.2010.5639549.

[18] Tesfamikael, H. H., Fray, A., Mengsteab, I., Semere, A. & Amanuel, Z. (2021). Construction of Mathematical Model of DC Servo Motor Mechanism with PID controller for Electric Wheel Chair Arrangement. Journal of Electronics and Informatics, 3(1), 49-60. doi:10.36548/jei.2021.1.005

[19] Tesfamikael, Hadish Habte, Adam Fray, Israel Mengsteab, Adonay Semere and Zebib Amanuel. "Simulation of Eye Tracking Control based Electric Wheelchair Construction by Image Segmentation Algorithm." (2021).

[20] R. Paul and M. P. Selvan, "A Study On Naming and Caching in Named Data Networking," 2021 Fifth International Conference on I-SMAC (IoT in Social, Mobile, Analytics and Cloud) (I-SMAC), 2021, pp. 1387-1395, doi: 10.1109/I-SMAC52330.2021.9640947.

**IEEE *Xplore*®**    Browse ⌄    My Settings ⌄    Help ⌄    **Institutional Sign In**    ◈IEEE

All ▼    [              ] 🔍

ADVANCED SEARCH

# Malware Image Classification using VGG16

**Publisher: IEEE**   [ Cite This ]   [ 📄 PDF ]

K Deepa◄  Dept Of Computer Science, SCMS School Of Engineering &Technology, VidyaNagar, Ernakulam, Palissery  Authors

**2** Cites in Papers    **248** Full Text Views

Ⓡ   <   ©   📁   🔔

**Need Full-Text** access to IEEE *Xplore* for your organization?

**CONTACT IEEE TO SUBSCRIBE ▸**

**Abstract**

**Abstract:**

set used here is the "Mailing" dataset, which contains a pictorial representation of well-known malware families. This paper proposes a methodology for identifying malware images and classifying them into various families. The classification is based on image features. The features are extracted using the pre-trained model namely VGG16. The samples of malware are depicted as byteplot grayscale images. Features are extracted employing the convolutional layer of a VGG16 deep learning network, which uses ImageNet dataset for the pre-training step. The features are used to train different classifiers which employ SVM, XGBoost, DNN and Random Forest for the classification task into different malware families. Using 9339 samples from 25 different malware families, we performed experimental evaluations and demonstrate that our approach is effective in identifying malware families with high accuracy.

II. Related Work

III. Proposed System

IV. Experiments and Results

V. Conclusion

Authors

Figures

References

Citations

Keywords

Metrics

**Published in:** 2022 International Conference on Computing, Communication, Security and Intelligent Systems (IC3SIS)

**Date of Conference:** 23-25 June 2022    **DOI:** 10.1109/IC3SIS54991.2022.9885587

**Date Added to IEEE *Xplore*:** 15 September 2022    **Publisher:** IEEE

**Conference Location:** Kochi, India

▼ **ISBN Information:**

Electronic ISBN:978-1-6654-6883-1

Conferences > 2022 International Conference... ❓

# Attendance Management System Using Facial Recognition

**Publisher: IEEE**    [ Cite This ]    [ 🗎 PDF ]

P Sarath Krishnan ; Athira Manikuttan    **All Authors**

| **1** | **182** |
|---|---|
| Cites in Paper | Full Text Views |

Ⓡ    ⌘    ©    📁    🔔

## Abstract

**Abstract:**

---

**Abstract**

**Document Sections**

I. Introduction

II. Related Works

III. Work Description

4. Results

5. Future Scope

Show Full Outline ▾

Authors

Figures

References

Citations

Keywords

**Abstract:**

In a classroom, keeping track of attendance is a difficult and time-consuming task. Here comes the importance of automated techniques for attendance marking. Facial recognition is necessary for automated attendance tracking methods. This suggested study uses face detection algorithms to provide an attendance marking system. The primary goals of this endeavor are to accurately record attendance and speed up the procedure. This lessens peoples' workloads as well. This Proposed system is implemented using 4 Steps such as Finding all faces, Posing and working faces, Encoding faces, Finding the person's name from the encoding

**Published in:** 2022 International Conference on Computing, Communication, Security and Intelligent Systems (IC3SIS)

**Date of Conference:** 23-25 June 2022

**Date Added to IEEE *Xplore*:** 15 September 2022

**DOI:** 10.1109/IC3SIS54991.2022.9885693

**Publisher:** IEEE

**Conference Location:** Kochi, India

▼ ISBN Information:

Electronic ISBN:978-1-6654-6883-1

Print on Demand(PoD)

Feedback

← → C 🔒 https://ieeexplore.ieee.org/document/9885425 ☆ ⬇ Ⓟ ⋮

IEEE.org | IEEE *Xplore* | IEEE SA | IEEE Spectrum | More Sites     Subscribe     Donate | Cart | Create Account | Personal Sign In

**IEEE** *Xplore®*     Browse ⌄   My Settings ⌄   Help ⌄   **Institutional Sign In**     ◈**IEEE**

All ⌄  [                    ] 🔍

ADVANCED SEARCH

# Personality Prediction using Machine Learning

**Publisher: IEEE**   [ Cite This ]   📄 **PDF**

Hima Vijay ; Neenu Sebastian   **All Authors**

Department of Computer Application, SCMS School of Engineering & Technology, Vidya Nagar, Karukutty, Ernakulam

4
Cite
Pap

**Need Full-Text** access to IEEE *Xplore* for your organization?

**CONTACT IEEE TO SUBSCRIBE >**

---

**Abstract**

**Document Sections**

I. Introduction

II. Proposed System

II. K-Means Clustering Algorithm

III. Datasets

IV. Results

Show Full Outline ▾

Authors

Figures

References

Citations

Keywords

**Abstract:**

This paper uses the k-means clustering machine learning technique to classify people's personalities. Several prior studies have attempted to estimate a person's personality type automatically. One of the most important applications of machine learning algorithms is to distinguish individuals based on their personality types. There are many benefits to classifying people according to their categories. Identifying one's personality can contribute a lot in today's world with great opportunities. Each individual can choose their career or other interests based on these predictions. In present world many organizations rely on these personality predictions while shortlisting candidates as this increase the efficiency of the work because the person is working in what he is good at than what he is forced to do. The project classifies personalities using K-means clustering algorithms and big five model.

**Published in:** 2022 International Conference on Computing, Communication, Security and Intelligent Systems (IC3SIS)

**Date of Conference:** 23-25 June 2022     **DOI:** 10.1109/IC3SIS54991.2022.9885425

**Date Added to IEEE *Xplore*:** 15 September 2022     **Publisher:** IEEE

**Conference Location:** Kochi, India

▾ **ISBN Information:**

Electronic ISBN: 978-1-6654-6883-1

# Sentence Similarity - A State of Art Approaches

Nora Raju T [*], Rahana P A [†], Raichel Moncy [‡], Sreedarsana Ajay [§], Sindhya K Nambiar [¶]
Department of Computer Science
SCMS School of Engineering and Technology
Ernakulam, Kerala, India
Email: [*]noraraju361@gmail.com, [†]rahanarazak66@gmail.com, [‡]raichelmoncy2002@gmail.com,
[§]sreedarsana101@gmail.com, [¶]sindhya@scmsgroup.org

*Abstract*—This paper draws up a summary of the different approaches to sentence similarity methods. Sentence similarity has a important place in different applications of natural language processing. Plagiarism check, question answering, information retrieval, text summarization, text classification are some of the natural language processes where sentence similarity finds its applications. The existing works on text similarity have been discussed by approaching through 3 methods: String-based, Knowledge-based, and Corpus-based similarity. Relatedness between short texts is measured by each approach based on a specific perspective. Moreover, the introduction of datasets that are mostly used as benchmarks for the evaluation of techniques in this field provides an absolute view on this issue. Better results are obtained when approaches that combine more than one perspective are used.

*Index Terms*—Semantic Similarity, Lexical similarity, Plagiarism, word embedding, jaccard similarity, cosine similarity

## I. INTRODUCTION

Amidst the evolution of the digital world, the internet has become the ultimate information hub. New data keeps getting added on a regular account. Moreover, the addition of all human languages and the digitalization of all data calls for the need for sentence similarity.

Sentence similarity is how we measure the similarities between sentences. This has become a major need to avoid the unnecessary addition of data and plagiarism. This can be better understood when we have to search the internet for information. That is, suppose we have to search for a better diet plan. This can be done in several ways. We can either search for 'Diet plans' or 'What to eat for a healthier lifestyle'. Both of these questions must yield similar answers. Another application might be, when data is added to the internet that is already there, which becomes unwanted. This causes a lot of memory wastage. Hence sentence similarity becomes an unavoidable aspect of natural language processing.

Sentence similarity could be checked through two different methods. The first method is through lexical similarity. And the second method is through semantic similarity. Lexical similarity is when you treat a sentence as a series of characters and check for its similarity. While in semantic similarity you go for the general meaning of sentences.

Semantic similarity also has three major approaches. The first is corpus-based sentence similarity, where the data is analyzed by breaking it into a big corpus. This might include checking for common word order similarity and second-order co-occurrence. The second approach is knowledge-based

sentence similarity, which makes use of the semantic net. The most commonly used semantic net is WordNet, providing a series of English nouns, adverbs, adjectives, and verbs put together semantically to make a word definition. The third approach is the string-based similarity method.

This review paper provides the reader with particulars about the various techniques that came to be in place to measure the similarities between sentences. The rest of this paper discusses the variety of methods as follows. Section II gives a rundown on sentence similarity and the methods used to measure sentence similarity. The paper is then concluded in section III.

## II. SENTENCE SIMILARITY

With the immense amount of reliance that has been placed upon the internet, natural language processing applications have become a vitality. A humongous data quantity needs to be added to the internet every day. And natural language processes have helped to do so without any strain. Sentence similarity is a pivotal element that makes up natural language processes. Whether it be text summarization or checking for plagiarism, sentence similarity helps us with it. New and improved methods have been developed to check the similarity between sentences to whole paragraphs of textual data. The following part of this paper discusses methods and techniques that have been in place to perform sentence similarity.

The types of sentence similarities have been divided into two:
i. Lexical similarity and
ii. Sentence similarity

Lexical similarity compares the two strings on the equality of characters and number of times word occurs, whereas in semantic similarity the general meaning of the two sentences is taken. Below we go into the methods used for lexical similarity and semantic similarity.

### A. Types of sentence similarity

*1) Lexical Similarity:* In lexical similarity, each sentence or word is treated as a set of characters. Measuring similarity would mean checking the similarity of a sentence character by character or statement matching.

Lexical similarity gives the similarity degree between more than one sentences in the same or distinct languages. The result yielded by checking lexical similarity can be between 0 and 1 or in percentage. If the result yielded is found to be 1 or 100

percent, this means that there was a 100 percent overlap in vocabulary. While if the result yielded is 0, it simply means that there are no repeated words or sequence of characters between the two textual inputs.

The lexical similarities between any two languages can also be checked. For example, English and French have a lexical similarity of about 25 percent (0.25); meanwhile, Spanish and Portuguese have a lexical similarity of about 86 percent (0.86). Usually, this means that languages with a lexical similarity above 85 percent (0.85) are more likely to be dialects.

Lexical similarity is less ideal than semantic similarity since semantic similarity provides a more thorough check for similarity as it compares the meanings of the sentences.

*2) Semantic Similarity:* Semantic Similarity, or Semantic Textual Similarity, deals within the scope of Natural Language Processing. Semantic similarity is a metric defined among texts or documents. Semantic Similarity between two parts of text measures how close their meaning is. This is common in Natural Language Processing and linguistic fields. It gets involved in applications for informatics sciences.

Different types of semantic similarities are as follows:

- Corpus-Based Similarity
- Knowledge-Based Similarity
- String-Based Similarity

STRING-BASED SIMILARITY String-based similarity checks comparability between two strings. It works on string sequence and also character composition. The similarity of the two strings is calculated by the distance between texts. The classification of String-based similarity are

- Character Based Similarity
- Term Based Similarity

1) Character-Based Similarity

- Longest Common Substring(LCS): It's to find the lengthy string among substring of two or more strings.
- Damerau-Levenshtein: It measure dissimilarity between two different strings by computing the least number of operations from a set of operations which converts a string to another string.
- Jaro: It finds similarity between two strings among common characters. The value ranges from 0 to 1. The value 1 indicates the strings are equal and the value 0 indicates there is no similarity between the two strings. The formula to calculate Jaro similarity of two strings s1 and s2 is given by

$$sim = \left\{ \frac{1}{3}\left( \frac{m}{|s_1|} + \frac{m}{|s_2|} + \frac{m-t}{m} \right) \right. \tag{1}$$

where:

  – $|s_i|$ is the length of the respective string
  – $m$ is the number of matching characters
  – $t$ is the number of transpositions

The two characters of s1 and s2 are considered to be matching if and only if they are the same and not greater than

$$\left\lceil \frac{max(|s_1|, |s_2|)}{2} \right\rceil$$

characters.

- Jaro-Wrinkler: It is used to compare smaller strings like words and names.
  If there are two strings s1 and s2, the Jaro-Winkler similarity is given by

$$sim_w = sim_j + lp(1 - sim_j), \tag{2}$$

  where:

  – $sim_j$ is the Jaro similarity
  – $l$ is the length
  – $p$ is a constant scaling factor

- Needleman-Wunsch: It helps to compare biological sequences.It is to align protein or nucleotide sequences.
- Smith-Waterman: It will perform local sequence alignment. It is to determine common regions among the two.
- N-gram: In a continuous sequence of words we can determine the similarity of subsequences of n items from a text.

2) Term-Based Similarity

- Block distance: It calculates the distance travelled to get a point in a road grid.
- Cosine Similarity: It determines the similarity between two vectors by computing the cosine of angle connecting the pair of vectors.
- Dice's Coefficient: It is double the number of similar words in strings compared divided by the complete number of terms in the pair strings.
  The formula to find the dice's coefficient is as follows:

$$d_{Dice}(s1, s2) = 1 - \left( \frac{2|s1 \cap s2|}{|s1| + |s2|} \right) \tag{3}$$

- Euclidean distance: It is the square root of the sum of differences of squares among correlated components of two vectors.
  The formula is written as:

$$d(x, y) = \sqrt{\sum_{k=1}^{n} (x_k - y_k)^2}$$

where x and y are the two vectors.

3) Jaccard similarity: It is calculated by the quantity of divided expression over union among all the terms in both strings.

The formula to calculate the Jaccard coefficient of two variables A and B is given as:

$$J(A, B) = \frac{|A \cap B|}{|A \cup B|} \quad (5)$$

4) Matching coefficient: It add up the number of terms that are alike.
5) Overlap coefficient: When two strings are completely matched, then one of them is a subgroup of the other string.

KNOWLEDGE-BASED SIMILARITY This similarity is mainly measured using the concept of knowledge graphs. If we consider 2 concepts as C1 and C2, considering the semantic distance between their paths with the help of a knowledge graph is the most intuitive semantic information which we could get. As the distance between the paths decreases more easily, we could find semantic similarity. Some of the ontologies used to find similarities include WordNet. WordNet uses the method of grouping the adjectives, nouns, adverbs and verbs into synonyms which are cognitive and are called synsets. WordNet is formed by the combination of a dictionary and thesaurus that forms the WordNet. The synsets are arranged in such a way that the relation between them can be extracted easily. is-a-part-of, is-a-kind-of, is-a-specific-example-of are some examples that can be seen in semantic relation. Some of the methods are:

- Ganggao Zhu, et al [13]: This paper introduces a combination of knowledge based and corpus based similarity. This method provided high performance in the form of accuracy and F score.
- Nilma Sandip Gite: The answer books can be valued mainly using a method introduced in this paper.In a server machine,the descriptive answers of the candidates are compared with the standard descriptive answers stored in that machine. Text mining is the approach on which this method mainly depends.
- Kunal Khadikar, et al [14]: This paper introduced a method used to find the copyright of documents with the help of knowledge graphs.Synonyms/phrases having the same meaning are detected which was difficult for plagiarism checking software.

CORPUS BASED SIMILARITY Corpus-based methods constitute a large number of proposed approaches in word similarity. A big corpus has to be analyzed and valuable information is extracted in this method and this is useful in determining the similarity between words according to the gained information. A large collection of spoken or written texts that can be used for language research is known as a corpus. Statistical analysis of a corpus can be done in two different ways. Latent semantic analysis and deep learning are the two different ways of statistical analysis.

1) Latent Semantic Analysis (LSA):
LSA is one of the most popular approaches to corpus-based analysis. Occurence of words that are closed in meaning, in similar pieces of text is the assumption

used in LSA. A vector, based on statistical computation is used to represent each word in LSA. Construction of a word matrix and analysing a big text is used to construct these vectors. Words and paragraphs can be represented in rows and columns respectively in this matrix. In order to reduce dimensionality the Singular Value Decomposition (SVD) can be applied. This is a well-known mathematical technique applied to LSA. Cosine similarity can be used to calculate the similarities of the words based on the constructive word vector.

2) Word Embedding:
Word Embedding: Words can be represented semantically using another method known as deep learning. In a semantic space, corpus similarity is training to find word representations. The co-occurrence of words in the corpus determines the generated word representation. Developing a model for guessing a word, provided the surrounding words is the concept behind deep learning. Learning the vector representation for words can be done. The semantic representation of words has shown good results in using deep learning methods. Word similarity can be measured using the cosine similarity between words' vectors. The semantic similarity can be found using the following word embedding models.
Word embedding models which are most widely used for finding the semantic similarity are

- Word2Vec developed by Google
- GloVe developed by Stanford
- fastText developed by Facebook

Cosine Similarity:The similarity of documents irrespective of their size, is measured by using the mathematical method known as cosine similarity. The cosine angle of the projected vectors in a three-dimensional space is measured here. The values of similarity measures range from -1 to 1. Cosine similarity is not only 1 of the best-known similarity checking methods but also a method for normalizing document length during the comparison. Since the term frequencies cannot be negative values, the cosine similarity of the 2 documents will range from 0-1.

$$similarity(A, B) = cos(\theta) = \frac{A.B}{\|A\| \times \|B\|}$$
$$= \frac{\sum_{i=1}^{n} A_i B_i}{\sqrt{\sum_{i=1}^{n} A_i^2} \sqrt{\sum_{i=1}^{n} B_i^2}} \quad (6)$$

The angle between the 2-term frequency vectors will not be greater than 90 degree.

Generalized Latent Semantic Analysis (GLSA) :
Computation of semantically motivated term and document

TABLE I
SUMMARY OF THE LITERATURE SURVEY

| Paper Title | Author(Year) | Methodology |
|---|---|---|
| Computing Semantic Relatedness using Wikipedia-based Explicit Semantic Analysis [1] | Gabrilovich E. & Markovitch, S. (2007) | Explicit Semantic Analysis (ESA)-by the cosine measure between the vector representation of two text. |
| Sentence Semantic Similarity based on Word Embedding and WordNet [2] | Mamdouh Farouk(2018) | wordssimilarity-WordNet and word embedding similarities is combined to calculate the words similarity |
| The Google Similarity Distance [3] | Cilibrasi, R.L., Vitanyi, P.M.B. (2007) | Normalized Google Distance (NGD)-by the Google search engine for a given set of keywords. |
| A Wikipediabased multilingual retrieval model [4] | . Martin, P., Benno, S. & Maik, A (2008) | The cross-language explicit semantic analysis (CLESA)-by the cosine similarity between the corresponding vector representations. |
| Generalized latent semantic analysis for term representation [5] | Matveeva, I., Levow, G., Farahat, A. and Royer, C.(2005) | Generalized Latent Semantic Analysis (GLSA)- computing semantically motivated term and document vector |
| Mining the web for synonyms: PMIIR versus LSA on TOEFL [6] | Turney, P. (2001) | Pointwise Mutual Information - Information Retrieval (PMI-IR)- for computing the similarity between pairs of words, |
| Zhu, Ganggao, and Carlos A. Iglesias. "Computing semantic similarity of concepts in knowledge graphs." IEEE Transactions on Knowledge and Data Engineering 29.1 (2016): 72-85.<br>Semantic text similarity using corpus-based word similarity and string similarity [7] | Islam, A. and Inkpen, D.(2008) | Semantic Text Similarity-combination between semantic and syntactic information |
| Second Order Cooccurrence PMI for Determining the Semantic Similarity of Words [8] | Islam, A. and Inkpen, D. (2006) | Second-order co-occurrence pointwise mutual information (SCO-PMI)- co-occur with the same neighboring words. |
| Experiments on the difference between semantic similarity and relatedness [9] | Peter, K.(2009) | Extracting DIStributionally similar words using Co-occurrences (DISCO) -simply retrieves their word vectors from the indexed data, and computes the similarity according to Lin measure |
| Plagiarism Detection across Distant Language Pairs [10] | Alberto, B. , Paolo, R., Eneko A. & Gorka L (2010) | N-gram-by dividing the number of similar n-grams by maximal number of n-grams |
| Using of jaccard coefficient for keywords similarity [11] | .Niwattanakul S, Singthongchai J, Naenudorn E, Wanapu S (2013) | jaccard distance- to measure similarity between words based on string matching |
| Assessing sentence similarity using WordNet based word similarity [12] | Liu H, Wang, Fei P(2013) | WordNet-to find word similarity |

vectors is done using this framework. The LSA approach is extended by GLSA focusing on terms of vectors. The GLSA can combine any kind of similarity measure into a suitable method using dimensional reduction. The term-document matrix which is traditional, is used in such a way that the last step provides the linear combination of term vectors. One of the advantages of term-based GLSA document representation is that it does not have the out-of-sample problem for new documents. It provides a representation for documents that reflects their general semantics. The GLSA document representation can be easily extended to contain more specific information such as the presence of proper names, dates, or numerical information.

Explicit Semantic Analysis (ESA):
Computation of semantic relatedness between two arbitrary contents is done using this measure. Using the Wikipedia-Based technique terms can be represented as high-dimensional vectors in which each vector entry presents the TF-IDF weight between the term and one Wikipedia article. The cosine measure between the corresponding vectors expresses the semantic relatedness between two terms. ESA is an

TABLE II
COMPARISON OF DIFFERENT APPROACHES OF SEMANTIC SIMILARITY

| Methodology | Principle | Measure | Feature | Advantage | Disadvantage |
|---|---|---|---|---|---|
| Path Based | Length of the path linking different word senses | Shortest Path | Number of edges between the concepts | Simple measure | Different pairs of equal length and shortest path will have same similarity |
| | | Wu & Palmer | Path length augmented by subsumer path to root | Simple Measure | Different pairs having lowest common subsume and equal length of path will have same similarity |
| | | L & C | Number of edges between the concepts | Simple Measure | Different pairs of equal length and shortest path will have same similarity |
| Information Content Based | The concepts sharing common information are similar | Resnik | Information content of the lowest common subsumer | Simple Measure | Different pairs having lowest common subsume will have same similarity |
| | | Lin | Information content of the lowest common subsumer and compared concepts | Considers the information content of compared concepts | Different pair having the same summation of information content will have same similarity |
| Feature Based | The concepts having common features are similar | Tversky | Compares features of the concepts | Considers features while computing similarity | Computationally complex |

unsupervised algorithm for feature extraction. It uses existing knowledge base concepts as features instead of the derived latent features such as singular value decomposition and latent dirichlet allocation. The area of text processing, most notably semantic relatedness, and explicit topic modelling finds a large number of applications of ESA.

Second-order co-occurrence point-wise mutual information (SCO-PMI) :

The major benefit of using SOC-PMI is the calculation of similarity between two words that does not co-occur frequently because they transpire with the same neighbouring words. This may be helpful as a tool aiding in the automatic construction of the word synonyms .

Normalized Google Distance (NGD):

It is done by measuring the number of hits returned by the Google search engine for a given number of keywords. In units of Google distance, keywords having the same meaning in a natural languages sense is considered to be 'close' while words having dissimilar meanings are considered to be farther apart. The normalized Google distance between two search terms x and y is infinite if they never occur together on the same web-page but occur separately. The NGD of two terms is zero or identical to the coefficient of x squared and y squared, if both terms always occur together.

Extracting DIStributionally similar words using COoccurrences (DISCO) :

For a given word, DISCO returns the second-order word vector, if the required word is the foremost distributionally similar one. The 2 major similarity measures are DISCO1 and DISCO2. DISCO1 computes, the primary order similarity between the 2 input words supported by their collocation set. The second-order similarity between the 2 input words is supported by a set of distributionally similar words.
The summary of various approaches is provided in tableI

## III. COMPARISON OF DIFFERENT SEMANTIC SIMILARITY MEASURES

The table II shows the review of various approaches of semantic similarity.Table 1 shows the research approaches taken to address the issue of semantic similarity from 2005 to the present year. The method adopted by Alberto[10] was the most common approach taken to solve the issue semantic similarity. He introduced the method of N-gram-by dividing the number of similar n-grams by maximal number of n-grams. Though this method could achieve high accuracy, the computational speed/time was exeptionally high. Thus in future, this method could be optimized to achieve a better complexity value.

## IV. CONCLUSION

In short finding the sentence similarity has proved to be crucial part of all Natural Language Processing Applications. In

this paper, we have discussed all the major methods to measure sentence similarity, by approaching the methods through two techniques. One is by the lexical method of approach and the other by the semantic aproach. Semantic similarity has been discussed in depth since it is the most used technique so far. All important data regarding sentence similarity that plays a major role in Natural Language Processing methods has been discussed.

## REFERENCES

[1] Gabrilovich, Evgeniy, and Shaul Markovitch. "Computing semantic relatedness using Wikipedia-based explicit semantic analysis." IJcAI. Vol. 7. 2007.

[2] Farouk, Mamdouh. "Sentence semantic similarity based on word embedding and wordnet." 2018 13th International Conference on Computer Engineering and Systems (ICCES). IEEE, 2018.

[3] Cilibrasi, Rudi L., and Paul MB Vitanyi. "The google similarity distance." IEEE Transactions on knowledge and data engineering 19.3 (2007): 370-383.

[4] Potthast, Martin, Benno Stein, and Maik Anderka. "A wikipedia-based multilingual retrieval model." European conference on information retrieval. Springer, Berlin, Heidelberg, 2008.

[5] Matveeva, Irina, et al. "Generalized latent semantic analysis for term representation." Proc. of RANLP. 2005.

[6] Turney, Peter D. "Mining the web for synonyms: PMI-IR versus LSA on TOEFL." European conference on machine learning. Springer, Berlin, Heidelberg, 2001.

[7] Islam, Aminul, and Diana Inkpen. "Semantic text similarity using corpus-based word similarity and string similarity." ACM Transactions on Knowledge Discovery from Data (TKDD) 2.2 (2008): 1-25.

[8] Islam, Aminul, and Diana Inkpen. "Second order co-occurrence PMI for determining the semantic similarity of words." Proceedings of the Fifth International Conference on Language Resources and Evaluation (LREC'06). 2006.

[9] Kolb, Peter. "Experiments on the difference between semantic similarity and relatedness." Proceedings of the 17th Nordic conference of computational linguistics (NODALIDA 2009). 2009.

[10] Barrón-Cedeno, Alberto, et al. "Plagiarism detection across distant language pairs." Proceedings of the 23rd International Conference on Computational Linguistics (Coling 2010). 2010.

[11] Niwattanakul, Suphakit, et al. "Using of Jaccard coefficient for keywords similarity." Proceedings of the international multiconference of engineers and computer scientists. Vol. 1. No. 6. 2013.

[12] Liu, Hongzhe, and Pengfei Wang. "Assessing Sentence Similarity Using WordNet based Word Similarity." J. Softw. 8.6 (2013): 1451-1458.

[13] Zhu, Ganggao, and Carlos A. Iglesias. "Computing semantic similarity of concepts in knowledge graphs." IEEE Transactions on Knowledge and Data Engineering 29.1 (2016): 72-85.

[14] K. Khadilkar, S. Kulkarni and P. Bone, "Plagiarism Detection Using Semantic Knowledge Graphs," 2018 Fourth International Conference on Computing Communication Control and Automation (ICCUBEA), 2018, pp. 1-6, doi: 10.1109/ICCUBEA.2018.8697404.

**IEEE** *Xplore*®

Browse ∨    My Settings ∨    Help ∨    Institutional Sign In

◆IEEE

All ▾    [search]    🔍

ADVANCED SEARCH

Conferences > 2022 International Conference... ❓

# Speech Emotion Recognition Using Bagged Support Vector Machines

Cite This    📄 PDF

Bini Omman
Department of computer science and engineering, SCMS School of Engineering and Technology, Ernakulam, India

**131**
Full
Text Views

Back to Results | Next >

---

← → C 🔒 https://ieeexplore.ieee.org/document/9885578    ☆ ⬇ P ⋮

II. Related Works

III. System Overview

IV. Experimental
Setup

V. Results

Show Full Outline ▾

Authors

Figures

References

Keywords

Metrics

used is difficult to build and train using HMM and neural networks,Low detection accuracy,High computational power and time.In this work we executed emotion category on corpora — the berlin emodb, and the ryerson audio-visible database of emotional speech and track (Ravdess). A mixture of spectral capabilities was extracted from them which changed into further processed and reduced to the specified function set. When compared to single estimators, ensemble learning has been shown to provide superior overall performance. We endorse a bagged ensemble model which consist of support vector machines with a gaussian kernel as a possible set of rules for the hassle handy. Inside the paper, ensemble studying algorithms constitute a dominant and state-of-the-art approach for acquiring maximum overall performance.

All ▼   [  ]  🔍

ADVANCED SEARCH

Conferences  >  2022 International Conference...  ❓

Back to Results

# A comparitative study of machine learning models for the detection of Phishing Websites

**Publisher: IEEE**   Cite This   🗎 PDF

Josna Philomina ◄  Glory Elizabeth Elias ;  Abhinaya A Menon   **All Authors**

Computer Science and Engineering SCMS School Of Engineering And Technology, Ernakulam, India

**2** Cites in Papers

**107** Full Text Views

Ⓡ  🔗  ©  📁  🔔

---

https://ieeexplore.ieee.org/document/9885595

V. Conclusion

learning, are discussed in this study.In this light, the study's major goal is to propose a unique, robust ensemble machine learning model architecture that gives the highest prediction accuracy with the lowest error rate, while also recommending a few alternative robust machine learning models.Finally, the Random forest algorithm attained a maximum accuracy of 96.454 percent. But by implementing a hybrid model including the 3 classifiers- Decision Trees,Random forest, Gradient boosting classifiers, the accuracy increases to 98.4 percent.

Authors

Figures

References

Citations

Keywords

Metrics

I. Introduction

RESEARCH-ARTICLE

# Multi-Domain Network Traffic Analysis using Machine Learning and Deep Learning Techniques

Authors: Dincy Arikkat, Rafidha Rehiman K A, Vinod, Suleiman Y. Yerima, Manoja, Pooja, Shilpa Sekhar, Sohan James,

Josna Philomina

SCMS School Of Engineering And Technology, India

View Profile

---

ACM DIGITAL LIBRARY

## ABSTRACT

Recent heterogeneous computing facilities and data explosion introduce challenges in network traffic analysis and demand intelligence-based approaches to ensure cyber security and the protection of online digital services. Researchers have been proposing various machine and deep learning approaches for network traffic analysis in different problem domains. However, it is also crucial to understand how these algorithms perform across the different domains. Hence in this research work we extend an analysis of diverse machine learning and deep learning techniques across three different problem domains: DDoS attack detection, Malicious URL detection and Tor traffic classification. We employ three publicly available datasets to train eight different machine learning and six deep learning models for both multi-class and binary classification in our comparative study. Our experiments show that Random Forest achieved superior performance compared to other machine learning models with F-measure of 92% for multi-class traffic classification and 100% for binary classification problems. For the deep learning models, Autoencoder with Random Forest achieved superior performance with an F-measure of 89% and 100% for multi-class and binary problems respectively.

# Performance of Hybrid Satellite-UAV NOMA Systems

Christina Gamal [1], Kang An [2], Xingwang Li [3], Varun G. Menon [4], Ragesh G. K. [5],
Mostafa M. Fouda [6], Basem M. ElHalawany [1,*]

[1]Faculty of Engineering at Shoubra, Benha University, Egypt
[2]Sixty-third Research Institute, National University of Defense Technology, Nanjing, China
[3]Physics and Electronic Information Engineering, Henan Polytechnic University, China
[4]SCMS School of Engineering and Technology, Ernakulam 683576, India
[5]Indian Institute of Information Technology Kottayam, India
[6]Department of Electrical and Computer Engineering, Idaho State University, Pocatello, ID, USA
*Corresponding Author, Email: basem.mamdoh@feng.bu.edu.eg

*Abstract*—**This paper investigates the performance of non-orthogonal multiple access (NOMA) based hybrid satellite-unmanned aerial vehicle (UAV) systems, where a low Earth orbit (LEO) satellite communicates with the ground users via a decode and forward (DF) UAV relay. We investigate a two NOMA users system, where a far user (FU) and a near user (NU) are served by the UAV which is located at a certain height above the origin of the coverage circle. The channel between satellite and UAV is assumed to follow a Shadowed-Rician fading and the channels between UAV and users are assumed to follow a Nakagami-m fading. New closed-form expressions of the outage probabilities for the two users and the system are derived. Different from other work in literature, we take into consideration different parameters affecting the total link budget. Additionally, we propose an algorithm for minimizing the system outage probability. The mathematical analysis is verified by extensive representative Monte-Carlo (MC) simulations. Finally, simulations are provided to demonstrate the impact of important parameters on the considered system as well as the superiority of the NOMA scheme the over reference scheme.**

*Index Terms*—**Outage Probability, Unmanned Aerial Vehicle, Satellite, Non-Orthogonal Multiple Access.**

## I. INTRODUCTION

Recently, satellite communication (SatCom) has withdrawn an increasing research interest due to the several advantages offering over conventional terrestrial communication such as wide coverage area, covering harsh and isolated geographical regions where conventional wired or wireless communication can't reach including maritime, deserts, and jungles. Moreover, SatCom serves well in disaster areas where the terrestrial networks are compromised. Additionally, SatCom can provide a wide range of flexible applications in the field of navigation, TV and Radio broadcasting services, Weather prediction and climate monitoring, Internet access, and satellite telephony [1]. On the other hand, SatCom networks face several challenges including operation cost [2], propagation delay [3], and signal degradation due to rain and atmospheric disturbances. Additionally, antenna-pointing errors angle caused by satellite perturbation or by the other side's mobility may lead to communication outage [4]. Furthermore, the line-of-sight (LOS) link may be blocked by heavy shadowing or obstacles that retard communication between the satellite and terrestrial users [5]. To combat such issues, hybrid satellite-terrestrial networks (HSTNs) based on relaying have been proposed in many literature [2], [5]–[7] to increase efficiency, and enhance the performance of the user whose direct link is unavailable or deteriorated. Satellites

can be stationed in a variety of orbits including Low Earth orbit (LEO), medium Earth orbit (MEO), highly elliptical orbit (HEO), and geosynchronous orbit (GEO) [8]. Recently, LEO satellites constellation networks have withdrawn a great interest due to their small propagation delay, high data rate, and lower transmit power [9]. Consequently, we consider a LEO satellite setup in this work.

On the other hand, unmanned aerial vehicles (UAVs) have been used as a wireless flying base station, mobile relay, or backhaul to improve the coverage, flexibility, and reliability of the network [1] in order to provide a variety of applications including reconnaissance, surveillance, disaster management, traffic control, healthcare, emergency search, military, agriculture, and communication relay [10], [11]. Thus, the combination of a UAV and a satellite has the potential to provide a technological breakthrough for communication networks due to the UAV's flexible mobility [12]–[14]. However, UAVs communication have their own challenges including limited bandwidth and limited battery [9], which mandates the exploitation of spectrum and energy efficient techniques in both transmission and mobility.

Non-orthogonal multiple access(NOMA) is one of the most promising and spectrum efficient techniques with a significant attention. NOMA improves the spectrum efficiency by serving more than one user at the same time with the same frequency resource [15], [16]. The power-domain NOMA (PD-NOMA) is the most widely used type NOMA at which a superposition of users' signals is transmitted using different power levels. However, this type of non-orthogonality causes interference at the receiver. To cope with this, successive interference cancellation (SIC) is used at the receiver to successively decode users' information one by one from the superimposing signal in the order of the received signal strength [17]. Improved spectrum efficiency, high connectivity, multiplexes many users, flexible power control method between strong and weak users, and low latency are all benefits of the NOMA scheme [18]. In contrast, the orthogonal multiple access (OMA) scheme is not the best choice to achieve the requirements for SatCom as OMA provides limit number of served users and reduced resource efficiency [4]. NOMA has been investigated for several network architectures and applications and proved to be an efficient technology [19]–[22].

To satisfy the higher throughput, low latency, higher reliability, and massive connectivity requirements of beyond fifth-generation (5G) and six-generation (6G) communications, network designers have to adopt a heterogeneous architecture that makes the best use of the advantages of different technologies [23]. This motivates researchers to investigate the performance of heterogeneous architectures of HSTN NOMA-based systems. The authors in [5] have considered the fairness issue in a NOMA-based HSTN system, where the terrestrial network acts as a cooperative relay. In [24], the NOMA-based integrated satellite-terrestrial relay networks (ISTNs) with multiple terrestrial relays was proposed, where a satellite communicates with two terrestrial users with the help of a selected relay out of multiple terrestrial relays under imperfect SIC. The performance of energy-harvesting terrestrial relay-based HSTNs network is investigated, where both amplify-and-forward (AF) [25] and decode-and-forward (DF) relay is powered from the satellite signals under NOMA transmission [2]. In [26], the authors investigated the outage probability of HSTN NOMA-based system, at which one user receives its signal directly from the satellite, while the other user relies on a multiple antenna DF relay. Further, the secrecy outage probability (SOP) of the HSTRN was investigated in [27] using physical layer security (PLS) technique in the presence of multiple eavesdroppers.

Moreover, the exploitation of aerial UAV relays is a promising direction to improve the performance of HSTRN systems. In [1], the PLS of a HSTN system with multiple mobile UAV DF relays was investigated. In [6], the authors have proposed a hybrid satellite-UAV architecture operated by a 5G non-orthogonal terrestrial network. The authors have investigated the outage probability and the asymptotic behavior where a satellite communicates with ground users with the help of a NOMA-based DF UAV relay. However, those investigations don't take into consideration the path-losses associated with satellite communication besides the antenna pointing errors [4]. This motivates researchers to investigate the performance of a practical heterogeneous HSTN NOMA system, where a UAV is used as a flying relay node. We investigate the system performance under free-space path loss and antenna pointing error, while the satellite-to-UAV and UAV-to-Terrestrial users channels undergo Shadowed-Rician and Nakagami-m fading channels, respectively. Mainly, the contributions of this work can be summarized as follows:

- We investigate the performance of a downlink NOMA-based HSTRN system that consists of a LEO satellite, DF UAV relay, and two NOMA terrestrial users. We take into consideration both small and large scale fading of satellite to UAV link under the effects of satellite beam gain, satellite antenna gain, receive antenna gain, antenna pointing error, free space loss, and noise power.
- We derive closed-form expressions for the outage probabilities (OPs) of the two users and the system OP.
- We propose an optimization algorithm that tweaks the power allocation factor to minimize the system OP.
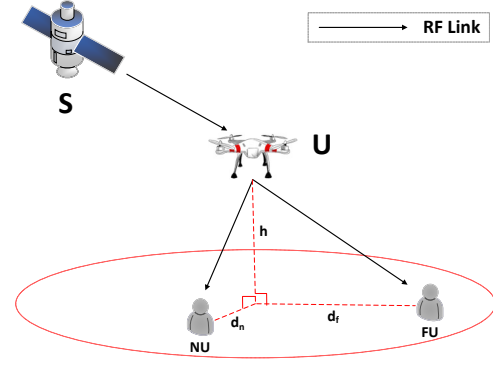- Validate the analytical derivations by extensive Monte-



Figure 1. The system model.

Carlo simulations, and then we study the impact of system parameters on the OPs. Finally, we carried out a comparison with a benchmark system.

## II. SYSTEM MODEL AND CHANNEL STATISTICS

### A. System Model

We consider a downlink Satellite scenario, at which a LEO Satellite ($S$) communicates with terrestrial NOMA users with the aid of a DF UAV ($U$) relay node deployed at a constant height $h$ from the ground, as shown in figure 1. We consider two users NOMA group, namely the far user (FU) and the near user (NU). We assume a half-duplex communication mode for all nodes, which are equipped with a single antenna. We further suppose that due to the obstruction or severe large-scale fading, direct links between the satellite and the users are unavailable, which encourages relying on the UAV as a relaying node.

Following DF relaying mechanism, $S$ transmits a superposing signal to the two NOMA users via the UAV relay. It is assumed that the NU and FU are located inside a circle while UAV is located above the origin of the circle. We assume perfect channel state information (CSI) of all links, where the S-U link, $h_s$, undergoes Shadowed Rician fading distribution, whereas the links between $U$ and ground users are subject to the Nakagami-m fading distribution. We take into consideration the free-space path loss, the receiver antenna gain, the satellite antenna gain, antenna pointing error, shadowing, and channel fading in the S-U link. Therefore, the entire link budget of the S-U link, without the small-scale fading, can be given as [28]

$$LB_s = \frac{G_s(\phi_s) \, G_u}{L_s \, L_p},  \tag{1}$$

where $G_u$ is the UAV antenna gain, and $G_s(\phi_s)$ is the beam gain and can be formulated as $G_s(\phi_s) = G_s\left(\frac{J_1(u_s)}{2u_s} + 36\frac{J_3(u_s)}{u_s^3}\right)^2$ [4] with $G_s$ denotes the satellite antenna gain, $J(.)$ denotes the Bessel function, and $u_s = 2.07123 \frac{d}{R}$ as $R$ is the radius of the coverage area, $d$ is the distance between the beam center and the UAV. $L_s$ is the free-space loss, $L_s = \frac{4\pi f_s H}{c}$, where the downlink carrier frequency at satellite is $f_s$, the height of the satellite is $H$ and the light velocity is $c$, and $L_p$ is the pointing error loss and can be given in dB as $L_p = 2.7211 \times 10^{-20} \, f_s^2 \, D_s^2 \, \theta_e^2$ [29] with $D_s$ being

the diameter of antenna aperture, and $\theta_e$ is the pointing error angle. Assuming a NOMA-based DF relaying, the end-to-end communication process from the satellite to the ground users happens in two-time slots. In the first time slot, $S$ broadcasts a superimposing signal $x_s$ to $U$, whereas $x_s = \sqrt{a_1 P_s} x_1 + \sqrt{a_2 P_s} x_2$, given that $x_1$ and $x_2$ are the signals for $FU$ and $NU$, respectively. Thus, the received signal at $U$ can be expressed as $y_{s_u} = h_s \sqrt{LB_s} x_s + n_s$, where $P_s$ is the transmit power at $S$, $a_1$ and $a_2$ denote the power allocation factors for $FU$ and $NU$, respectively, where $a_1 > a_2$ and $a_1 + a_2 = 1$. $n_s \sim \mathcal{CN}(0, \sigma_s^2)$ represents the additive white Gaussian noise (AWGN) with zero mean and variance $\sigma_s^2 = K\,T\,B$, where $K = 1.38 * 10^{-23}\ J/K$ is a Boltzmann's constant, $B$ is the noise bandwidth, and $T$ is the noise temperature. Based on the DF relaying strategy, the UAV first decodes the received signal then forwards it to the two users. So, the UAV relay decodes the signal with the high effective channel gain first then SIC is applied to decode the other signal. Thus, the received signal to interference and noise ratio (SINR) at $U$ for signal $x_1$ and $x_2$ can be written as

$$\gamma_{x_1}^U = \frac{\gamma_s\, LB_s\, a_1 |h_s|^2}{\gamma_s\, LB_s\, a_2 |h_s|^2 + 1}, \tag{2a}$$

$$\gamma_{x_2}^U = \gamma_s\, LB_s\, a_2 |h_s|^2, \tag{2b}$$

where $\gamma_s = \frac{P_s}{\sigma_s^2}$ denotes the transmit SNR at $S$, and $|h_s|^2$ is the channel power gain of satellite link that follows a shadowed Rician fading model. In the second time slot, the UAV forwards a combined version, $x_u$, of both decoded symbols to the paired users. Thus, the received signal at $FU$ and $NU$ can be expressed as $y_f = h_f \sqrt{P_f} x_u + n_f$, $y_n = h_n \sqrt{P_n} x_u + n_n$ respectively, where $x_u = \sqrt{b_1 P_u} x_1 + \sqrt{b_2 P_u} x_2$, $P_u$ is the transmit power at $U$, $h_f$ and $h_n$ are the channel gain coefficients of FU and NU, respectively. $P_n$ and $P_f$ are the path losses at $NU$ and $FU$ respectively and can be written as $\frac{\delta_l}{(\sqrt{d_i^2 + h^2})^\alpha}$, $d_i$ represents the propagation distance between the UAV and ground user, $\delta_l$ denotes the frequency dependent channel power at the reference distance of 1m, and $\alpha$ is the path-loss exponent [30]. $n_f \sim \mathcal{CN}(0, \sigma_f^2)$ and $n_n \sim \mathcal{CN}(0, \sigma_n^2)$ represent the additive white Gaussian noise (AWGN) at $FU$ and $NU$ respectively. $b_1$ and $b_2$ denote the power allocation factors for $FU$ and $NU$ respectively, where $b_1 > b_2$ and $b_1 + b_2 = 1$. Thus, the received SINR at $FU$ is:

$$\gamma_{x_1}^f = \frac{\gamma_f\, P_f\, b_1 |h_f|^2}{\gamma_f\, P_f\, b_2 |h_f|^2 + 1}, \tag{3}$$

where $\gamma_f = P_u / \sigma_f^2$ denotes the transmit SNR at $U$ to $FU$. The near user decode $FU$'s signal first then SIC is applied to get $NU$'s signal. Thus, the received SINR at $NU$ for $x_1$ and $x_2$ can be expressed as

$$\gamma_{x_1}^n = \frac{\gamma_n\, P_n\, b_1 |h_n|^2}{\gamma_n\, P_n\, b_2 |h_n|^2 + 1}, \tag{4a}$$

$$\gamma_{x_2}^n = \gamma_n\, P_n\, b_2 |h_n|^2, \tag{4b}$$

where $\gamma_n$ denotes the transmit SNR at $U$ to $NU$, and $\gamma_n = \gamma_f = \gamma_u$.

B. *Channel Statistics*

The satellite to UAV link undergoes a shadowed-Rician fading, where the probability density function (PDF) of $|h_s|^2$ is [27]:

$$f_{|h_s|^2}(x) = \alpha_s \exp\left(-\beta_s x\right) {}_1F_1\left(m_s; 1; \delta_s x\right), \tag{5}$$

where $\alpha_s = \frac{1}{2 b_s}\left(\frac{2 b_s m_s}{2 b_s m_s + \Omega_s}\right)^{m_s}$, $\beta_s = \frac{1}{2 b_s}$, and $\delta_s = \frac{\Omega_s}{2 b_s (2 b_s m_s + \Omega_s)}$. ${}_1F_1(.;.;.)$ is the confluent hypergeometric function of the first kind [31, Eq. (9.14.1)], $m_s$ denotes the fading severity parameter, $\Omega_s$ represents the average power of line-of-sight (LOS) and $2 b_s$ represents the multipath components. With the aid of equations [32, (07.20.03.0009.01)] and [33, (07.02.03.0014.01)], ${}_1F_1$ function can be expressed as

$$ {}_1F_1\left(m_s; 1; \delta_s x\right) = e^{\delta_s x} \sum_{k=0}^{m_s-1} \frac{(-1)^k (1-m_s)_k (\delta_s x)^k}{(k!)^2}, \tag{6}$$

where $(.)_n$ is the pochhammer symbol [31, p. xliii]. Let $\zeta(k) = \frac{(-1)^k (1-m_s)_k (\delta_s)^k}{(k!)^2}$. With the help of equation [31, (3.351.2)], the cumulative distribution function (CDF) of the $|h_s|^2$ is expressed as

$$F_{|h_s|^2}(x) = 1 - \alpha_s\, e^{-(\beta_s - \delta_s)x} \sum_{k=0}^{m_s-1} \zeta(k) \\ \times \sum_{l=0}^{k} \frac{k!}{l!} x^l\, (\beta_s - \delta_s)^{-(k-l+1)}. \tag{7}$$

The links between the UAV relay and the $FU$ and $NU$ are assumed to follow the Nakagami-m fading whose PDF $|h_i|^2$, $i \in \{f, n\}$ can be expressed as [34]

$$f_{|h_i|^2}(x) = \left(\frac{m_i}{\Omega_i}\right)^{m_i} \frac{x^{m_i-1}}{\Gamma(m_i)}\, e^{-\frac{m_i}{\Omega_i} x}, \tag{8}$$

and the CDF of $|h_i|^2$ is expressed as

$$F_{|h_i|^2} = 1 - e^{-\frac{m_i}{\Omega_i} x} \sum_{n=0}^{m_i-1} \left(\frac{m_i}{\Omega_i} x\right)^n \frac{1}{n!}, \tag{9}$$

where $m_i$ is the severity parameter for user i.

III. OUTAGE PROBABILITY ANALYSIS

In this section, we investigate the reliability of the proposed system, where the reliability is characterized in terms of the users and system outage probabilities (OPs). The OP is the probability that a specific SINR falls below a certain threshold value. In the following, we derive the OPs of both users and the system OP as follows:

*1) OP of NU ($OP_n$):* The OP event for NU occurs when neither the UAV nor the NU correctly decodes $x_1$ and $x_2$, which can be mathematically expressed as [6]

$$OP_n = \Pr(\min(\frac{\gamma_{x_1}^U}{\gamma_{th_f}}, \frac{\gamma_{x_2}^U}{\gamma_{th_n}}) < 1) + \\ \Pr(\min(\frac{\gamma_{x_1}^U}{\gamma_{th_f}}, \frac{\gamma_{x_2}^U}{\gamma_{th_n}}) \geq 1,\ \min(\frac{\gamma_{x_1}^n}{\gamma_{th_f}}, \frac{\gamma_{x_2}^n}{\gamma_{th_n}}) < 1) \\ = 1 - \Pr(\gamma_{x_1}^U \geq \gamma_{th_f},\ \gamma_{x_2}^U \geq \gamma_{th_n}) \\ \times \Pr(\gamma_{x_1}^n \geq \gamma_{th_f},\ \gamma_{x_2}^n \geq \gamma_{th_n}), \tag{10}$$

where $\gamma_{th_f} = 2^{2R_f} - 1$ and $\gamma_{th_n} = 2^{2R_n} - 1$ are the target SINR threshold at FU and NU, respectively. $R_f$ and $R_n$ are

the target data rates for FU and NU respectively. From (2) and (4), the $OP_n$ in (10) can be written as,

$$OP_n = 1 - \Pr(|h_s|^2 \geq \max(\frac{\gamma_{th_f}\,\omega_1}{a_1 - a_2\,\gamma_{th_f}}, \frac{\gamma_{th_n}\,\omega_1}{a_2}))$$
$$\times \Pr(|h_n|^2 \geq \max(\frac{\gamma_{th_f}\,\omega_2}{b_1 - b_2\,\gamma_{th_f}}, \frac{\gamma_{th_n}\,\omega_2}{b_2})) \quad (11)$$
$$= 1 - (1 - F_{|h_s|^2}(A\,\omega_1)) \times (1 - F_{|h_n|^2}(B\,\omega_2)),$$

such that $a_1 - a_2\gamma_{th_f} > 0$ and $b_1 - b_2\gamma_{th_f} > 0$ and $OP_n = 1$ otherwise, where $A = \max\left(\frac{\gamma_{th_f}}{a_1 - a_2\,\gamma_{th_f}}, \frac{\gamma_{th_n}}{a_2}\right)$, $B = \max(\frac{\gamma_{th_f}}{b_1 - b_2\,\gamma_{th_f}}, \frac{\gamma_{th_n}}{b_2})$, $\omega_1 = \frac{1}{\gamma_s L B_s}$, and $\omega_2 = \frac{1}{\gamma_u P_n}$. By substituting (7), and (9) into (11), the closed-form expression for the $OP_n$ can be expressed as,

$$OP_n = 1 - \alpha_s\, e^{-(\beta_s - \delta_s)A\omega_1} \sum_{k=0}^{m_s - 1} \zeta(k) \sum_{l=0}^{k} \frac{k!}{l!}\,(A\omega_1)^l$$
$$\times (\beta_s - \delta_s)^{-(k-l+1)}\, e^{-\frac{m_n}{\Omega_n}B\omega_2} \sum_{n=0}^{m_n - 1} (\frac{m_n}{\Omega_n}B\omega_2)^n \frac{1}{n!}. \quad (12)$$

*2) OP of FU ($OP_f$):* The outage event will occur for the FU when the UAV is unable to decode $x_1$, $x_2$, or when the UAV is able to decode $x_1$ and $x_2$, but the FU is unable to decode its signal. Consequently, the $OP_f$ can be stated as [6]

$$OP_f = \Pr(\min(\frac{\gamma_{x_1}^U}{\gamma_{th_f}}, \frac{\gamma_{x_2}^U}{\gamma_{th_n}} < 1) +$$
$$\Pr(\min(\frac{\gamma_{x_1}^U}{\gamma_{th_f}}, \frac{\gamma_{x_2}^U}{\gamma_{th_n}} \geq 1), \frac{\gamma_{x_1}^f}{\gamma_{th_f}} < 1)$$
$$= \Pr(\min(\frac{\gamma_{x_1}^U}{\gamma_{th_f}}, \frac{\gamma_{x_2}^U}{\gamma_{th_n}}, \frac{\gamma_{x_1}^f}{\gamma_{th_f}}) < 1) \quad (13)$$
$$= 1 - \Pr(\gamma_{x_1}^U \geq \gamma_{th_f}, \gamma_{x_2}^U \geq \gamma_{th_n}, \gamma_{x_1}^f \geq \gamma_{th_f}).$$

Similar to the derivation of the $OP$ for the NU, the closed-form expression for $OP_f$ can be expressed as

$$OP_f = 1 - \alpha_s\, e^{-(\beta_s - \delta_s)A\omega_1} \sum_{k=0}^{m_s - 1} \zeta(k) \sum_{l=0}^{k} \frac{k!}{l!}\,(A\omega_1)^l$$
$$\times (\beta_s - \delta_s)^{-(k-l+1)}\, e^{-\frac{m_f}{\Omega_f}C\omega_3} \sum_{n=0}^{m_f - 1} (\frac{m_f}{\Omega_f}C\omega_3)^n \frac{1}{n!}, \quad (14)$$

where $C = \frac{\gamma_{th_f}}{b_1 - b_2\,\gamma_{th_f}}$, and $\omega_3 = \frac{1}{\gamma_u P_f}$.

*3) The System OP ($OP_{sys}$):* can be expressed as

$$OP_{sys} = 1 - \Pr(\gamma_{x_1}^U \geq \gamma_{th_f}, \gamma_{x_2}^U \geq \gamma_{th_n})$$
$$\times \Pr(\gamma_{x_1}^f \geq \gamma_{th_f}, \gamma_{x_1}^n \geq \gamma_{th_f}, \gamma_{x_2}^n \geq \gamma_{th_n}), \quad (15)$$

By substituting (2), (3), and (4) into (15), and using (7) and (9), the closed form expression of the $OP_{sys}$ is given as

$$OP_{sys} = 1 - \alpha_s\, e^{-(\beta_s - \delta_s)A\omega_1} \sum_{k=0}^{m_s - 1} \zeta(k) \sum_{l=0}^{k} \frac{k!}{l!}\,A\omega_1^l$$
$$\times (\beta_s - \delta_s)^{-(k-l+1)}\, e^{-\frac{m_n}{\Omega_n}B\omega_2} \sum_{n=0}^{m_n - 1} (\frac{m_n}{\Omega_n}B\omega_2)^n \frac{1}{n!}$$
$$\times e^{-\frac{m_f}{\Omega_f}C\omega_3} \sum_{u=0}^{m_f - 1} (\frac{m_f}{\Omega_f}C\omega_3)^u \frac{1}{u!}. \quad (16)$$

## IV. OPTIMIZATION ALGORITHM FOR POWER ALLOCATION

In this section, we propose the following optimization algorithm for adjusting the power allocation factor to obtain the

Table I
SYSTEM PARAMETERS.

| Parameter | Value |
|---|---|
| Height of LEO satellite (iridium ) | 780 Km |
| Downlink carrier frequency at satellite | 1.55 GHz |
| UAV antenna gain | 1 dB |
| Satellite antenna gain | 30 dB |
| Diameter of satellite antenna aperture | 2 m |
| Pointing error angle of satellite | 1° |
| Carrier frequency at UAV | 2 GHz |
| The height of UAV | 100 m |
| Horizontal distance from the UAV to the near user | 50 m |
| Horizontal distance from the UAV to the far user | 100 m |
| Coverage radius of spot beam from satellite (R) | 200 Km |
| The distance from the beam center to the UAV | 0.3R m |
| Noise bandwidth | 12 MHz |
| Temperature noise | 290 K |

minimum system OP. We assume that $a_1 = b_1 = f_1$ and $\gamma_{th_n} = \gamma_{th_f} = \gamma_{th}$, which can be written as:

$$\min_{f_1}\ OP_{sys} \quad (17a)$$
$$s.t.\ \frac{\gamma_{th}}{1 + \gamma_{th}} < f_1 < 1 \quad (17b)$$

The problem in (17) is convex and can be solved using any commercial solver such as Matlab and Mathematica. Figure 2 depicts the variations of the three OPs versus $f_1$ to show the convexity graphically. By setting the parameters in Table I and set $\gamma_{th} = 1$, the optimal system OP is achieved at $f_1^* = 0.7302$. In Section V, this optimization algorithm is used in all figures unless otherwise mentioned. Additionally, the convexity of the problem in (17) can be proved mathematically by differentiating $OP_{sys}$ in (16). Based on the definition of A = B = $\max(\eta_1, \eta_2)$ for $b_1 = a_1$, where $\eta_1 = \frac{\gamma_{th}}{f_1 - f_2\,\gamma_{th}}$, $\eta_2 = \frac{\gamma_{th}}{f_2}$, $f_2 = 1 - f_1$, we divide (16) into two intervals according to the value of $f_1$. The first interval is $\frac{\gamma_{th}}{1 + \gamma_{th}} < f_1 < \frac{1 + \gamma_{th}}{2 + \gamma_{th}}$, where $\eta_1 > \eta_2$ and A = B = $\eta_1$. By substituting in (16) and with some simple mathematical manipulation, the partial derivative $\frac{\partial OP_{sys}}{\partial f_1}$ can be proved to be a negative value, which means a decreasing function of $f_1$. Moreover, within the second interval, $\frac{(1 + \gamma_{th})}{(2 + \gamma_{th})} < f_1 < 1$, we can substitute A = B = $\eta_2$, where the derivative can be proved to be positive. This proves that the system OP shows an inflection point at $\frac{(1 + \gamma_{th})}{(2 + \gamma_{th})}$. Additionally, the second derivative $\frac{\partial^2 OP_{sys}}{\partial f_1^2}$ can be easily proved to be a positive value showing the convexity of the function with respect to $f_1$.
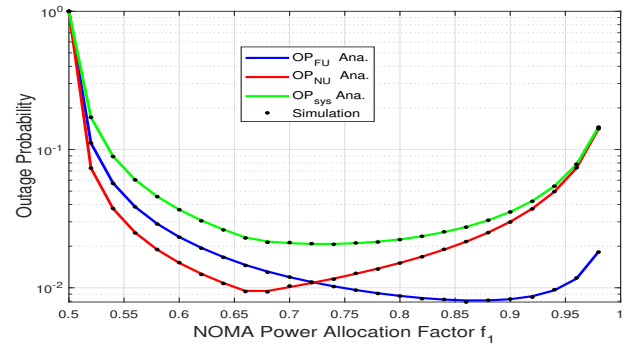


Figure 2. Outage probability versus power allocation $f_1$.

## V. RESULTS AND DISCUSSIONS

In this section, we validate the analytical results using representative numerical simulations. We evaluate the outage probability of both the satellite-UAV-terrestrial users and the system in addition to investigating the impact of key parameters on the performance. Monte-Carlo simulation is implemented to verify the accuracy by averaging over $10^6$ channels realizations. For numerical analysis, we set the power allocation factor to the output of the optimal power allocation algorithm in (17). The target rates of near user and far user are assumed to be equal, where $R_n = R_f = 0.5$ unless mentioned otherwise, while $\alpha = 2$ is the path-loss factor and $\sigma_f{}^2 = \sigma_n{}^2 = $ -70 dB. The link among satellite and UAV undergoes frequent heavy shadowing (FHS), the channel coefficients of terrestrial link are $m_n = m_f = 1$, $\Omega_n = \Omega_f = 1$. The settings are summarized in Table I [35].

Figure 3 plots the variations of OPs of FU, NU, and the overall system versus the transmit power compared with OMA scheme, where the transmit power $(P_t) = P_s = P_u$. The results show that the curves of theoretical analysis coincide with the Monte Carlo simulation curves, which validates our analysis. The results show that the OP improves with the increase of the transmitted power for both users under both NOMA and OMA schemes. The OPs of the far and near users are notably reduced by adopting the NOMA scheme compared with OMA scheme.

Figure 4 plots the variations of the OPs of both users as a function of the UAV height for an $P_t = 35$ dB for both Satellite and UAV. The results show that OP decreases when the UAV is close to the ground. It is noteworthy that FU is more sensitive to the height of the UAV than NU.

Figure 5 plots the OPs for both users versus the satellite antenna pointing error angle $\theta_e$ at fixed $P_t = 35$ dB. It is shown that the pointing error angle has a significant effect on the outage performance of both users, where the OP deteriorates as the pointing error angle increases. It is noteworthy that the results show a complete outage, i.e., OP = 1, for a pointing error angle around $\theta_e = 12°$. The results in Figure 6 support those in Figure 5, it can be clearly seen that $\theta_e$ significantly influences the OP at a low value (i.e. $\theta_e = 7°$ or $9°$), the OPs for both far and near user significantly decrease for the entire range of the transmitted power.

Figure 7 depicts the impact of shadowing parameters for the shadowed Rician link of the $S$-$U$ channel on the OP


Figure 4.   OP versus the height of UAV.
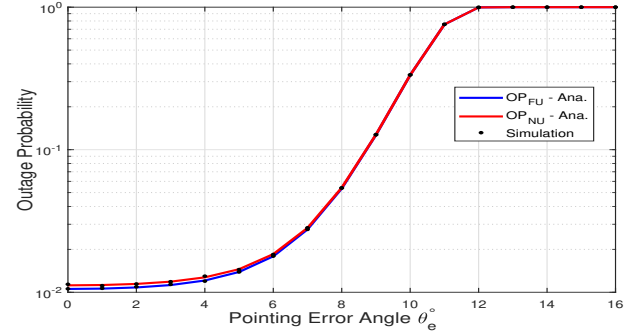

Figure 5.   OP versus Pointing Error Angle.
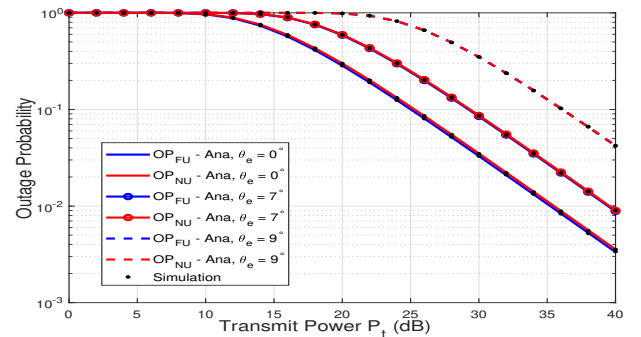

Figure 6.   OP versus $P_t$ for different pointing error angle.
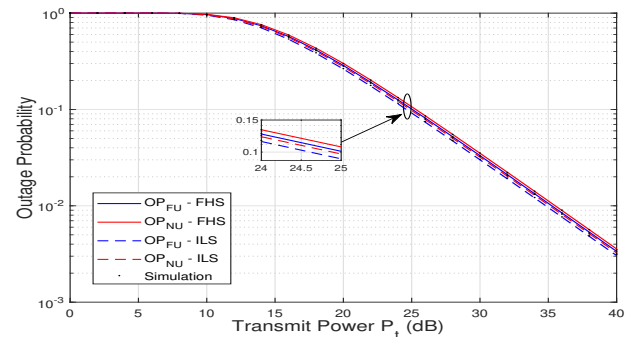

Figure 7.   OP versus $P_t$ for various shadowing parameters.

performance. We compare the OP performance for two different shadowing scenarios, i.e., FHS, and infrequent light shadowing (ILS) whose channel parameters are given in Table II [24]. The results show that the OPs of both users under FHS scenario are slightly higher than the OPs of ILS due to the impact of communication conditions between satellite and UAV.


Figure 3.   OP versus $P_t$ at $R_n = R_f = 0.5$.
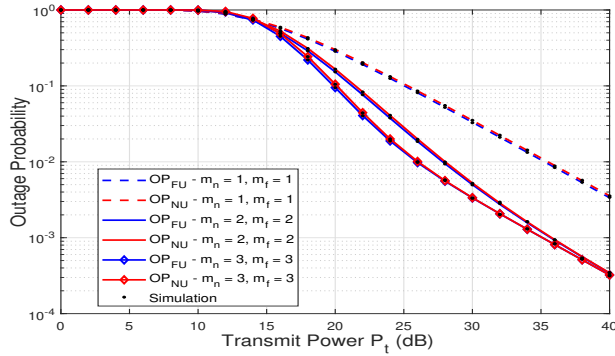
Figure 8.  OP versus $P_t$ for different Nakagami-m severity factor.

Table II
SHADOWING PARAMETERS.

| Shadowing | $m_s$ | $b_s$ | $\Omega_s$ |
|---|---|---|---|
| Frequent heavy shadowing | 1 | 0.063 | 0.0007 |
| Infrequent light shadowing | 10 | 0.158 | 1.29 |

Figure 8 indicates the impact of different severity conditions for the terrestrial link on the OP. The severity parameters of the terrestrial link have a significant impact on the OP. It can be seen that the OP degrades as the fading severity increases with decreasing $m_i$. This is because of the fact that the performance of the system enhances as the fading severity decreases.

## VI. CONCLUSION

In this article, we studied the performance of the hybrid satellite-UAV-terrestrial downlink NOMA system where the closed-form expression for the outage probability is derived and evaluated with the presence of path loss and antenna-pointing error loss. We showed the impact of various parameters on the considered system. We also showed how the power allocation factor affects the total system OP and how to get an optimal power allocation. The numerical results showed the superiority of the NOMA over OMA system.

## REFERENCES

[1] P. K. Sharma and D. I. Kim, "Secure 3D mobile UAV relaying for hybrid satellite-terrestrial networks," *IEEE Transactions on Wireless Communications*, vol. 19, no. 4, pp. 2770–2784, 2020.

[2] D.-T. Do et al., "Hybrid satellite-terrestrial relay network: Proposed model and application of power splitting multiple access," *Sensors*, vol. 20, no. 15, p. 4296, 2020.

[3] B. Di, L. Song, Y. Li, and H. V. Poor, "Ultra-dense LEO: Integration of satellite access networks into 5G and beyond," *IEEE Wireless Commun.*, vol. 26, no. 2, pp. 62–69, 2019.

[4] X. Yan, H. Xiao, K. An, G. Zheng, and S. Chatzinotas, "Ergodic capacity of NOMA-based uplink satellite networks with randomly deployed users," *IEEE Systems Journal*, vol. 14.

[5] X. Zhang et al., "Performance analysis of NOMA-based cooperative spectrum sharing in hybrid satellite-terrestrial networks," *IEEE Access*, vol. 7, pp. 172 321–172 329, 2019.

[6] X. Li et al., "A unified framework for HS-UAV NOMA networks: Performance analysis and location optimization," *IEEE Access*, vol. 8, pp. 13 329–13 340, 2020.

[7] X. Yan et al., "Hybrid satellite terrestrial relay networks with cooperative non-orthogonal multiple access," *IEEE Commun. Lett.*, vol. 22, no. 5, pp. 978–981, 2018.

[8] A. H. Hashim, F. D. Mahad, S. M. Idrus, and A. S. M. Supa'at, "Modeling and performance study of inter-satellite optical wireless communication system," in *International Conference On Photonics 2010*, 2010.

[9] M. R. H. Khan, M. O. Ziad, S. M. Chowa, M. Mehedi *et al.*, "A comparative study of intelligent reflecting surface and relay in satellite communication," Ph.D. dissertation, Brac University, 2021.

[10] X. Lei, L. Yang, J. Zhang, G. Li, and J. Chen, "LAP-based FSO-RF cooperative NOMA systems," in *Proc. IEEE VTC2020-Fall*, 2020.

[11] S. H. Alsamhi et al., "Green internet of things using UAVs in B5G networks: A review of applications and strategies," *Ad Hoc Networks*, p. 102505, 2021.

[12] M. Petkovic and M. Narandzic, "Overview of UAV based free-space optical communication systems," in *International Conference on Interactive Collaborative Robotics*.   Springer, 2019, pp. 270–277.

[13] R. Ruby, B. M. ElHalawany, and K. Wu, "Impact of UAV mobility on physical layer security," in *Proc. IEEE MSN 2021*, 2021.

[14] R. Ruby, K. Wu, Q.-V. Pham, and B. M. ElHalawany, "Aiding a disaster spot via an UAV-based mobile AF relay: Joint trajectory and power optimization," in *Proc. ACM Symposium on Mobility Management and Wireless Access*, 2020, p. 105–113.

[15] M. V. Jamali, S. M. Azimi-Abarghouyi, and H. Mahdavifar, "Outage probability analysis of uplink NOMA over ultra-high-speed FSO-backhauled systems," in *Proc. IEEE GC Wkshps*, 2018.

[16] B. M. ElHalawany et al., "Performance analysis of downlink NOMA systems over $\kappa$-$\mu$ shadowed fading channels," *IEEE Trans. on Vehic. Tech.*, vol. 69, no. 1, pp. 1046–1050, 2020.

[17] F. Aveta and H. H. Refai, "Free space optical non-orthogonal multiple access experimentation," in *Free-Space Laser Communications XXXI*, vol. 10910.   International Society for Optics and Photonics, 2019, p. 109101O.

[18] M. Najafi, V. Jamali, P. D. Diamantoulakis, G. K. Karagiannidis, and R. Schober, "Non-orthogonal multiple access for FSO backhauling," in *Proc. IEEE WCNC*, 2018.

[19] W. U. Khan et al., "Energy efficiency maximization for beyond 5G NOMA-enabled heterogeneous networks," *Peer-to-Peer Netw. Appl.*, vol. 14, no. 1, p. 3250–3264, 2021.

[20] W. U. Khan, F. Jameel, T. Ristaniemi, B. M. Elhalawany, and J. Liu, "Efficient power allocation for multi-cell uplink NOMA network," in *Proc. IEEE VTC2019-Spring*, 2019.

[21] W. U. Khan, M. A. Javed, T. N. Nguyen, S. Khan, and B. M. Elhalawany, "Energy-efficient resource allocation for 6G backscatter-enabled NOMA IoV networks," *IEEE Trans. Intell. Transp. Syst.*, 2021, doi: 10.1109/TITS.2021.3110942.

[22] M. Elsayed, A. Samir, A. A. A. El-Banna, X. Li, and B. M. ElHalawany, "When NOMA multiplexing meets symbiotic ambient backscatter communication: Outage analysis," *IEEE Trans. Vehic. Technology*, vol. 71, no. 1, pp. 1026–1031, 2022.

[23] P. S. Bithas et al., "A survey on machine-learning techniques for UAV-based communications," *Sensors*, vol. 19, no. 23, p. 5170, 2019.

[24] H. Shuai, K. Guo, K. An, and S. Zhu, "NOMA-based integrated satellite terrestrial networks with relay selection and imperfect SIC," *IEEE Access*, vol. 9, pp. 111 346–111 357, 2021.

[25] B. M. ElHalawany, M. Elsabrouty, O. Muta, A. Abdelrahman, and H. Furukawa, "Joint energy-efficient single relay selection and power allocation for analog network coding with three transmission phases," in *Proc. IEEE VTC Spring*, 2014.

[26] L. Han, W.-P. Zhu, and M. Lin, "Outage of noma-based hybrid satellite-terrestrial multi-antenna df relay networks," *IEEE Wireless Communications Letters*, vol. 10, no. 5, pp. 1083–1087, 2021.

[27] V. Bankey et al., "Physical layer security in hybrid satellite-terrestrial relay networks," in *Physical Layer Security*.   Springer, 2021, pp. 1–28.

[28] X. Zhang et al., "NOMA-based proactive content caching in hybrid satellite-aerial-terrestrial networks," in *Proc. IEEE WCNCW*, 2021.

[29] G. Maral, M. Bousquet, and Z. Sun, *Satellite communications systems: systems, techniques and technology*.   John Wiley & Sons, 2020.

[30] A. A. Khuwaja, Y. Chen, and G. Zheng, "Effect of user mobility and channel fading on the outage performance of UAV communications," *IEEE Wireless Commun. Lett.*, vol. 9, no. 3, pp. 367–370, 2019.

[31] D. Zwillinger and A. Jeffrey, *Table of integrals, series, and products*. Elsevier, 2007.

[32] Wolfram, the wolfram functions site, 2017. [Online]. Available: http://functions.wolfram.com/PDF/Hypergeometric1F1.pdf

[33] Wolfram, the wolfram functions site, 2017. [Online]. Available: http://functions.wolfram.com/PDF/LaguerreLGeneral.pdf

[34] S. M. Ibraheem et al., "Outage performance of NOMA-based DF relay sharing networks over Nakagami-m fading channels," in *Proc. ICCES*, 2018, pp. 512–517.

[35] S. Dey, D. Mohapatra, and S. Archana, "An approach to calculate the performance and link budget of LEO satellite (iridium) for communication operated at frequency range (1650–1550) mhz," *Int. J. Latest Trends Eng. Technol.*, vol. 4, no. 4, pp. 96–103, 2014.

# Context-aware gender and age recognition from smartphone sensors

Cite This

PDF

Sajana T S ; Susmi Jacob ; Vinod P ; Varun G Menon ; Shilpa P C   All Authors

Computer Science & Engineering SCMS
School of Engg and Technology, APJ
Abdul Kalam Technological University,
Thiruvananthapuram, Kerala, India

## Abstract

Document Sections

I. Introduction

II. Related Works

III. Theoritical
    Concepts

**Abstract:**
Smartphones include multiple sensors to track a device's movement. This research investigated the capability of smartphone motion sensors to determine the user's gender and age in different contexts. A subject's context is an action they engage in, such as sitting or standing. This paper is based on the differences in behavior between male and female smartphone users, precisely, how they hold and manage their devices. To build our approach, we use the MotionSense Dataset. This dataset contains data from accelerometer and gyroscope sensors over time (attitude, gravity, acceleration, and rotationRate). In this study, we consider multiple contexts such as walking, sitting, standing, and jogging. Our method

I. Introduction

II. Related Works

III. Theoritical
     Concepts

IV. Methodology

V. Evaluation

Show Full Outline ▾

Authors

Figures

References

Keywords

Metrics

age in different contexts. A subject's context is an action they engage in, such as sitting or standing. This paper is based on the differences in behavior between male and female smartphone users, precisely, how they hold and manage their devices. To build our approach, we use the MotionSense Dataset. This dataset contains data from accelerometer and gyroscope sensors over time (attitude, gravity, acceleration, and rotationRate). In this study, we consider multiple contexts such as walking, sitting, standing, and jogging. Our method proposes to use smartphone sensors to detect an individual's age and gender with an accuracy of 99.89% if they are seated.

**Published in:** 2022 International Conference on Computing, Communication, Security and Intelligent Systems (IC3SIS)

**Date of Conference:** 23-25 June 2022     **DOI:** 10.1109/IC3SIS54991.2022.9885610

**Date Added to IEEE *Xplore*:** 15 September 2022     **Publisher:** IEEE

**Conference Location:** Kochi, India

▼ ISBN Information:
   **Electronic ISBN:**978-1-6654-6883-1
   **Print on Demand(PoD)**
   **ISBN:**978-1-6654-6884-8

# Towards energy-efficient UAV-assisted 5G Internet of Underwater Things

Sandeep Verma
G. S. Sanyal School of Telecommunications Indian Institute of Technology, Kharagpur, India
sandeepverma@ieee.org

Shahbaz Akhtar
G. S. Sanyal School of Telecommunications, Indian Institute of Technology, Kharagpur, India
mdsakhtar@iitkgp.ac.in

Aneek Adhya
G. S. Sanyal School of Telecommunications, Indian Institute of Technology, Kharagpur, India
aneek@gssst.iitkgp.ac.in

Varun G Menon
Department of Computer Science and Engineering
SCMS School of Engineering and Technology, India
varunmenon@scmsgroup.org

## ABSTRACT

Adhering to the requirements of Fifth Generation (5G) communication for seamless data gathering, especially from underwater resources, Unmanned Aerial Vehicles (UAVs)-assisted 5G Internet of Underwater Things (IoUT) have been leaving an everlasting impression. However, the resource-constrained underwater sensor nodes limit the potential of IoUT for reliable data dissemination due to their shorter operational period. To extenuate this concern, in this paper we present an Energy-Efficient Unmanned Aerial Vehicle (UAV)-assisted Routing Architecture (EEURA) for 5G IoUT. The Cluster Head (CH) is selected using Improved-Tunicate Swarm Algorithm (I-TSA). We use Energy-Harvesting (EH)-enabled nodes and a single UAV for data collection from the underwater deployed sensor nodes to extenuate hot-spot problem. It is evident from the simulation investigation that EEURA performs exclusively better than the state-of-the-art routing methods in IoUT.

## CCS CONCEPTS

• Networks → Network design and planning algorithms.

## KEYWORDS

Cluster-Head (CH), Energy-Harvesting (EH), Internet of Underwater Things (IoUT), Routing, UAV, 5G

## 1 INTRODUCTION

The advent of Fifth Generation (5G) technology has given rise to continuously increasing demands for greater data rates, extensive connectivity, dependability, and the smallest achievable latency of less than 1 millisecond [2]. The implementation of the 5G framework faces a number of difficulties due to the constantly increasing demands placed on the usage of 5G technology and the growing number of users. Unmanned Aerial Vehicles (UAVs)-assisted networks have proven helpful in addressing these issues, including infrastructure failure during natural disasters and 5G system malfunctions brought on by an unexpected rise in user volume [1]. UAVs-assisted 5G technology has not only helped in proliferating the speed of data dissemination in its network coverage, but has also helped the users to reach out to various remote locations for example monitoring of underwater resources [11].

Internet of Underwater Things (IoUT) consists of various sensor nodes deployed underwater to monitor various aquatic activities [15]. Due to the challenging environment of IoUT, the communication among the sensor nodes gets heavily influenced. Therefore, it becomes crucial to design a routing protocol compatible with acoustic communication. A plethora of research efforts is reported presenting the energy-efficient routing techniques for IoUT [1, 6, 10, 14]. However, due to the multi-hop communication, the hot-spot problem arises and eventually degrades the performance of the network.

**Table 1: Comparative analysis of state-of-art protocols in IoUT**

| Protocol and Reference | Targeted attributes | Significance | Shortcomings |
|---|---|---|---|
| CUWSN [1] | CH and coordinate node selection | Increased network longevity | Hot-spot problem |
| QOSRP [5] | Congestion | Enhanced throughput | Doesn't consider energy consumption |
| LRP [6] | Hot-spot problem | Reduced energy consumption | Shortest queue strategy |
| QERP [7] | Non-reliable data transmission | Enhanced throughput | void hole issues |
| MLCEE [9] | Non-balanced transmission | Qualitative link, balanced energy expenditure | Delay in data transmission, void hole problem |
| EGBLOAD [10] | Relay nodes | Enhanced network longevity | Proliferated energy consumption |
| MFOBR [11] | Fault resilience routing | Decreased delay, network longevity | Hot-spot problem |
| TORA [13] | Data collection constraints | Localization efficacy and network longevity | Proliferated energy expenditure |
| CSO[14] | Identified articulation points | Enhanced throughput | Hot-spot problem, Complex architecture |
| SEECR [15] | Security aspects | Optimally enhanced performance of network | Larger size of communication overhead, creation of void |
| LFEER [16] | Acoustic medium limitations | Network longevity enhanced | Complex algorithm, non-reliability in link |

**CUWSN** - Cluster based Underwater WSN; **QoSRP** - QoS channel-aware Routing Protocol; **LRP** - Link quality-aware queue-based spectral clustering Routing Protocol; **QERP** - Quality-of-service (QoS) aware Evolutionary Routing Protocol; **MLCEE** - A Multi-Layer Cluster; **EGBLOAD** - Energy Grade and Balance LOAD distribution; **MFOBR** - Moth Flame Optimization based Fault resilient routing; **TORA** - Totally Opportunistic Routing Algorithm; **CSO** - Cat Swarm Optimization based algorithm; **SEECR** - Secure Energy Efficient and Cooperative Routing protocol; **LFEER** - Localization Free Energy Efficient and cooperative Routing

Furthermore, it is observed through the retrospective survey, Energy-Harvesting (EH)-enabled sensor nodes can re-energize themselves, particularly in the Terrestrial Wireless Sensor Network (TWSN). However, when it comes to IoUT, the concept of EH has not been adapted significantly due to the challenging conditions of an aquatic environment. As far as designing the routing protocol for IoUT is concerned, cluster-based routing has led to the reduced energy expenditure of sensor nodes, and hence, it has been comprehensively adopted by various researchers. A tabular study of state-of-the-art routing protocols stating their merits and demerits is given in Table 1. The proposed work in this manuscript is motivated by the fact that none of these strategies made use of UAVs or EH-enabled sensor nodes and hence, mitigating the hot-spot problem.

In lieu of research gaps discussed above, our major contributions are discussed as given below.

- We present Energy-Efficient UAV-assisted Routing Architecture (EEURA) for 5G IoUT. We deploy a fixed number of EH-enabled sensor nodes that act as gateway nodes to collect data from the underwater deployed nodes as shown in Figure 1. It is done so to mitigate hot-spot problem in IoUT.
- A UAV is made to hover over the target area to gather the information from the gateway nodes. Thereafter, UAV sends the collected data to the base station through the 5G network.
- We adapt cluster-based routing method for the underwater sensor nodes wherein the CH is selected using Improved-Tunicate Swarm Algorithm (I-TSA) [8] based on some crucial parameters namely, residual energy, distance from the EH-enabled nodes, network's average energy, and fault tolerant characteristic of a node.

To the best of our knowledge, it is the first ever work that presents the holistic approach for mitigating hot-spot problem while utilizing the EH-enabled sensor nodes and also the UAV-assisted 5G communication for reliable data dissemination.

Henceforth, the manuscript is organized as follows. Section 2 details about the proposed system model and simulation results are discussed in Section 3. Finally, the conclusion is given in Section 4.
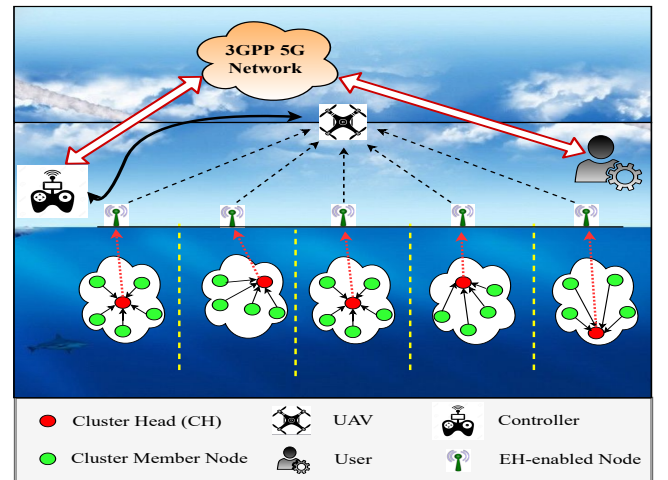


**Figure 1: Proposed routing architecture of EEURA**

## 2 PROPOSED SYSTEM MODEL OF EEURA

Since the proposed architecture follows cluster-based routing mechanism hence, it undergoes two phases of operation namely, network establishment and data transmission phase. For these phases of operation, we consider following network assumptions.

- It is assumed that the deployed sensor nodes don't have any recharging source which could re-energize them. Hence, once the energy of these nodes is exhausted, it is assumed to be dead. Further, when it happens to all nodes, the whole network is said to be dead.
- The EH-enabled nodes are used to gather the data from the underwater nodes. Further, it is assumed that these nodes are energized through the solar harvesting ambient energy.
- A single UAV is used to collect data from these EH-enabled nodes, and it is assumed that UAV has no constraint of energy. Any other hindrance in data collection is not considered as the ideal scenario is assumed while UAV is operating.
- The deployed sensor nodes are assumed to be homogeneous in the context of the energy.
- The security provisioning is out of scope for this work, as the network is assumed to be secured.
- The sensor nodes deployed underwater and EH-enabled nodes are stationary and are fixed in a way that they don't move from their deployed position.

## 2.1 Acoustic Energy Model

For computing path loss factor, the channel model is detailed as following. The transmission loss incurred due to spreading and absorption, is computed as follows [4].

$$Tx_{loss} = 10 \log rg + \alpha \times rg \times 10^{-3} \qquad (1)$$

In above equation, $\alpha$ denotes the absorption coefficient and is expressed in units dB/km. The variable $rg$ is range of communication that are given in yards and $fq$ is the frequency in kHz. For the frequencies of low values, the Thorps equation is used as follows.

$$\alpha = \frac{0.1 f_q^2}{1 + f_q^2} + \frac{40 f_q^2}{4100 + f_q^2} + 2.75 \times 10^{(-4)} f_q^2 + 0.003 \qquad (2)$$

Here, $\alpha$ is in dB/km.

## 2.2 Network establishment phase of EEURA

The sensor nodes deployed underwater forms a cluster in a distributed fashion. Since, the nodes join a CH to form a cluster, the CH selection has been focused in this work predominantly. The CH selection is performed using I-TSA by optimizing the fitness parameters that helps in its selection. Algorithm 1 illustrates the whole operation of EEURA. We devise fitness function to be optimized by I-TSA [8], as follows.

A. **Fitness parameters for selecting CH using I-TSA:** The fitness parameters that are essential for selecting CH are discussed below.

---

**Algorithm 1** Operational steps of EEURA

---

**Input:** $Un$ (number of nodes deployed underwater), $It_{max}$ (maximum iterations), $UAV$
**Output:** Z = $CH\_S$ (selected CH), $D_{nod}$ (dead nodes), $A_{nod}$ (alive nodes), LND (Last Node Dead)

1: **procedure** EEURA
2:     Sensor nodes deployment in underwater
3:     $CH\_S = 0$
4:     **for** $It_{current} = 1\ to\ It_{max}$ **do**
5:         $A_{nod} = Un$
6:         $D_{nod}=0$
7:         **for** i= 1 to $Un$ **do**
8:             **if** $E_{rd}(i) == 0$ **then**
9:                 $D_{nod}=D_{nod}+1$
10:                 **if** $D_{nod}==Un$ **then**
11:                     $LND=It_{current}$
12:                 **end if**
13:                 $Av_{nod} = A_{nod} - D_{nod}$
14:             **end if**
15:         **end for**
16:         **for** i= 1 to $Un$ **do**
17:             **if** $E_{rd}(i) > 0$ **then**
18:                 Equations (1-7) for selecting CH
19:                 $CH\_S = CH\_S + 1$
20:             **else**
21:                 $i^{th}$ node ← TDMA scheduling
22:                 Update $E_{rd}(i)$ w.r.t equations (1-2) [1, 4]
23:             **end if**
24:         **end for**
25:         **if** $D_{nod}=Un$ **then**
26:             break
27:         **end if**
28:     **end for**
29:     return Z
30: **end procedure**

---

I. Residual energy factor : The computation of residual energy for the sensor nodes is done through the equation (3).

$$F_1 = \sum_{i=1}^{n} \frac{E_{rd}(i)}{E_{in}(i)} - Tx_{loss}(i) \qquad (3)$$

Higher the value of $F_1$, more will be chances for a node to be selected as CH. In equation (3), $E_{rd}$ and $E_{in}$ denote the residual and initial energy of the node, further $n$ denotes the total number of nodes.

II. Distance between the node and the EH-enable node:

$$F_2 = \sum_{i=1}^{n} \frac{Davg_{n-EH}(i)}{D_{n-EH}(i)} \qquad (4)$$

$$Davg_{n-EH}(i) = \frac{1}{n} \times \sum\nolimits_{i=1}^{n} D_{n-EH}(i) \tag{5}$$

Ratio of average distance of a node from EH-enabled node, to the distance of a node from EH node is considered as given in equation (4). The equation (5) shows the computation of average distance for a node to EH node. Higher value of $F_2$ for a node ensures its selection as a CH.

III. Network's average energy:

$$F_3 = \frac{1}{n} \times \sum\nolimits_{i=1}^{n} E_{rd(i)} \tag{6}$$

The third fitness parameter, $F_3$, is used to calculate the network's average energy, which is provided in equation (6). The selection of CH in the IoUT is favoured by a greater network energy value.

IV. Fault tolerant characteristic of a node:

$$F_4 = \frac{CH_{(n-i)} \times CH_{nxt(i)}}{Dead_{CH(i)}} \tag{7}$$

In equation (7), $F_4$ gives the ratio in the context of selected CH and also the dead CHs. In numerator, the $CH_{(n-i)}$ denotes selected CH and $CH_{nxt(i)}$ shows the next node to be selected as CH. In denominator, the $Dead_{CH(i)}$ represents $i^{th}$ dead CH.

B. **Fitness Function:** Once the above discussed fitness parameters are computed, the fitness function is determined while considering the linear combination of these parameters as given by equation (8).

$$F = \frac{1}{\gamma 1 \times F_1 + \gamma 2 \times F_2 + \gamma 3 \times F_3 + \gamma 4 \times F_4} \tag{8}$$

$$\gamma 1 + \gamma 2 + \gamma 3 + \gamma 4 = 1 \tag{9}$$

In above equation (9), $\gamma 1$, $\gamma 2$, $\gamma 3$, and $\gamma 4$ denote weighted parameters which are given values based on a particular application.

## 2.3 Data transmission phase

As soon as the CH is selected, the data is forwarded to EH-enabled nodes. These nodes aggregate the collected data and forward to hovering UAV. From this UAV, data is sent to the user through the 3GPP 5G network. As the whole communication is single hop, the hot-spot problem is completely mitigated. The steps involved in data transmission phase are illustrated in Algorithm 2.

## 3 SIMULATION INVESTIGATION

The proposed architecture is simulated in MATLAB software and different parameters used, are assigned values as given in Table 2. Different performance metrics namely, stability

---

**Algorithm 2** Data transmission phase

1: **procedure** EEURA
2:     **for** i= 1 to $Un$ **do**
3:         **if** $E_{rd}(i) > 0$ **then**
4:             $i^{th}$ node ← TDMA scheduling (for cluster member)
5:             $CH\_S$ node ← underwater cluster member node
6:             $CH\_S$ node ← Data aggregation
7:             $EH_{enabled}$ node ← $CH\_S$ node
8:             **if** $EH_{enabled} > ThEH_S$ **then**
9:                 $UAV$ ← $EH_{enabled}$ node
10:             **else**
11:                 no transmission to UAV
12:             **end if**
13:         **end if**
14:     **end for**
15: **end procedure**

---

period, network lifetime, throughput, network's residual energy, etc. are considered for performance evaluation. The competitive protocols of IoUT namely, CUWSN [1], Energy Efficient Layered CH Rotation (EE-LCHR) [3], MFOBR [11] and DEKCS [12], and are considered for performance evaluation of proposed protocol i.e., EEURA while examining it for aforementioned performance metrics.

**Table 2: Experimental Values**

| Parameters | Values |
|---|---|
| Underwater area considered | $100 \times 100 \ meter^2$ |
| EH-enabled nodes' location | (10, 50), (20, 50), (30, 50), (40, 50) and (50, 50) |
| Number of EH-enabled nodes | 6 |
| Number of underwater sensor nodes (except EH-enabled nodes) | 100 |
| Initial value of energy of a node | 0.25 Joule |
| Number of UAVs | 1 |
| $ThEH_S$ (Energy threshold for EH-enabled node) | 0.25 Joule |
| $f_q$ | 10kHz |
| $\gamma 1$, $\gamma 2$, $\gamma 3$, and $\gamma 4$ | 0.25 |

## 3.1 Performance evaluating metrics

There are various performance metrics which are considered for examining the performance of EEURA. In this work, we consider stability period, network lifetime, throughput, network's residual energy, etc. The overall performance of EEURA in comparison to other protocols is given in Table 3.

**Table 3: Overall performance investigation of EEURA against the competitive protocols**

| Performance | Underwater Routing Protocols | | | | |
|---|---|---|---|---|---|
| metrics | CUWSN [1] | MFOBR [11] | DEKCS [12] | EE-LCHR [3] | **EEURA** |
| S.P. | 1180 | 1405 | 1005 | 1307 | **1518** |
| HND | 1512 | 1719 | 2228 | 2518 | **2756** |
| N.L. | 1803 | 2126 | 2771 | 3009 | **3596** |
| THPT | 37635 | 40865 | 101676 | 112353 | **135719** |

S.P - Stability Period; HND - Half Network Dead; THPT - Throughput
N.L - Network Lifetime

*3.1.1*    ***Stability Period:*** In IoUT, due to the challenging aquatic environment, the sensor nodes consume a lot of energy. This metric states about the stability of the network by ensuring the dissemination of significant information. We define stability period by the number of rounds completed till 10% nodes are dead. From Figure 2, it is evident that EEURA improves stability period by 16.14% and 51.1% as compared to EE-LCHR and DEKCS protocols, respectively. It is due to the use of EH-enabled nodes and the selection of CH using I-TSA algorithm that help in preserving the energy of sensor nodes.
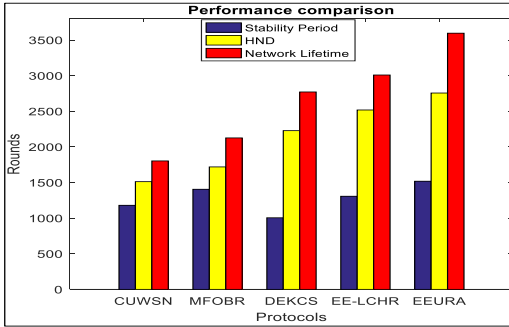


**Figure 2: Overall performance of EEURA against the IoUT routing protocols**

*3.1.2*    ***Network lifetime:*** This is one of the crucial metrics that helps in deciding the fate of the network in IoUT. When all nodes are non-operational attributing to their gradual energy consumption, it is terms as network lifetime. As observed from the Figures 3 and Table 3, the EEURA acquires the improvement of 19.5% and 29.77% as compared to EE-LCHR and DEKCS, respectively. Further, the investigation for number of alive nodes is presented for proposed work in Figures 3. For both cases, the protocol EEURA outperforms other protocols and improves network performance significantly. The use of EH-enabled nodes and UAV-assisted communication help in mitigating the hot-spot problem that prolongs the lifetime of the network.
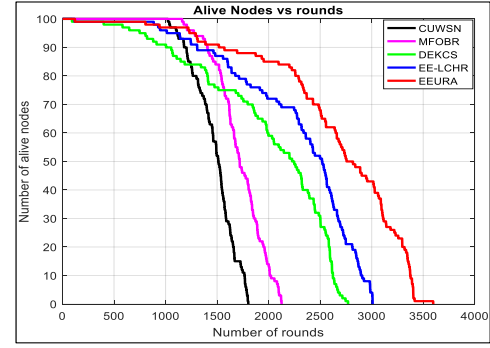


**Figure 3: Comparison of EEURA against IoUT routing protocols for alive nodes versus rounds**

*3.1.3*    ***Network's remaining energy:*** In this metric, the gradual energy consumption of the proposed work is investigated. It is evident from the Figure 4 that EEURA significantly improves the network's remaining energy with the passage of rounds as compared to EE-LCHR, DEKCS, etc.
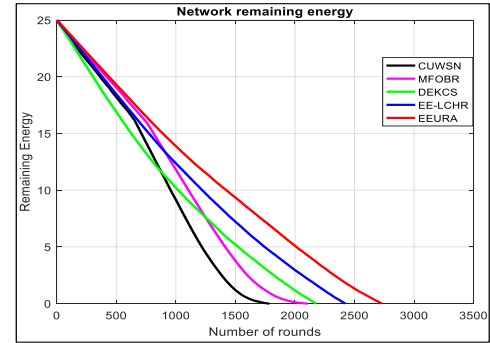


**Figure 4: Comparison of EEURA against IoUT routing protocols for network's remaining energy versus rounds**

*3.1.4*    ***Packets sent to UAV:.*** Once the data transmission in commenced, the EH-enabled nodes send data packets directly to the hovering UAV. The proposed protocol is examined for number of packets it sends to the UAV for a unit round. As shown in Figure 5, the protocol EEURA outperforms other protocols for sending number of data packets. EEURA improves throughput by 20.1% and 33% as compared to EE-LCHR and DEKCS protocols, respectively.

## 4   CONCLUSION AND FUTURE DIRECTIONS

In this paper, the primary focus has been on enhancing the network lifetime of the underwater sensor nodes by proposing an energy-efficient routing architecture i.e., EEURA. The
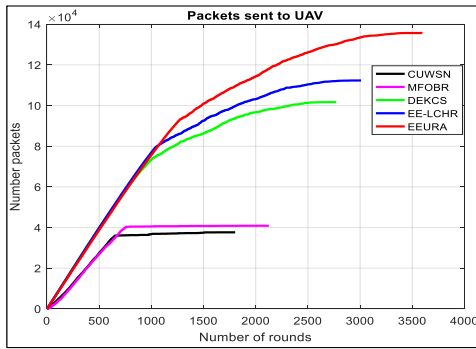
**Figure 5: Comparison of EEURA against IoUT routing protocols for throughput**

use of EH-enabled nodes along with UAV-assisted data collection not only help in mitigating the hot-spot problem but also improves the network energy-efficiency. The simulation investigation reveals the improvement reported by the EEURA against the competitive underwater routing protocols namely, CUWSN [1], MFOBR [11], DEKCS [12], and EE-LCHR [3]. It is contemplated that EEUR acquires the amelioration of 16.14% and 51.1% in stability period against EE-LCHR and DEKCS protocols and also it improves network lifetime by 19.5% and 29.77% against the aforementioned protocols, respectively.

There are some crucial concerns which we wish to address in our future work. We consider some network assumptions that assume the ideal scenarios for environment and considering secured network which may be realized to investigate the performance in real time. Further, the task of managing the operation of UAV is tedious and is subjected to the availability of recharging source. The EH-enabled nodes are assumed to be charged through the ambient energy of solar harvesting resource. However, there might be situation when the EH-enabled nodes are not charged enough to be able to transmit data.

## 5 ACKNOWLEDGMENTS

## REFERENCES

[1] Kamalika Bhattacharjya, Sahabul Alam, and Debashis De. 2019. CUWSN: energy efficient routing protocol selection for cluster based underwater wireless sensor network. *Microsystem Technologies* (2019), 1–17.

[2] Lalit Chettri and Rabindranath Bera. 2020. A Comprehensive Survey on Internet of Things (IoT) Toward 5G Wireless Systems. *IEEE Internet of Things Journal* 7, 1 (2020), 16–32. https://doi.org/10.1109/JIOT.2019.2948888

[3] Amrita Datta and Mou Dasgupta. 2022. Energy Efficient Layered Cluster Head Rotation Based Routing Protocol for Underwater Wireless Sensor Networks. *Wireless Personal Communications* (2022), 1–18.

[4] Mari Carmen Domingo and Rui Prior. 2008. Energy analysis of routing protocols for underwater wireless sensor networks. *Computer communications* 31, 6 (2008), 1227–1238.

[5] Muhammad Faheem, Rizwan Aslam Butt, Basit Raza, Hani Alquhayz, Muhammad Waqar Ashraf, Syed Bilal Shah, Md Asri Ngadi, and Vehbi Cagri Gungor. 2019. QoSRP: A cross-layer QoS channel-aware routing protocol for the Internet of underwater acoustic sensor networks. *Sensors* 19, 21 (2019), 4762.

[6] Muhammad Faheem, Gurkan Tuna, and Vehbi Cagri Gungor. 2017. LRP: Link quality-aware queue-based spectral clustering routing protocol for underwater acoustic sensor networks. *International Journal of Communication Systems* 30, 12 (2017), e3257.

[7] Muhammad Faheem, Gurkan Tuna, and Vehbi Cagri Gungor. 2017. QERP: Quality-of-service (QoS) aware evolutionary routing protocol for underwater wireless sensor networks. *IEEE Systems Journal* 12, 3 (2017), 2066–2073.

[8] Essam H Houssein, Bahaa El-Din Helmy, Ahmed A Elngar, Diaa Salama Abdelminaam, and Hassan Shaban. 2021. An improved tunicate swarm algorithm for global optimization and image segmentation. *IEEE Access* 9 (2021), 56066–56092.

[9] Wahab Khan, Hua Wang, Muhammad Shahid Anwar, Muhammad Ayaz, Sadique Ahmad, and Inam Ullah. 2019. A multi-layer cluster based energy efficient routing scheme for UWSNs. *IEEE Access* 7 (2019), 77398–77410.

[10] Zahoor Ali Khan, Ghazanfar Latif, Arshad Sher, Imran Usman, Mahmood Ashraf, Manzoor Ilahi, and Nadeem Javaid. 2019. Efficient routing for corona based underwater wireless sensor networks. *Computing* 101, 7 (2019), 831–856.

[11] Sangeeta Kumari, Pavan Kumar Mishra, and Veena Anand. 2020. Fault resilient routing based on moth flame optimization scheme for underwater wireless sensor networks. *Wireless Networks* 26, 2 (2020), 1417–1431.

[12] Kenechi G Omeke, Michael S Mollel, Metin Ozturk, Shuja Ansari, Lei Zhang, Qammer H Abbasi, and Muhammad Ali Imran. 2021. DEKCS: A dynamic clustering protocol to prolong underwater sensor networks. *IEEE Sensors Journal* 21, 7 (2021), 9457–9464.

[13] Ziaur Rahman, Fazirulhisyam Hashim, Mohd Fadlee A Rasid, and Mohamed Othman. 2018. Totally opportunistic routing algorithm (TORA) for underwater wireless sensor network. *Plos one* 13, 6 (2018), e0197087.

[14] Madhuri Rao and Narendra Kumar Kamila. 2021. Cat Swarm Optimization based autonomous recovery from network partitioning in heterogeneous underwater wireless sensor network. *International Journal of System Assurance Engineering and Management* (2021), 1–15.

[15] Khalid Saeed, Wajeeha Khalil, Sheeraz Ahmed, Iftikhar Ahmad, and Muhammad Naeem Khan Khattak. 2020. SEECR: secure energy efficient and cooperative routing protocol for underwater wireless sensor networks. *IEEE Access* 8 (2020), 107419–107433.

[16] Sahar Shah, Anwar Khan, Ihsan Ali, Kwang-Man Ko, and Hasan Mahmood. 2018. Localization free energy efficient and cooperative routing protocols for underwater wireless sensor networks. *Symmetry* 10, 10 (2018), 498.

# Deep learning architectures for Brain Tumor detection: A Survey

Divya K S
Research Scholar, KTU
Department of CSE
Adi Shankara Institute of
Engineering and Technology
Kalady, Kerala.
divya.it@adishankara.ac.in.

Dr. Manish T I
Professor, Department of CSE
SCMS School of Engineering
and Technology, Kerala.
manish@scmsgroup.org

*Abstract*-Deep learning methods are used in various fields of medical imaging like medical image localization/Detection segmentation, classification, and registration. Various medical conditions can be detected, monitored, and treated with deep learning techniques. One such condition is brain tumors. The main cause of brain tumors is the fast and uncontrolled development of brain cells. Over time, numerous techniques for detecting brain tumors have been developed. Manual analysis of brain tumor images will be time-consuming and it requires expert radiologists. Deep learning techniques can solve this issue since it is a fully automated process. Various deep learning architectures are used nowadays for different pattern recognition tasks in medical imaging. This survey aims to deliver different recent deep learning models developed to detect brain tumors and to present the drawbacks of existing techniques.

*Keywords*—Deep learning (DL), Transfer Learning (TL), Reinforcement Learning (RL), Evolutionary Algorithms (EA) Convolutional neural networks (CNN), Medical Images, and classification.

## I. INTRODUCTION

In medical systems, the analysis of medical image services is significant in many fields like Magnetic Resonance Imaging (MRI), Radiography, endoscopy, Computed Tomography, Mammography Images, Ultrasound images, Positron Emission Tomography (PET), etc. Due to the lack of radiologists, manually analyzing medical images requires a significant amount of effort. Thus emerges different deep learning models for analyzing medical images. The most significant models are Convolutional neural networks which belong to the category of supervised deep learning algorithms. Unsupervised algorithms mainly include Generative Adversarial Networks (GAN) and Autoencoders.

The unregulated development of brain cells leads to brain tumors. It needs to be detected at an early stage. To plan the treatment and to improve patients' survival rates, brain tumor identification at an early stage is necessary. There are different types, features, and treatments available for brain tumors. So manual brain tumor detection is susceptible to error. Here comes the significance of automated analysis of brain tumor images implemented with the help of deep learning architectures.

Benign and malignant tumors are the two main types of brain tumors. The benign tumor is not life-threatening and does not affect the surrounding tissues. But the malignant tumor is harmful and will spread into surrounding tissues. World health organization classifies brain tumors into four groups namely Metastatic, Meningioma, Glioblastoma, and Astrocytoma. For cancer/ tumor diagnosis various imaging modalities can be used. But compared to CT, MRI is safer because it uses high-density magnetic fields, which are non-toxic to analyze body parts. Several studies were done for classifying the tumors in the brain. They are based on pre-trained models of different CNN variants. Some of them developed the models from scratch. In some of the works transfer learning technique was implemented. Deep learning models were mainly used for extracting features from medical images and for classification machine learning techniques were used. This paper aims to deliver recent deep learning architectures used for brain tumor detection and also presents various databases used, their accuracy, and finally their drawbacks.

## II. DEEP LEARNING TECHNIQUES FOR BRAINTUMOR DETECTION

Woźniak et al. [1] presented a new learning technique known as correlation learning.It consists of CNN and artificial neural network (ANN)together in the training phase. Palettes of CNN architecture were used to get the best possible result. A parallel processing model was used to implement this technique where a multithreading mechanism chooses thenumber of threads. This model obtained an accuracy of 96%.

Sadad et al. [3] introduced brain tumor detection using Unet. The base model was ResNet50. To get accurate results on smaller data sets, data augmentation is performed. An optimized framework called NASNet is used for optimization tasks. This method relies on the concept of the idea of EA also and RL. It also compares NASNet Model with recently evolved brain tumor classificationmethods. Data used is from Figshare, which is a publically available brain tumor data set containing three tumor types. The accuracy of this model is 99.6%.

Mesut et al. [4] presented a detection technique for classifying tumors. The data set employed includes two labels, normal images, and

abnormal images. This detection technique consists of three techniques. The first one is attention modules, the second one is hyper column technique and the third is residual blocks. Relevant areas on the brain MR imagecan be analyzed by attention modules. Residual blocks are used to make the gradients smooth. The hypercolumn retrieves features from the previous layers and significant features can be selected. For this, the model saves the series of activation maps of each pixel of the images. Finally, it is converted to an array. The dataset used is BRATS. This model has an accuracy of 96.05.

Sajja et al. [6] implemented a hybridized CNN classier for the identification of brain tumors. Hybridized CNN model is used for classification. It consists of 10 layers including a fully connected layer. The activation function used is RELU. The data set used isBRATS and obtained an accuracy of 96.1

Kang et al. [7] presented a model for classifying brain tumors using ML and model combination schemes. In this model deep features are extracted using a pre-trained model and transfer learning techniques. ML techniques are used to select the best features and the top three features whichhas the highest score are selected and combined to form ensemble features. These ensemble features are fed to different ML classifiers for prediction. The model is compared with 13 pre-trained models and achieved the greatest accuracy of 98.83.

Çinar et al. [10] proposed a deep learning network using CNN to perform tumor detection. The base model used was Resnet 50. From the Resnet50 model, the last5 layers have been removed. In addition to that 10 newlayers were added. The accuracy of this model was 97.2%. Additional layers added mainly consist of drop out, Relu, Max pooling, Fully Connected, Softmax, and Classification layers. Brain tumor images are also classified using various pre-trained models and found that accuracy was high for this hybrid model.

Deepak et al. [12] implemented a classification system to classify three types of brain tumors. In this method modified Google Net model was implemented to extract the features. The features are then classified using classifiers support vector machines and the KNearest neighbor classifier.

Saba et al. [13] implemented a Grab cut method to separate tumors using MRI. In this method, deep features were extracted using VGG Main features of the image such as LBP and HOG are manually extracted. Both deep features and manually extracted features are combined. The combined features are given to different ML classifiers for classification and the SVM classifier gives the greatest classification accuracy.

Mohsen et al. [14] proposed a classifier that is a combination of two techniques. The first one is the discrete wavelet transform (DWT) method and the second one is the principal components analysis (PCA). For feature extraction, DWT is used and for feature reduction, PCA is used. Tumors were segmented using the Fuzzy C-means technique. Finally, for classification Deep Neural networks were used. The

accuracy of this model was 96.97 which is high compared to traditionalclassifiers like KNN and LDA.

Raza et al. [16] developed an architecture known as DeepTumorNet which will classify three types of tumors. The base architecture for this model was the pre-trained model GoogLeNet. In this classification model, the last five layers of GoogLeNet were removed, and new 15 layers were introduced in addition to those five layers. The activation function usedwas a leaky ReLU. The accuracy of this model was 99.67, which is the highest compared to the accuracy of other pre-trained models.

Alanazi et al. [18] implemented a deep learning model based on transfer learning for detectingpituitary, meningioma, and glioma-type tumors. Three CNN models were developed from scratch whichconsists of nineteen, twenty-two, and twenty-five layers respectively. 22-layer isolated CNN gives the highest accuracy.

Ayadi et al [22] presented a new CNN architecture for classifying tumors which is powerful in extracting features of MRI datasets. This model uses 3x3 kernels for convolutional layers. The size of theinput image is 256 × 256. For extracting features 10 convolutional layers are used. The activation functions used are Sigmoid, ReLu, leaky ReLU, and ELU. Thedata set used is Figshare Dataset, Radiopaedia Dataset, and REMBRANDT Dataset. Data augmentation was performed before classification to improve accuracy.

Sharif et al [25] implemented a pre-trained model Densenet201 for feature extraction. For improved feature extraction. This paper uses two methods. The first technique is the Entropy-based method and the second method is based on genetic algorithms. The deep features are further filtered using the threshold function. Classification is performed using. The data sets used are the SVM classifier. BRATS2018 and BRATS2019 are the data set used and the accuracy of themodel was 99%.

Kumar S et al. [26] presented an improved CNN technique for classifying tumors in the brain. The main steps in this model were preprocessing of images, segmentation of the affected region, feature extraction, and finally classification. For segmentation fuzzy deformable fusion model is used. For extracting features LBP model is used and finally, the deep CNN model is used for classification. The data sets used areBRATS and SimBRATS and got an accuracy of 96.3%.

Abd El Kader et al. [27] implemented a CNN model with five convolutional layers and five pooling layers. To identify an object basic features such as edges and corners and differential convolution feature maps are employed. The dataset used was obtained from TUCMD .The accuracy obtained with this model was 99.25.

TABLE 1 gives an overview of various deep learning architectures for brain tumor detection, their accuracy, and their drawbacks.

TABLE 1. OVERVIEW OF DIFFERENT DEEP LEARNING ARCHITECTURES FOR
BRAIN TUMOR DETECTION

| Sl No: | Reference | Year | Dataset | Method/ Model used | Application | Accuracy | Drawbacks |
|---|---|---|---|---|---|---|---|
| 1 | [25] | 2022 | BRATS2018 and BRATS2019 | Densenet201 | Multimodal brain tumor classification | 99 | The accuracy of the model is affected due to the reduction in features .Computational time is increased due to fusion process. |
| 2 | [18] | 2022 | [19],[20],[21] | Isolated CNN | Classification of glioma, meningioma and pituitary tumors | 95.75 | Model complexity is increased |
| 3 | [16] | 2022 | CE-MRI dataset[17] | GoogLeNet | Classification of three types of tumors namely glioma, meningioma, and pituitary tumors | 99.67 | Total layers after modification increased from 144 to 154 |
| 4 | [22] | 2021 | Figshare Dataset[2],Radiopaedia Dataset[23], REM BRANDT Dataset[24] | CNN | Classification of three types of tumors namely glioma, meningioma, and pituitary tumors | 98.43 | Training and testing time not specified |
| 5 | [27] | 2021 | TUCMD | Differential deep-CNN | Classification oftumor and non-tumor cells | 99.25 | Preprocessing of images not mentioned  Training and testing time not specified |
| 6 | [1] | 2021 | [2] | CNN, ANN | Brain tumor detection | 96 | The developed training model was based on multithreading and its performance depends on the CPU |
| 7 | [7] | 2021 | [5],[8],[9] | Ensemble learning | Brain tumor detection | 98.83 | Image augmentation is required since the data set is small |

## III. CONCLUSION

In this paper various recently developed deep learning architectures for brain tumor detection have been studied. In all the above methods either the model is developed from scratch or applied the technique of transfer learning for the classification of brain tumors. Some of the challenges mentioned in the above papers are small data set, imbalanced data set, and lack of annotated medical images. The challenges can be resolved by efficient data augmentation and unsupervised deep learning techniques. Thus deep learning methods have great significance in the area of analyzing medical images and are applied in various challenging areas.

## REFERENCES

[1] Woźniak, Marcin, Jakub Siłka, and Michał Wieczorek. "Deep neural network correlation learning mechanism for CT brain tumor detection." *Neural Computing and Applications* (2021): 1-16.

[2] Cheng, Jun (2017): brain tumor dataset. figshare. Dataset. https://doi.org/10.6084/m9.figshare.1512427.v5

[3] Sadad, Tariq, et al. "Brain tumor detection and multi-classification using advanced deep learningtechniques." *Microscopy Research and Technique*84.6 (2021): 1296-1308.

[4] Toğaçar, Mesut, Burhan Ergen, and Zafer Cömert. "BrainMRNet: Brain tumor detection using magnetic resonance images with a novel convolutional neural network model." *Medical hypotheses* 134 (2020): 109531.

[5] Chakrabarty N. Brain MRI Images for BrainTumor Detection | Kaggle n.d. https://www.kaggle.com/navoneel/brain-mri- images-for-brain-tumor-detection (accessed June10, 2019).

[6] Sajja, Venkata Rama Krishna, and Hemantha Kumar Kalluri. "Classification of Brain Tumors Using Convolutional Neural Network over Various SVM Methods." *Ingénierie des Systèmesd Inf.* 25.4 (2020): 489-495.

[7] Kang, Jaeyong, Zahid Ullah, and Jeonghwan Gwak. "Mri-based brain tumor classification usingensemble of deep features and machine learning classifiers." *Sensors* 21.6 (2021):

[8] https://www.kaggle.com/ahmedhamada0/braintumor-detection .

[9] https://www.kaggle.com/sartajbhuvaji/brain- tumor-classification-mri (accessed on 1 August2020)

[10] Çinar, Ahmet, and Muhammed Yildirim. "Detection of tumors on brain MRI images using the hybrid convolutional neural network architecture." *Medical hypotheses* 139 (2020): 109684

[11] Kaggle, https://www.kaggle.com/datasets.

[12] Deepak, S., and P. M. Ameer. "Brain tumor classification using deep CNN features via transfer learning." *Computers in biology and medicine* 111 (2019): 103345

[13] Saba, Tanzila, et al. "Brain tumor detection using fusion of hand crafted and deep learning features."*Cognitive Systems Research* 59 (2020): 221-230

[14] Mohsen, Heba, et al. "Classification using deep learning neural networks for brain tumors." Future Computing and Informatics Journal 3.1 (2018): 68-71

[15] http://www.med.harvard.edu/AANLIB/home.htm

[16] Raza, Asaf, et al. "A Hybrid Deep Learning-Based Approach for Brain Tumor Classification." Electronics 11.7 (2022): 1146.

[17] BT. Data Set. Available online: https://figshare.com/articles/dataset/brain_tumor_ dataset/1512427

[18] Alanazi, Muhannad Faleh, et al. "Brain tumor/mass classification framework using magnetic-resonance-imaging-based isolated and developed transfer deep-learning model." Sensors 22.1 (2022): 372.

[19] Jun, C. Brain Tumor Dataset. 2017. Available online:https://figshare.com/articles/dataset/brain_tumor _dataset/1512427

[20] https://www.kaggle.com/ahmedhamada0/brain- tumor-detection/metadata

[21] Bhuvaji, S.; Kadam, A.; Bhumkar, P.; Dedge, S.;Kanchan, S. Brain Tumor Classification (MRI) Dataset. 2020.Availableonline: https://www.kaggle.com/sartajbhuvaji/brain- tumor-classification-mri

[22] Ayadi, W., Elhamzi, W., Charfi, I., & Atri, M. (2021). Deep CNN for brain tumor classification. *Neural Processing Letters*, *53*(1), 671-700

[23] Radiopaedia. https ://radiopaedia.org/

[24] Clark K, Vendt B, Smith K, Freymann J, Kirby J, Koppel P, Tarbox L (2013) The cancer imag-ing archive (TCIA): maintaining and operating apublic information repository. J Digit Imaging 26(6):1045–1057

[25] Sharif, M. I., Khan, M. A., Alhussein, M., Aurangzeb, K., & Raza, M. (2022). A decision support system for multimodal brain tumor classification using deep learning. *Complex & Intelligent Systems*, *8*(4), 3007-3020

[26] Kumar, S., & Mankame, D. P. (2020). Optimization driven deep convolution neural network for brain tumor classification. Biocybernetics and Biomedical Engineering, 40(3), 1190-1204.

[27] Abd El Kader, I., Xu, G., Shuai, Z., Saminu, S., Javaid, I., & Salim Ahmad, I. (2021). Differential deep convolutional neural network model for brain tumor classification

# Comparative Performance Evaluation of Wire-bonded Micro Heat Pipes with Acetone and Water as Working fluid

Back to Results

**Publisher: IEEE**  Cite This  📄 PDF

Rag R L ; Rupesh S    All Authors

43
Full
Text Views

**More Like This**

Analytical methods for estimating equivalent thermal conductivity in impregnated electrical windings formed using Litz wire

2017 IEEE International Electric Machines and Drives Conference (IEMDC)

Feedback

**Abstract**

Document Sections

I. Introduction

II. FORMULATION

III. SOLUTION

**Abstract:**

Thermal management of high-heat-flux dissipation-rate micro-electro-mechanical systems (MEMS) using micro heat pipes is an exciting new field. Desktop computers are cooled using heavy metal sinks and fans. Wire sandwiched micro heat pipes are analysed computationally; they are a novel type of micro heat pipe that uses an array of wires sandwiched between two metallic plates to create the flow channels. Work fluid is carried through the system by the sharp corners between the wires and plates, which serve as liquid arteries. The temperature

II. FORMULATION

III. SOLUTION
PROCEDURE

IV. THE
TEMPERATURE
PROFILE

V. PERFORMANCE
EVALUATION

Show Full Outline ▾

Authors

Figures

References

Keywords

Metrics

they are a novel type of micro heat pipe that uses an array of wires sandwiched between two metallic plates to create the flow channels. Work fluid is carried through the system by the sharp corners between the wires and plates, which serve as liquid arteries. The temperature distribution in the micro heat pipes is obtained by solving the numerical model with a finite difference approach. By calculating effective thermal conductivity values from the temperature profiles, we can compare the heat pipe's performance using acetone and water as the working fluid. With an effective thermal conductivity of 168.83 kW/m$^2$ K, acetone shows substantial improvement over water in heat pipes.

formed using Litz wire

2017 IEEE International Electric Machines and Drives Conference (IEMDC)

Published: 2017

Effective Thermal Conductivity Calculation and Measurement of Litz Wire Based on the Porous Metal Materials Structure

IEEE Transactions on Industrial Electronics

Published: 2020

**Show More**

**Published in:** 2022 International Conference on Innovations in Science and Technology for Sustainable Development (ICISTSD)

**Date of Conference:** 25-26 August 2022    **DOI:** 10.1109/ICISTSD55159.2022.10010562

**Date Added to IEEE *Xplore*:** 13 January 2023    **Publisher:** IEEE

▾ **ISBN Information:**    **Conference Location:** Kollam, India

**Electronic ISBN:**978-1-6654-9936-1

**Print on Demand(PoD)**
**ISBN:**978-1-6654-9937-8

# Comparative Performance Evaluation of Wire-bonded Micro Heat Pipes with Acetone and Water as Working fluid

Rag R L
*Mechanical Engineering*
*SCMS School of Engineering and Technology*
Cochin, India
ragrajanl@gmail.com

Rupesh S
*Mechanical Engineering*
*PES College of Engineering,* Mandya
Karnataka, India
mailtorupeshs@gmail.com

*Abstract—* **Thermal management of high-heat-flux dissipation-rate micro-electro-mechanical systems (MEMS) using micro heat pipes is an exciting new field. Desktop computers are cooled using heavy metal sinks and fans. Wire sandwiched micro heat pipes are analysed computationally; they are a novel type of micro heat pipe that uses an array of wires sandwiched between two metallic plates to create the flow channels. Work fluid is carried through the system by the sharp corners between the wires and plates, which serve as liquid arteries. The temperature distribution in the micro heat pipes is obtained by solving the numerical model with a finite difference approach. By calculating effective thermal conductivity values from the temperature profiles, we can compare the heat pipe's performance using acetone and water as the working fluid. With an effective thermal conductivity of 168.83 kW/m$^2$K, acetone shows substantial improvement over water in heat pipes.**

*Keywords- acetone, effective thermal conductivity, micro heat pipe, water*

Nomenclature

| | | |
|---|---|---|
| *A* | = | *area of cross-section in m$^2$* |
| *k* | = | *thermal conductivity in W/m K* |
| *L* | = | *length of the heat pipe in m* |
| *Q* | = | *heat in W* |
| *q* | = | *heat flow rate in W/m$^2$* |
| *T* | = | *temperature in K* |
| *ΔT* | = | *temperature difference, $T-T_{amb}$ in K* |

Subscripts

| | | |
|---|---|---|
| *c* | = | *cross-section* |
| *eff* | = | *effective* |

## I. Introduction

Progress in modern technology is often driven by innovations in microelectronics, aims at progress in the ability of computing with improvement in speed of processing, and reduction in the size of components and devices. The challenges in the miniaturization of silicon components and the enhancement of their performance have led to the development of high-power electronic devices and CPUs with high packing densities. This has opened the way for the advancement of electronic devices with very high levels of heat generation rates, for a variety of industrial applications. As modern electronics demands very rigid specifications regarding miniaturization, reliability and power-component density, optimal thermal management of microelectronics has become a key issue for the designer and the engineer in recent times.

In general, for cooling electronic devices, there are many existing conventional methods. Passive air cooling is one basic way of cooling electronic devices, where the convective currents occur without the support of external power. The difference in temperature and subsequent changes in the density of the medium causes the flow. Forced air cooling systems are used as a common method for cooling in CPUs, where a fan will enhance the flow over the heat sinks for effective cooling. Liquids like water are used in forced liquid systems which are another set of cooling techniques used in electronic cooling. Of all the three methods, the second one has a prominent usage in electronic cooling due to its simplicity in design and manufacturing and cost-effective nature. Though the method is common and simple, bulky heat sinks utilize more material for manufacturing. The fan also increases the dust deposit over the components which in turn forms to be an insulator as the thickness of the deposit increases.

To remove heat from the source with smaller dimensions to a remote location, micro heat pipes are the best options. The micro heat pipe, as defined by Cotter (1984) has 'channels which are so small, that the mean curvature of the vapour–liquid interface is comparable in magnitude to the reciprocal of the hydraulic radius of the flow channel' [1]. Even though micro heat pipes poses evaporator, adiabatic and condenser sections and rely on the thermal phenomenon similar to that in conventional heat pipe [2], [3], they are physically distinct and compact from the former due to the absence of wick. In micro heat pipes, liquid arteries formed by the non-circular cross sections enables the transfer of working fluid from the condenser to evaporator sections. [7]. Micro heat pipes and heat spreaders continue to be the optimal solution for heat sinks and miniature equipments and devices respectively,

owing to their effective heat transport capability with trivial temperature gradient in the flow direction (high thermal conductance).

The wire-sandwiched micro heat pipe essentially consists of an array of channels, developed from sandwiching an array of wires within the metal plates. The ease in its construction, simple structure and adaptability to many heat-generating surfaces, made the micro heat pipes with wire bonds, a favorable option for cooling electronic devices. Each channel in the array acts as an individual micro heat pipe as depicted in Fig. 1. It comprises of an evaporator which is externally heated, an adiabatic segment devoid of any heat transfer and a condenser experiencing convective cooling. The area of cross-section of the liquid and the vapour change longitudinally from the evaporator end to the condenser end is displayed in Fig 1(c).

The conceptual wire-bonded micro heat pipes were initially presented by Wang and Peterson [4] as a one-dimensional analytical-steady-state model. The liquid-vapour phase interactions were analysed in the model and found the highest heat transfer performance. The fabrication easiness, better integration capability with electronic devices, and suitability for spacecraft applications were major attractions of the new model. The experimental validation in the studies proved the feasibility of the design and determined the optimum values for the design. The combination of aluminium - fluid acetone was used in the proposed design.

The performance investigation of a wire-bonded micro heat pipe array was done by Launay et al. [5]. A copper-water system was used to determine the capillary limitations in the temperature field and experimentally compare the charged micro heat pipes with empty channels. A numerical model was also used for predicting the effects of angle of contact, quantity of charge and fluid distribution.

To evaluate the efficiency of wire-bonded micro heat pipes, Rag and Sobhan [6] created a transient one-dimensional model. In order to derive the velocity, pressure, and temperature distributions, a fully implicit finite difference approach was used to solve the mass, momentum, and energy conservation equations. The efficiency of the wire-bonded micro heat pipe was determined by computing its effective thermal conductivity. Using the working fluid's constant thermo-physical properties, the equations accounted for longitudinal area fluctuations, phase shift, and frictional effects. Rag and Sobhan [7] used the same one-dimensional transient model to analyse the effects of operational and geometrical variables on effective thermal conductivity. Maximum values of effective thermal conductivity were achieved by optimising these parameters within the usable range. The transient variation of thermo-physical parameters was incorporated into a numerical model and quantitative measures of thermal conductivity were obtained by varying the input heat flux at the evaporator and condenser heat transfer coefficient by Rag et al. [8]. More realistic operational and performance characteristics were obtained when it comes to a wide variety of operational parameters.

In the present analysis, the temperature profiles are predicted computationally using an in-house code and evaluated the efficacy of a wire-bonded micro heat pipe which can be used for replacing the existing heat sink in a desktop computer. The already developed transient one-dimensional model is modified to accommodate two different working fluids, water and acetone, compatible with copper as the material of the micro heat pipes [2]. An experiment using acetone-aluminum system was used in a previous study [4] for validation of results in another study [6], acetone is considered as the second fluid for the present analysis. The dimension details of the micro heat pipes were listed in Table 1.
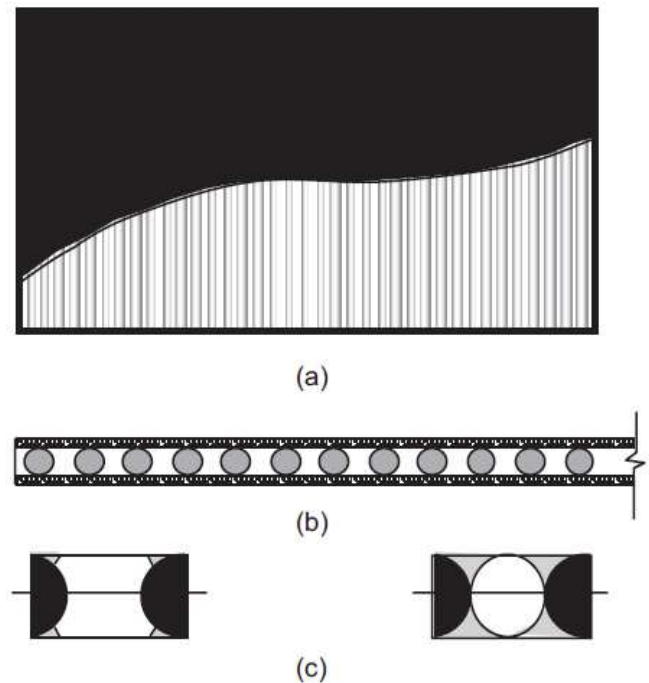


Fig. 1. Schematic of a wire sandwiched micro heat pipe

TABLE I.      PHYSICAL PROBLEM DETAILS

| Parameter | Value |
| --- | --- |
| Solid Material | Copper |
| Working Fluids | Acetone/ Water |
| Heat Pipe length | 125 mm |
| Wire radius | 0.8 mm |
| Wire-pitch | 2 mm |
| Evaporator length | 20 mm |
| Adiabatic section length | 85 mm |

## II. FORMULATION

Line connections are only present at either end of the wires wedged between the parallel plates. Any two such wires

form a miniature heat pipe, with vapour flowing along the middle and liquid moving around the edges of the plate and wires. The wire-bonded micro heat pipe can be broken down into an evaporator section that takes in heat and releases it to the surroundings, an adiabatic section that does not exchange heat with anything else, and a condenser section that releases heat to the surroundings or the cooling media that is circulating around it. The analysis takes into account the fact that the vapour and liquid cross-sectional areas will change along the length. A one-dimensional numerical model is employed for transient analysis since the most significant changes in flow characteristics occur along the flow's longitudinal axis. These presumptions constitute the basis for the formulation of the governing equations:

    1. Vapor and liquid laminar flow.
    2. No-slip liquid and vapour boundary conditions.
    3. Vapor saturation.
    4. Meniscus radius of curvature consistency.

For a quasi-steady state, the Laplace Young equation can be used to connect the pressure differential between the liquid and vapour phases to the meniscus radius at a given axial point. Pressure, velocity, and temperature profiles are analysed to determine the micro heat pipes' efficiency by solving the equations for mass, momentum, and energy in differential form for the liquid and vapour phases. As a function of the radius of the meniscus, the longitudinal area of the liquid and vapour phases are accounted for in their respective governing equations. The equation of state establishes a connection between the vapour pressure and temperature, which is then restated in terms of vapour momentum to ensure convergence. The liquid pressure is approximated using the Hagan-Poisseuille equation, but for more converged results, the numbers are re-entered into the liquid momentum equation. Although triangle-shaped micro heat pipes [5, 9] use the same approach and mathematical formulation, the calculations must account for unique area characteristics. Previous papers contain the area parameters and the governing equations.

### III. SOLUTION PROCEDURE

A custom FORTRAN programme is used to implement a Finite Difference technique to solve the governing equations. The first and second-order derivatives in the finite difference formulation were calculated using central differences. The thermo-physical qualities that vary with temperature are accounted for in the programme. In addition to the conventional solution procedure's [6]-[8] phases, a new function is introduced to define the working fluid's characteristics. Choosing the working fluid allowed the code to make use of the fluid's temperature-dependent thermophysical features and produce more accurate predictions. The heat balance test and the grid independent test of the code were conducted and shown in the previous publications extensively [6].

### IV. THE TEMPERATURE PROFILE

In this analysis for acetone and water as working fluid, the input heat flux supplied is taken as 2.4 W/cm$^2$ and the coefficient of heat transfer in the condenser is taken as 650W/m$^2$K, which are reasonable values in electronic devices generating heat [6]–[8]. From Fig. 2 it is clear that the temperature profiles are as anticipated based on the previous literature [6]–[8]. The influence of the evaporator is observed in the smooth behaviour of temperature distribution at the evaporator-adiabatic junction and that of the condenser is seen at the adiabatic-condenser junction. Since the state equation is used to approximate vapour pressure, both vapour temperature and vapour pressure exhibit a consistent longitudinal fluctuation. Micro heat pipe performance is analysed by determining the effective thermal conductivity using the vapour temperature distributions.

### V. PERFORMANCE EVALUATION

To evaluate the relative performance of different micro heat pipe designs, researchers use effective thermal conductivity [6]–[8]. According to Fourier's rule of thermal conduction, it is defined as follows:

$$k_{eff} = \frac{Q}{A_c \frac{\Delta T}{L}} \quad (1)$$

Wire-bonded micro heat pipes using acetone as the working fluid are shown to have an effective thermal conductivity of 168.83 kW/mK, while water only has an effective thermal conductivity of 127.27 kW/mK. Acetone is showing better effective thermal conductivity in the selected heat flux input and heat transfer coefficient of a condenser.
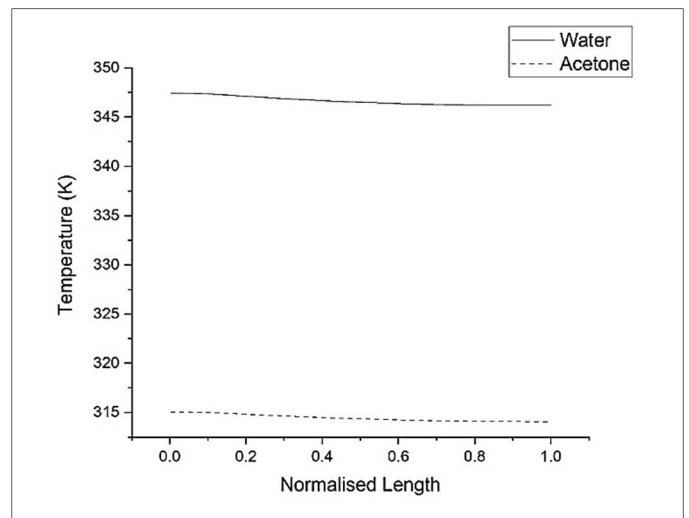


Fig. 2. Temperature profile for 2.4 W/cm$^2$ input heat flux and 650 W/m$^2$K condenser heat transfer coefficient

## VI. CONCLUSIONS

In order to compare the efficiency of wire-bonded micro heat pipes using acetone and water as working fluid and copper as material, a computational analysis is carried out.

Using a fully implicit finite difference approach, the mathematical model is solved to obtain the temperature profiles for both working fluids. With an effective thermal conductivity of 168.83 kW/mK, acetone proves to be a great medium for a heat pipe, outperforming even water.

### REFERENCES

[1] T. P. Cotter, "Principles and prospects for micro heat pipes," in *Proceedings of the 5th International Heat Pipe Conference*, Tsukuba, Japan, Jan. 1984, vol. 1984, pp. 328–335. Accessed: Apr. 27, 2022. [Online]. Available: https://www.osti.gov/biblio/5246927

[2] G. P. Peterson, *An introduction to heat pipes: modeling, testing, and applications*. New York: Wiley, 1994.

[3] C. Sobhan, R. Rag, and G. Peterson, "A review and comparative study of the investigations on micro heat pipes," *Int. J. Energy Res.*, vol. 31, pp. 664–688, May 2007, doi: 10.1002/er.1285.

[4] Y. Wang and G. Peterson, "Analysis of Wire-Bonded Micro Heat Pipe Arrays," *J. Thermophys. Heat Transf. - J THERMOPHYS HEAT Transf.*, vol. 16, pp. 346–355, Jul. 2002, doi: 10.2514/2.6711.

[5] J. P. Longtin, B. Badran, and F. M. Gerner, "A One-Dimensional Model of a Micro Heat Pipe During Steady-State Operation," *J. Heat Transf.*, vol. 116, no. 3, pp. 709–715, Aug. 1994, doi: 10.1115/1.2910926.

[6] R. L. Rag and C. B. Sobhan, "Computational Analysis of Fluid Flow and Heat Transfer in Wire-Sandwiched Microheat Pipes," *J. Thermophys. Heat Transf.*, vol. 23, no. 4, pp. 741–751, 2009, doi: 10.2514/1.44101.

[7] R. L. Rag and C. B. Sobhan, "Computational Analysis and Optimization of Wire-Sandwiched Micro Heat Pipes," *Int. J. Micro-Nano Scale Transp.*, vol. 1, no. 1, pp. 57–78, 2010.

[8] R. L. Rag, C. Sobhan, and G. Peterson, "Computational Analysis of Wire-Bonded Micro Heat Pipe: Influence of Thermophysical Parameters," *J. Thermophys. Heat Transf.*, vol. 32, pp. 1–8, Apr. 2018, doi: 10.2514/1.T5359.

[9] C. Sobhan and G. Peterson, "Modeling of the Flow and Heat Transfer in Micro Heat Pipes," Rochester, NY, Jan. 2004, pp. 883–890. doi: 10.1115/ICMM2004-2426.

Dean Vučinić
Vidya Chandran
Alam Md. Mahbub
C. B. Sobhan  *Editors*

# Applications of Computation in Mechanical Engineering

Select Proceedings of 3rd International Conference on Computing in Mechanical Engineering (ICCME 2021)

Springer

*Editors*
Dean Vučinić
(Editor-in-Chief), The Brussels School
of Governance
Vrije Universiteit Brussel
Brussels, Belgium

Vidya Chandran
Department of Mechanical Engineering
SCMS School of Engineering
and Technology
Ernakulam, India

Alam Md. Mahbub
Harbin Institute of Technology (Shenzhen)
University
Shenzhen, China

C. B. Sobhan
School of Materials Science
and Engineering
National Institute of Technology Calicut
Calicut, Kerala, India

# Contents

# A Review on Computational Techniques for Nanostructured Polymer Composite Materials

**G. R. Raghav** , **Gibin George** , **R. Sujith, and Nikhil Ashok**

**Abstract** This paper summarizes recent advancements in computational analysis of nanoparticle/nanofibers reinforced polymer matrix composites. The reinforcements vary from particle to fibers of varying shapes and sizes. In this review, various computational techniques such as computational micromechanics, integrated computational materials engineering (ICME) framework, and algorithms are discussed in detail. The multiscale modeling of polymer composites which includes mesoscale, microscale, nanoscale, and electronic scale modeling techniques can be carried out using various software packages available in the market. This review aims to explore the various research activities in polymer matrix composites using computational techniques for studying the microstructures and other mechanical behaviors which enables the readers for further exploration in this field.

**Keywords** Computational techniques · Polymers · Micromechanics · FEM

## 1 Introduction

In recent years, the utilization of polymer-based composites has increased drastically in the field of coatings, electronic devices, automobile, construction, and aerospace applications. Even though polymer-based composite materials have been widely preferred it has its disadvantages. The polymer matrix composites exhibit very poor toughness and thermal properties. Hence, many researchers are working to discover better mechanical properties from polymer matrix composites. In this process, many methods have been employed by the researchers such as trying new reinforcements such as nanoparticles, nanofibers, and nano cellulose. The addition of reinforcements has resulted in improving the properties such as micro-hardness, toughness, tensile strength, and thermal resistant properties. Even though the experimental studies are important and more works are there in exploring the properties of polymer-based composites, it is difficult to predict the mechanical properties through experimental

G. R. Raghav (✉) · G. George · R. Sujith · N. Ashok
SCMS School of Engineering and Technology, Ernakulam, India
e-mail: raghavmechklnce@gmail.com

# Optimisation of Parameters in Numerical Simulation of Hot Forging Using Taguchi Approach

**Sam Joshy, T. M. Anup Kumar, N. Nikhil Asok, R. Suraj, and Koshy P. Joseph**

**Abstract** Finite element analysis (FEA) is performed on the hot forging of a sample using DEFORM™ 3D in this research. The Taguchi method and Deform 3D simulation software was used to optimize the forging process. The responses to die stress in the hot forging process are investigated using Taguchi's $L_9$ orthogonal array to find the interactions and influences on the design parameters and process parameters such as die temperature, sliding velocity, and friction coefficient. For the simulations in Deform 3D, a design of experiment based on Taguchi's three-level, the three-parameter approach was used and was carried out on AISI 1025 steel, which is commonly used in making bolts. To ascertain the significant parameters of this operation, the Analysis of Variance (ANOVA) is utilized, and it was seen that the optimal factor settings for each performance characteristic were different. The results show that die temperature and die speed has the highest contribution in reducing die stress.

**Keywords** Forging · Deform 3D · Optimization · Taguchi analysis

## 1 Introduction

Forging, extrusion, and rolling are the most preferred manufacturing processes used for producing structural components [8, 13]. Forging is widely used to make near-net-shape parts with optimum material utilisation and superior mechanical properties.

S. Joshy · T. M. A. Kumar · N. N. Asok · R. Suraj · K. P. Joseph (✉)
SCMS School of Engineering and Technology, Ernakulam, India
e-mail: koshy@scmsgroup.org

S. Joshy
e-mail: samjoshy@scmsgroup.org

T. M. A. Kumar
e-mail: anupkumartm@scmsgroup.org

N. N. Asok
e-mail: nikhil@scmsgroup.org

R. Suraj
e-mail: surajr@scmsgroup.org

215

# Optimization of Geometrical Parameters in Magnetorheological Dampers Using Finite Element Modeling

**N. Nikhil Asok** ⓘ **, Sam Joshy** ⓘ **, R. Suraj** ⓘ **, Anjana Viswanath, and A. Rakesh**

**Abstract**  Magnetorheological (MR) dampers is widely used in semiactive vibration control in automobile suspension systems. The vibration control depends on the electromagnetic circuit used in these damping systems. To achieve the maximum damping performance, the geometric parameters of the piston is optimized. In the present work, a compact design of MR damper is presented, and optimization of geometric dimensions of the electromagnetic circuit is performed using design of experiments techniques. The pole length, inner radius and MR fluid gap are selected as factors, and the magnetic field density is taken as the response parameter. Amongst these factors, pole length has the highest contribution of 74.34 requires lower values of MR gap to produce highest damping characteristics.

**Keywords** Magnetorheological damper · Anova · Design of experiments · Taguchi · Optimization.

## 1  Introduction

Automobiles uses active suspension, in which these suspension systems uses an on-board system which responds according to the vertical movement of the body with respect to the chassis as against the passive systems which uses springs, the movement of which is controlled by road surface, whereas semi-active or adaptive suspension systems controls the damper properties to match with the road conditions. Such dampers uses solenoid valves (electrohydraulic dampers), and the damping is controlled by using fluids with controllable viscosity. Semi suspension systems offers higher reliability, versatility and adaptability of fully active damper, with a cost that is comparable to that of a passive system. Semi-active systems uses magnetorheological (MR) dampers. In these dampers, MR fluids are used to control damped vibration. These fluids comes under smart fluids, which allow electric or magnetic

N. Nikhil Asok (✉) · S. Joshy · R. Suraj · A. Viswanath · A. Rakesh
SCMS School of Engineering and Technology, Karukutty, India
e-mail: nikhil@scmsgroup.org

# Aerodynamic Analysis of Deployable Wing Arrangement for Space Shuttle

**Vidya Chandran** ⓘ**, Poornima Rajendran, Shabu Gopakumar,
K. S. Arun Kumar, C. A. Nikhilraj, and Sheeja Janardhanan** ⓘ

**Abstract**  The study space for morphing wings is astonishingly wide and provides ample scope for enhancements up against fixed wings. Morphing-wing research has accumulated considerable recognition in the aerospace community over the last decade, and a folding wing is a promising approach that can improve aircraft proficiency over multiple varieties of missions which conclusively enhance the capability of the space shuttle. In this paper, the conventional shape of the wings is being refashioned to serve the requirements for maintaining the flight and also for navigation. The idea was sparked by the traditional Japanese fan and has a hinged mechanism similar to that of the fan. This work introduces a novel concept for retractable dynamic wings on a space shuttle. Modeling of the spacecraft with modified wings is done in SOLIDWORKS. The aerodynamic analysis is performed using the computational fluid dynamics (CFD) method with ANSYS FLUENT® (2020 R1) as the solver. The aerodynamic force coefficients are estimated for five different specific deployment phases, viz., zeroth ($0°$), one quarter ($7.5°$), half ($15°$), three-quarter ($22.5°$), and full ($30°$) phases. The result reveals that the coefficient of drag drops and the coefficient of lift rises from the primary phase to the final phase providing promising inputs into the idea of retractable wings.

**Keywords**  Space shuttle · Retractable dynamic wings · CFD · Wing deployment

V. Chandran · P. Rajendran (✉) · S. Gopakumar · K. S. A. Kumar · C. A. Nikhilraj
Department of Mechanical Engineering, SCMS School of Engineering and Technology, Ernakulam, Kerala 683576, India
e-mail: poornimarar@gmail.com

V. Chandran
e-mail: vidyachandran@scmsgroup.org

S. Janardhanan
School of Naval Architecture and Ocean Engineering, Indian Maritime University, Visakhapatnam, Andhra Pradesh, India
e-mail: sheejaj@imu.ac.in

337

International Conference on Materials for the Millennium

MatCon-2023

January 12-14, 2023

# Conference Proceedings

Organized by

Department of Applied Chemistry

Cochin University of Science and Technology

Kochi-682022, India

Sponsored by

DST-SERB, DRDO, DBT, CUSAT

MatCon 2023

**Book of Proceedings**

**Publication Team**

Prof. (Dr.) K. N. Madhusoodanan, Vice Chancellor, CUSAT (Patron)
Prof. (Dr.) P. M. Sabura Begum, Head of the Department,
Department of Applied Chemistry (Chairman), CUSAT

**Editorial Board**
Prof. (Dr.) Manoj N. (Chief Editor)
Dr. Leena R. (Chief Editor)
Dr. Suja Haridas (Chief Editor)
Ms. Shamna S. (Associate Editor)
Ms. Athira M. P (Associate Editor)
**Members**

Prof. K. Girish Kumar
Pof. K. Sreekumar
Prof. P.V. Mohanan
Smt. Bindu S.
Prof. Yoosaf Karuvath
Ms. Sumi P. M.
Prof. Jayasree E. G.
Prof. Jayasree E. G.
Dr. Sebastian Nybin Remello
Ms. Devika S. R.

Dr. Kala R.
Ms. Amoolya Chandran
Dr. Manoj E.
Ms. Saranya P. K.
Dr. Sindhu Mathai
Ms. Athira K. S.
Prof. S. Prathapan
Dr. Sanu K. Anand
Dr.Shandev P. P.
Ms. Ansa Santu

MXene: Preparation, properties, and applications," *Front. Phys.*, vol. 10, no. 3, pp. 276–286, 2015, doi: 10.1007/s11467-015-0493-x.

5.  L. Li *et al.*, "Carbon Dot-Regulated 2D MXene Films with High Volumetric Capacitance," *Ind. Eng. Chem. Res.*, vol. 59, no. 31, pp. 13969–13978, 2020, doi: 10.1021/acs.iecr.0c01440.

6.  E. E. Elemike, J. Adeyemi, D. C. Onwudiwe, L. Wei, and A. O. Oyedeji, "The future of energy materials: A case of MXenes-carbon dots nanocomposites," *Journal of Energy Storage*, vol. 50, 2022, doi: 10.1016/j.e st.2022.104711.

## PP 36

## Copper(II) Based Potential Pharamaceutical Drugs Against Cancer

Nithya Mohan* [a,b], Sreejith S.S [a], M.R.P. Kurup[a], P.V.Mohanan[a]*

*[a]Department of Applied Chemistry, Cochin University of Science and Technology, Kochi 682 022, Kerala, India, [b]SCMS School of Engineering & Technology (SSET),Vidya Nagar, Palissery, Karukutty - 683 576, Kerala, India.*

*\*nithyanedumpilly@gmail.com.*

The report of the World Health Organization on cancer reveals some fearful results and the report says that in 2020, 10 million people have succumbed to death worldwide owing to this deadly disease and it is the second most common cause of death after cardiovascular diseases. The recent report of Freddie Bray et.al[1]

reveals that by 2040 the rate of this disease is expected to be increased to 28.4 million. So, there is a pressing need to develop a drug which could effectively interact and destroy the affected cell. Herein, we are reporting our work on the developement of a potential metallodrug based on tetradentate Schiff base.

We have systematically designed and synthesized four Cu(II) salen compounds (**1** to **4**) (Figure 1) and characterized using various spectroscopic and analytical techniques. The binding affinity of the complexes with CT-DNA was explored by UV-visible and fluorescence techniques. The compounds exhibit excellent DNA binding and cleavage activities. The binding mechanism were probed by molecular docking studies. These results display high binding constant values owing to the intercalative type of binding. In addition, binding affinity of the compounds with protein were also studied *via in silico* molecular docking method using Human Serum Albumin as receptors. Cleavage of DNA strands was investigated by gel electrophoresis. All the tested compounds show high binding constant value with both DNA and protein. Preliminary *in vitro* studies with L929 (a mouse fibroblast cell line) and HeLa cells (human cervical cancer cell line) indicated the cytotoxic effect of the complexes; however, detailed molecular studies may be required to confirm the mode of anti-cancer mechanism. Considering the results and comparing the existing reports[2-3], we are proposing a promising candidate (compound **4**) for the development of efficient therapeutic drugs.
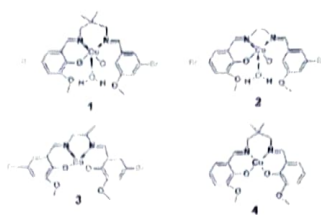
Figure 1. Synthesized pharmaceuticals drugs (**1-4**)

### References

1. S.S.Massoud,A.F.Louka,N.E.Bordelon,R.Fischer,F.A. Mautner, J.Vanco,J.Hošek,Z.Dvorak and Z.Travnicek, *New Journal of Chemistry,* **2019,** *43,* 6186-6196.

2. A.Paul, P.Singh, M.L.Kuznetsov, A.Karmakar, da Silva, B.Koch, A.J.Pombeiro, *Dalton Transactions,* **2021,** *50* (10), 3701-3716.

3. S.Banerjee, P.Ghorai, P.Brandão, D.Ghosh, S.Bhuiya, D.Chattopadhyay, S.Das, A.Saha, *New Journal of Chemistry,* **2018,** *42* (1), 246-259.

## PP 37

# Design and Development of Cobalt-based Single-Atom Catalyst for Efficient CO2 Utilization
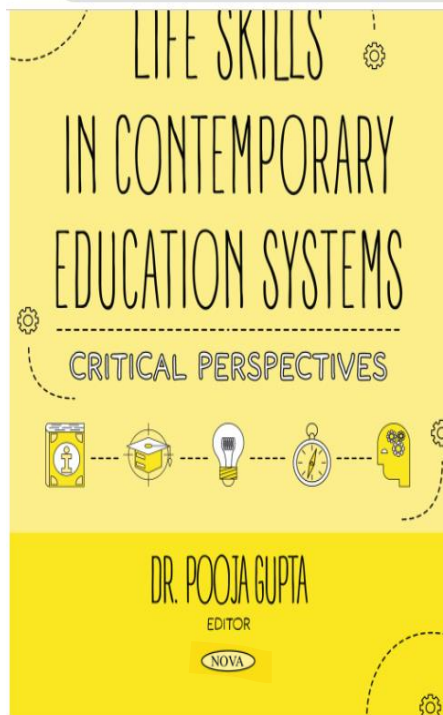
$82.00

**Pooja Gupta, PhD** – Assistant Professor, School of Liberal Studies, UPES, India

Life skills education has gained considerable momentum in recent times while grabbing the attention of education policymakers, researchers, and industry 4.0 for leading a more fulfilling life at personal as well as professional levels. This book is comprised of nine chapters written by experienced and passionate academicians and professionals from varied disciplines, which gives this book a multi-disciplinary outlook. The chapters include research pertaining to work-life balance, self-awakening techniques for overall development, and discussions on life skills essential for professional as well as personal growth. One of the focal points of the chapters is how to manage daily stress, develop stress reduction techniques, and understand the benefits of work-life balance confirming the research on the persuading elements of work-related stress and developing techniques to maintain work-life balance.

Binding

eBook    ⟳ Clear

Publication Date: April 20, 2023

[2]Sri Meenakshi Govt. Arts College for Women, Madurai, TN, India

**Chapter 5. Behavioural Economics and Emotional Quotient**

Pragati Bakshi

Assistant Professor in Economics, Yogoda Satsanga Mahavidyalaya, Ranchi, Jharkhand, India

**Chapter 6. Life-Skills Courses in an Indian Legal Education Framework**

Dr. Sujata Bali[1], Dr. Purnima Bali[2]and Bharti Nair Khan[1]

[1]School of Law, University of Petroleum and Energy Studies, Dehradun, India
[2]Department of English, Shoolini University, Solan, India

**Chapter 7. A 'Novel' Approach to Inculcating Life Skills**

Deepna Rao

Department of English, Jai Hind College (Autonomous), Affiliated with the University of Mumbai, Mumbai, India

**Chapter 8. Enhancing Life Skills in Learners of the New Age Economy**

Suruchi Sharma[1], PhD and Seema Verma[2], PhD

[1]School of Management, Graphic Era Hill University, Dehradun, Uttarakhand, India
[2]School of Aviation, Banasthali Vidyapith, Tonk, Rajasthan, India

**Chapter 9. Self-Awakening: An Important Life Skill**

Beena Puthillath

Department of EEE, SCMS School of Engineering and Technology, Ernakulam, Kerala, India

Index

# Malware Detection using Dynamic Analysis

Anandhi V[1], Vinod P[2], Varun G Menon[3], Abhijith Krishna E R[4], Akshay Shilesh[5], Akshay Viswam[6], and Amin Shafiq[7]

[1,3-7]Department of Computer Science and Engineering, SCMS School of Engineering and Technology, Ernakulam.
[1,3-7]Affiliated to APJ Abdul Kalam Technological University, Thiruvanthapuram, Kerala, India.
[2]Department of Computer Applications, Cochin University of Science and Technology, Kerala, India.
Email: [1]anandhi@scmsgroup.org, [2]vinod.p@cusat.ac.in, [3]varunmenon@scmsgroup.org, [4]abhijith.krishna@scmsgroup.org

*Abstract*—**Malware detection is an indispensable factor in the security of internet-oriented machines. The number of threats have been increased day by day. Malware analysis is a process of performing analysis and a study of the components and behavior of malware. The use of dynamic analysis will help the system to classify malware more accurately and to detect any malware samples. Dynamic analysis is a method in which the malware runs in a Sandbox environment, and artifacts are collected. The system uses Cuckoo Sandbox for executing the malware samples in a controlled environment. The system compares bidirectional long short-term memory and convolutional neural network models for machine learning algorithms to detect and classify the malware samples. Unlike a typical signature-based detection, where patterns are checked in the source file, a type of static detection, here, dynamic analysis is used to extract necessary reports, which are then preprocessed to get features like dynamic link library (dlls), kernel module names, services used, etc. to try creating a list of text, which can explain the behaviour of the executable file. These are tokenized and embedded to obtain numerical data, which is passed to the models. The accuracy of trained models is compared, which describes the performance of the models on the dataset. Thus providing grounds for testing future models and later building a better detection system based on it.**

*Index Terms*—**malware analysis, cuckoo sandbox, bidirectional long short-term memory, dynamic analysis**

## I. INTRODUCTION

Malware is malicious software distributed over a network that infects, steals, examines, or performs any function an attacker desires. Nowadays, malware detection is important as it serves as an essential alert system for the computer's security against cyber threats. It is the process of identifying malware on a host system and determining whether the particular software is harmful or not. It prevents hackers from gaining access to the computer, and avoids risking sensitive data, altering system settings or contents, or propagating through the network. The best measures against malware are antivirus monitoring and firewall software. The number of malware has expanded at an unprecedented rate due to the extensive use of computer systems and networks. With the expanding usage of susceptible online systems and various operating systems, a growing variety of dangers is emerging. As a result, the issue is to locate and identify risks that can be generalized to avoid future attacks on computer systems.

According to the Symantec threat report [1], 4818 unique websites were victims of form jacking code. Every month,

stolen credit card data is sold for up to $2.2 million to cyber criminals. Similarly, McAfee Labs reported that the DarkSide ransomware has resulted in a policy issue between the US and Russia [2]. In 2022, the Trellix company reported that the cyber attackers used the Log4shell flaw, a software vulnerability, and attacked Ukrainian Infrastructure. There were several campaigns conducted for the cyber threats in the region of Eurasia against Ukraine and identified HermeticWiper. This malware steals digital certificates and gains write access to various low-level data structures on the organizations [3].

In the research carried out, the main contributions of this paper are as follows:

- We develop a malware detection system using Convolutional Neural Network over two benchmark malware datasets namely Malware Bazaar and VirusShare.
- We conduct experiments on images using BiLSTMs to classify malware. and show significant improvement in the performance of deep learning models.
- We compare our proposed system with the state-of-the-art approaches and found that a combination of CNN and BiLSTM achieved better classification results.

The paper is organized as follows. Section II discusses related work on static and dynamic analysis. Section III covers the motivation, methodology used including the BiLSTM architecture. In Section IV, we present our dataset used with the experimental results obtained. Finally, Section V concludes the paper, and we mention future work.

## II. RELATED WORK

In today's world, the vulnerabilities of computer systems are well exploited by cybercriminals. There are several types of malware detection methods [4–7]. They are (a) static detection (b) dynamic detection (c) hybrid (d) ML-based detection (e) DL-based detection and (f) visualization.

In the static malware detection method, a malware file is examined without running the program. The main advantage of the static feature extraction method is that it reduces the feature size by considering the entire binary content, thereby detecting the invariants before runtime [8]. Dynamic analysis involves running the malware executable file and analyzing its behavior to eliminate the infection or prevent it from spreading to other systems [9].

Zhang [10] proposes a deep learning architecture that includes both a CNN layer and an LSTM layer where API call sequences are used to train the model. The CNN model consists of filters, LSTM layer, a dropout layer, and lastly fully connected layer for classification. The proposed model achieved an accuracy of nearly 100%.

Mishra et al. [11] proposed a BiLSTM based model to classify malware in a cloud-based system. CNN layer is the basic block and the model is trained on system call sequences. An accuracy of 90% was achieved. They also made a comparison by substituting the BiLSTM for a normal LSTM layer which resulted in a worse case of detection.

Mcdole et al. [12] records and analyzes the behavior of malware executables using dynamic analysis. The information collected during execution is the memory access, API calls, and network communications.

Usman et al. [13] proposed a novel cyber security techniques on hybrid approach based on dynamic malware analysis that can identify malicious Internet Protocol addresses before communication. Huang et al. [14] propose a malware detection method based on malware visualization and deep learning. The static visualization images are generated by Cuckoo Sandbox. It is used to generate dynamic visualization images. Then form hybrid images that merge the static and dynamic images. Finally, the model train the hybrid images yielding a test accuracy of 92.50% for the hybrid approach.

A novel method for detecting malware by deep learning-based analysis was proposed by Liu et al. [15] on API calls. They used cuckoo sandbox and Filtering techniques were employed to extract the API calls sequence of malicious programs. A comparison on the experimental results with standard models were done. The proposed LSTM has the best performance for malware detection, reaching the accuracy of 97.85%.

Wu et al. [16] proposed an architecture with CNN integrated with attention block used to extract effective features of the load impact factors. Then prediction is forecasted by the LSTM combined with BiLSTM layers and found that the proposed method has better forecasting performance than the state-of-art approaches. Peng et al. [17] proposed a deep learning model based on Bi-directional long short-term memory, sine cosine algorithm, and complete ensemble empirical mode decomposition with adaptive noise for forecasting and found that the model obtained higher prediction accuracy than the existing models.

## III. PROPOSED METHOD

The overall method consists of five different modules namely, input data preprocessing, feature representation, feature encoding, feature extraction, and classification.

### A. Motivation

The motivation of this paper is that the traditional classification methods have to be improved as there is various limitation in static and dynamic methods. Dynamic malware analysis of new samples is highly time-consuming and requires proper tuning to achieve good performance with an acceptable result.
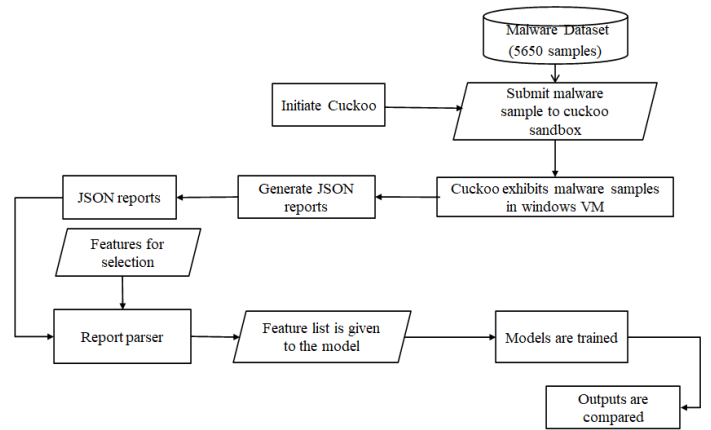


Fig. 1. Flow diagram of proposed system

### B. Methodology

Digital security is an important aspect of our daily life. This paper aims to contribute in the direction of classifying malware as accurately as possible. The proposed system is a malware classification system that uses BiLSTM and CNN model to analyse the behavior of malware samples in a controlled sandbox environment and have the model learn to properly identify a malware sample from a benign one. This system being dynamic, can actively classify malware that have not been classified before unlike current antivirus software. The samples are first fed into the sandbox and after receiving a log file containing the executed operations, it is fed into the models, and the results obtained are compared between the models. The proposed block diagram and its interconnection along with the various stages involved are depicted in Fig 1.

The significance of feature selection increases the accuracy and reduces the redundant features, thereby increasing the prediction time.

### C. Algorithm

The purpose is to parse the report.json files and extract wanted features into specific files. The input is the location to the output of dumps. The output is files written to the output directory which are text files that contain the features. The detailed step-by-step process is given in Algorithm 1.

### D. Cuckoo Sandbox

Basically, a cuckoo sandbox is a Linux Ubuntu host that in turn contains a nested Windows 7 machine in it [18]. The open-source tool called Cuckoo Sandbox is used to analyze malware automatically. This tool works in a controlled and secure environment. This tool makes an intention to the malware that it has affected a true host machine, which then records the malware activity. Finally generates a malware report on the activities done by the malware on the virtual machine (VM).

Linux commands or GUI can be used for accessing the cuckoo sandbox. The malware is submitted to the VM to the

**Algorithm 1** Parser Algorithm

**Require:** Iterate through each folder (classes) for batch folders

**Ensure:** For each file report file in each batch, perform the following steps to extract the features from JSON files

1: Extract dll from pe_imports
2: Extract name from pe_sections
3: Extract kernel_mod_name from modscan data
4: Extract service from svscan data
5: Extract proc_name from malfind data
6: Extract process from pslist data
7: Extract mut_name from mutscan data
8: Combine these values separated by newline

**Require:** Write output txt file with features for each malware sample in a fixed output directory

---

Windows guest. The malware once submitted runs on the VM. The malware behavior is recorded and this activity is fed to the Ubuntu host and a report is generated based on the activity.

### E. Bidirectional long short-term memory

Although LSTM is popular and has more advantages, it could not completely solve the vanishing gradient problem. This model uses more resources and takes more time to get trained. They use high memory and bandwidth because of the layers connected in serial fashion. Thus, LSTMs do not use the hardware efficiently.

LSTM requires more computation as more parameters are required. So Bidirectional long short-term memory or BiLSTM, is used. A Bidirectional Long Short-term Memory [19], is a model that processes information with two LSTMs in a forward and backward direction as shown in Fig. 2. The efficiency of the model is increased by understanding the context, which allows the model to learn the preceding and following words. Bidirectional recurrent neural networks are simply adding up two RNNs where one works forward and the other in a reverse direction.
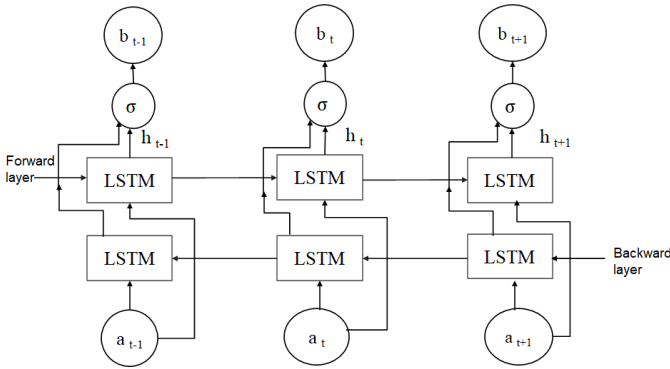


Fig. 2. BiLSTM structure

### F. Word Embedding

Word embedding is a technique where words of similar meaning are given the same pattern representation as real-valued vectors. There are fewer dimensions in this type of representation. This method is used to train on any natural language processing task as it is easy to understand.

### G. Text Vectorization

The process of converting text into numerical representation is Text Vectorization.

TF-IDF (Term Frequency–Inverse Document Frequency) captures the number of occurrences the word is available in the whole document. The words occurring frequently are given less weight. This inverse weighting for frequently occurring words is known as Inverse Document Frequency. This term gives the relative importance of words in a collection of texts or sets of documents. TF-IDF calculation is used in Natural Language Processing problems where the more frequently occurring words have less weight and words which are not repeated will have more weight. Let $w$ denote TF-IDF weight of any feature $x$, $tf(x)$ denote frequency of feature $x$, $N$ be the number of ransomware samples in the document, and $IDF$ denotes the instances that contain the feature $x$. The following steps are used for calculating TF-IDF as shown in Equation 1.

- Define the term frequency values
- Calculate inverse document frequency values (IDF)
- Multiply the above two values. This indicates how often the words occur in the document

$$w(x) = tf(x) * log\frac{N}{IDF(x) + 1} \qquad (1)$$

### H. Convolutional Neural Network

Convolutional neural networks have always become the predominant machine learning algorithm [20] since CNN is a simple feed-forward network that uses automatic feature extraction and uses adjacent pixel information to downsample the image effectively. CNN is a typical neural network in which at least one layer is a convolutional layer. In CNNs, with more hidden layers, the gradient vanishes which stops the learning phase.

## IV. EXPERIMENTAL RESULTS

The experiments are conducted using Precision, Recall, F1 measure, and Accuracy as evaluation metrics for the classification.

Categorical accuracy: Categorical accuracy measures the average accuracy rate across all predictions. This is calculated by comparing the one-hot vectors of truths and predictions and then taking an average over the vector. In the proposed system, accuracy is calculated using the metric given below for both training and validation.

$$Accuracy(A) = \frac{TP + TN}{TP + TN + FP + FN}. \qquad (2)$$

where True Positive ($TP$ - indicates the number of malware samples correctly identified as malware), True Negative ($TN$

- indicates the number of benign samples accurately identified as legitimate.), False Positive ($FP$ - is the number of benign samples misclassified as malware), and False Negative ($FN$ - indicates the number of wrongly classified malware images).

**Implementation and Setup:** The Linux OS system with Ubuntu 20.04 is installed on the Virtual Machine. The Cuckoo Sandbox and Python with windows are installed on a Virtual Machine. Now both OS can be used without using a separate boot system.

**Dataset:** The experiments are performed on two malware datasets, Malware Bazaar [21] and VirusShare [22]. In this paper, we used around 5650 executables belonging to 6 classes including 1471 benign samples. 70% of the dataset is used for training and the remaining 30% is reserved for testing. 3955 files for training and 1695 files for validation. A Windows operating system (OS) is installed in the cuckoo sandbox virtual machine and is used to extract the system calls from the malware executable samples.

By using the appropriate measures, the performance of the models is calculated. We conduct the three experiments on the dataset:

- **Experiment-1:** Performance of CNN model in detecting malware executables.
- **Experiment-2:** Performance of BiLSTM model in detecting malware executables.
- **Experiment-3:** Performance of CNN-BiLSTM model in detecting malware executables.

### A. Performance of CNN model in detecting malware executables

CNN model consisting of text_vectorization layer, word embedding, three CONV layers, each followed by a Pooling layer, Flattening, and finally the fully connected layer.

A convolutional neural network consists of the following layers:

- Convolutional layers - First layer is the convolution layer which is presented with training and testing malware images. A filter is convolved across the width and height of the input image to extract patterns specific to malware and benign files. Here the kernel size chosen is a $3\times3$ filter. The kernel is slided over the input and the product is computed at all positions. The convolution layer gives maximum information by reducing the noise in the input features. Parameters include stride, step filter size, and filter count, which is the number of filters used.
- Pooling layers - Next is the max pooling layer which reduces the data processing by taking the maximum value obtained in the first slide of the kernel. A $2\times2$ is the window size or the filter size used for the max pooling operation. Max pooling takes the maximum value from each group of neurons from the previous layer. This is also called the sub-sampling layer as the computation is performed by downsampling the features, thereby reducing the processing involved.
- Dense layers - Finally, the fully connected dense layer is incorporated where every neuron in one layer is con-
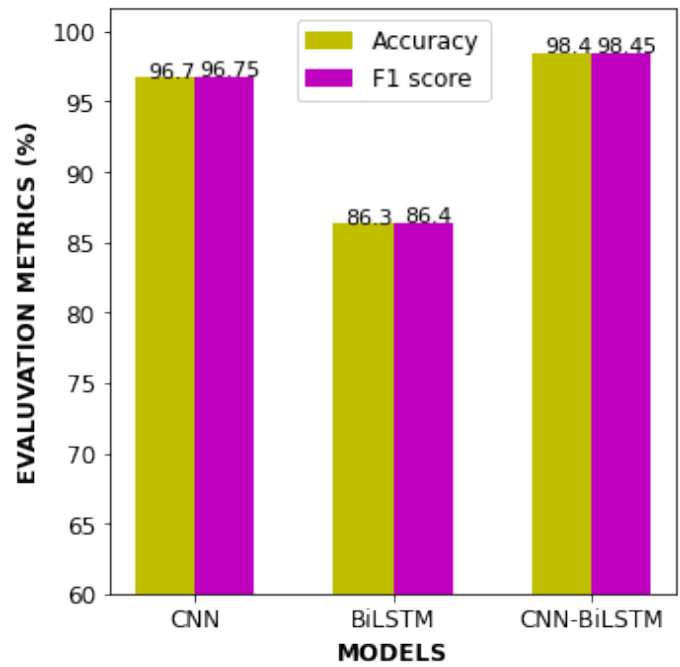


Fig. 3. Accuracy and F1 score for three models

nected to every other neuron in the other layer. The basic principle of CNN is the same as the multilayer perceptron. The flattened matrix after max pooling passes through the fully connected layer to classify the images. The network is trained by the back-propagation method where the weights and bias are updated and the loss is calculated. When the loss function is close to zero, the learning phase terminates.

The model produced an average accuracy of 96.7% as shown in Fig 3. Since the dataset is a balanced set, we get approximately the same scores.

### B. Performance of BiLSTM model in detecting malware executables

BiLSTM model consists of text_vectorization layer, input, embedding layer, two BiLSTM layers with dropout layers, and finally the dense layer. In the proposed model, the input to the BiLSTM is an array. By knowing the input, past, and future states of its local neighbors, BiLSTM can predict the present input. We have used a Dropout of 0.25 on the BiLSTM layer. Sigmoid is used as an activation function. Finally, the image vector representation passes through the dense layer. The activation function used by all feed-forward layers is Tanh and the final prediction is achieved using the softmax function. The model produced an average accuracy of 86.3% as shown in Fig 3.

## C. Performance of CNN-BiLSTM model in detecting malware executables

The proposed CNN-BiLSTM consists of text vectorization layer, an input layer, word embedding layer, two convolution layers, pooling layers (maxpool), BiLSTM layer, dropout layer, and finally the dense fully connected layer for classification. Figure 3 shows that the model produced an average accuracy of 98.4%.
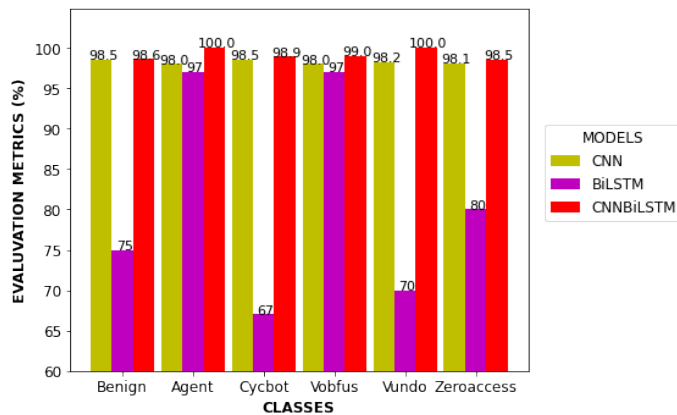


Fig. 4. Classification accuracy for three models

We considered 597 malware executables from agent, 936 from cycbot, 926 from vobfus, 600 from vundo, 1120 from zeroaccess malware families for the dynamic analysis, and 1471 benign files with a total of 5650 files belonging to 6 classes, where 3955 files were used for training and 1695 files for validation phase. Figure 4 shows the evaluation metrics for the six classes considered for all three models. It is observed that the average accuracy of 98.5% is obtained for a combination of CNN with BiLSTM for all families considered. The proposed model has shown efficient performance for the classification, which extracts useful features and better feature representation, resulting in achieving better accuracy.

## V. CONCLUSION AND FUTURE SCOPE

In recent times, the amount of malware affecting systems has become enormous and diverse in nature. Automating the detection and classification of new malware helps the forefront of defenders to rest a bit ease. The effectiveness of machine learning has encouraged peers to find methods to tackle this problem. The study here uses Dynamic analysis techniques to extract malware artifacts and process them using BiLSTM and CNN models and experiments with them to classify across five malware classes and a benign class. A combination of CNN-BiLSTM model produced an average accuracy of 98.4%. The CNN-BiLSTM model performs better than the BiLSTM model in classification and detection of malwares. There is a gradual increase in accuracy when compared with the other state of art methods.

In future work, we intend to include more models and more malware classes, specifically towards self-attention models to improve the overall accuracy further. We also intend to provide a web and android app interface, where one can submit a file, and get a report summary on the file, detecting any malicious instructions within the file. This would help the layman have free, and bleeding-edge access to a malware-detection system, which does not rely on signatures and similar concepts.

## REFERENCES

[1] https://docs.broadcom.com/docs/istr-04-march-en

[2] https://www.mcafee.com/enterprise/en-us/assets/reports/rp-ryuk-ransomware-targeting-webservers.pdf

[3] https://www.trellix.com/en-us/threat-center/threat-reports/apr-2022.html

[4] Roundy, Kevin A., and Barton P. Miller. "Hybrid analysis and control of malware", In International Workshop on Recent Advances in Intrusion Detection, pp. 317-338. Springer, Berlin, Heidelberg, 2010.

[5] Wang, Huanran, Weizhe Zhang, and Hui He, "You are what the permissions told me! Android malware detection based on hybrid tactics", Journal of Information Security and Applications 66, 2022.

[6] Ijaz, Muhammad, Muhammad Hanif Durad, and Maliha Ismail, "Static and dynamic malware analysis using machine learning", In 2019 16th International bhurban conference on applied sciences and technology (IBCAST), pp. 687-691, 2019.

[7] Nataraj, Lakshmanan, Sreejith Karthikeyan, Gregoire Jacob, and S. Manjunath, "Malware images: visualization and automatic classification", In Proceedings of the 8th international symposium on visualization for cyber security, pp. 1-7, 2011.

[8] Adel Abusitta, Miles Q. Li, Benjamin C.M. Fung, "Malware classification and composition analysis: A survey of recent developments", Journal of Information Security and Applications, vol. 59, 2021.

[9] Singh, Jagsir, and Jaswinder Singh. "A survey on machine learning-based malware detection in executable files." Journal of Systems Architecture 112, 2021.

[10] J. Zhang, "DeepMal: A CNN-LSTM Model for Malware Detection Based on Dynamic Semantic Behaviours," 2020 International Conference on Computer Information and Big Data Applications (CIBDA), pp. 313-316, 2020.

[11] Mishra, P., Khurana, K., Gupta, S., & Sharma, M. K., "VMAnalyzer: Malware Semantic Analysis using Integrated CNN and Bi-Directional LSTM for Detecting VM-level Attacks in Cloud", Twelfth International Conference on Contemporary Computing (IC3), 2019.

[12] Mcdole, Andrew & Gupta, Maanak & Abdelsalam, Mahmoud & Mittal, Sudip & Alazab, Mamoun, "Deep Learning techniques for Behavioral Malware Analysis in Cloud IaaS", 2020.

[13] Usman, Nighat, Saeeda Usman, Fazlullah Khan, Mian Ahmad Jan, Ahthasham Sajid, Mamoun Alazab, and Paul Watters, "Intelligent dynamic malware detection using machine learning in IP reputation for forensics data

analytics", Future Generation Computer Systems 118, pp. 124-141, 2021.

[14] Huang, Xiang, Li Ma, Wenyin Yang, and Yong Zhong, "A method for Windows malware detection based on deep learning", Journal of Signal Processing Systems 93, no. 2, pp. 265-273, 2021.

[15] Liu, Yingying, and Yiwei Wang, "A robust malware detection system using deep learning on API calls", In 2019 IEEE 3rd Information Technology, Networking, Electronic and Automation Control Conference (ITNEC), pp. 1456-1460, 2019.

[16] Wu, K., Wu, J., Feng, L., Yang, B., Liang, R., Yang, S., & Zhao, R., "An attention-based CNN-LSTM-BiLSTM model for short-term electric load forecasting in integrated energy system", International Transactions on Electrical Energy Systems, 31(1), 2020.

[17] Peng, T., Zhang, C., Zhou, J., & Nazir, M. S., "An integrated framework of Bi-directional long-short term memory (BiLSTM) based on sine cosine algorithm for hourly solar radiation forecasting", Energy, 221, 2021.

[18] Nunes, Matthew, Pete Burnap, Omer Rana, Philipp Reinecke, and Kaelon Lloyd, "Getting to the root of the problem: A detailed comparison of the kernel and user-level data for dynamic malware analysis", Journal of Information Security and Applications 48, 2019.

[19] Zhiyong Cui, Ruimin Ke, Ziyuan Pu, Yinhai Wang, "Deep Bidirectional and Unidirectional LSTM Recurrent Neural Network for Network-wide Traffic Speed Prediction", Computer and information sciences, 2018.

[20] Daniel Gibert, Carles Mateu, Jordi Planes, and Ramon Vicens, "Classification of Malware by Using Structural Entropy on Convolutional Neural Networks", The Thirtieth AAAI Conference on Innovative Applications of Artificial Intelligence, 2018.

[21] https://bazaar.abuse.ch/browse/

[22] https://virusshare.com

# Wearable Fabric Tactile Sensors for Robotic Elderly Assistance

Mary Catherine V G
*Division of Electronics*
Cochin University of Science and Technology
Cochin, India
marycatherinevg@cusat.ac.in

Binu Paul
*Division of Electronics*
Cochin University of Science and Technology
Cochin, India
binupaul@cusat.ac.in

Vinoj P G
*Department of ECE*
SCMS School of Engineering and Technology
Karukutty, India
vinojpg@scmsgroup.org

*Abstract*—**The demand for Robots in Elderly assistance is increasing due to the lack of human caregivers. In the context of Robot coexisting with the human beings in a home environment, for the safe and friendly interaction it is essential to endow the sense of touch through Tactile sensor systems. This paper proposes a novel scalable approach for tactile sensors based on low cost wearable conductive fabric. Fabric tactile sensor (FABTAC) is conformable with the robot body and can be used as a tactile sensing skin that perceives touch and force applied at the contact location. FABTAC sensors are developed as an array of touch sensors sewed on the cloth substrate with the stainless-steel conductive thread. The thermistor sensors are also sewed to fabric to perceive the temperature information. The FABTAC sensors are integrated on to the custom-made 3D printed Robotic hand and the tactile data is processed with a novel wearable electronic FLORA microcontroller platform. The acquired data can be used to provide a real time tactile feedback for performing assistive tasks like grasping objects of diverse profiles, avoiding slippage. The FABTAC sensors has the advantage of utilizing flexible, light weight sensors with good spatial and temporal resolution. Thus, the system can potentially aid the automation of daily life activities of the Elderly thereby enhancing the quality of their life.**

**Keywords—Tactile sensing, Human Robot Interaction, Wearable sensors, Fabric sensors, Tactile feedback**

## I. INTRODUCTION

The number of caregivers is not growing in tandem with the growth of the Elderly population. The high expense of elderly support is due to the relative scarcity of caregivers for the elderly. The enormous expense of providing care for the elderly could be significantly reduced by using robots in this scenario. Robots with a tactile sensing skin is required for interactions to be both secure and safe. Our human brain senses the touch with the somatosensory system containing a large network of nerve endings and touch receptors on skin, which transmit the tactile information to the brain which in turn tells the body how to react to different senses. The tactile sensors being the electronic counterpart of biological skin, enables the robot to perceive their environment and create a reactive behavior in response to human expectations.

Bioinspired, tactile sensing is important for robots which works in close interaction with the human beings as in elderly care applications. Tactile sensors can estimate the contact parameters like mechanical touch, pressure and temperature at the contact area [1].

Unlike the visual and auditory senses, human skin is not a localized sensory organ which makes the tactile sensing more challenging in terms of transduction technology [2]. And the sensors should be distributed throughout the body. As touch can take many forms-shapes, texture, force, pain, temperature it is not one physical property to be sensed which makes the sensor design more complex and thereby making it difficult to mimic the tactile sensing [3].

### A. Criteria for Selection of Tactile Sensors

The Criteria for selection of tactile sensors are reported below[3]

   a) Spatial resolution
   b) Contact Parameters to be measured
   c) Response profile
   d) Time resolution

### B. Transduction Techniques

Earlier, the research in the field of tactile sensing focused towards the transduction technology/sensor design.

Various tactile sensor systems have been proposed to cover the robot body for the grasping and manipulation of fine and fragile objects with dexterity. Capacitive tactile sensors are based on changes in the distance between the parallel plates on mechanical touch thereby changing capacitance. This effect can be utilized to detect static touch. They have high sensitivity and has a large dynamic range[4]-[7]. Piezoelectric tactile sensors works on piezoelectric effect where the materials generate an electrical voltage on application of external force . This effect can be utilized for dynamic touch sensing [9][10]. Optical tactile sensors utilizes changes in light intensity to detect external force applied at the point of touch as reported in [11][12].

## II. RELATED WORK

The human Interactive Robot RI-MAN [13] embedded with tactile sensors has been developed for assistive care applications to determine the contact load while carrying a dummy human. 320 tactile pressure-sensing elements are integrated on the body with each sensor sheet having 8 x 8 elements placed at the chest and forearms.

A tactile sensor suit, flexible and soft, that has 192 sensing regions has been proposed [14]. The designed robotic suit used electrically conductive cloth and string to build the sensor outfit. Each sensing region functions as a binary switch. The tactile sensing is based on a layered architecture.

A low-cost simple method has been reported [15] to transform a knitted glove to a scalable tactile glove with a sensor array of 548 sensors. The glove has a piezoresistive film connected to conductive thread electrodes. The glove can be utilised to recognise distinguish object and to estimate their weight while grasping.

A fabric-based stretchable tactile sensing skin to measure force and temperature parameters has been reported in [16]. The sensors were integrated on MEKA M1 Mobile Manipulator to make contact on the arms of human being which demonstrated the feasibility of the system for Human Robot Interactive environment.

## III. PROPOSED ARCHITECTURE

The Literature reports shows that the large area coverage of sensors at high spatial resolution comes at the expense of high cost technology requirements. This paper presents a novel low-cost approach to tactile sensors for robots based on conductive fabric which can sense human touch utilizing the capacitance transduction effects.

The experimental study was conducted towards creating a tactile sensing skin to perceive touch, force and temperature parameters at the contact area of touch. The work proposed here is the multimodal wearable approach to tactile sensing so as to utilize this tactile information for dynamic feedback control of robotic hand assistance to Elderly people.

The Hardware Configuration of Wearable FABTAC sensors integrated to robotic hand which can be used in grasping assitance for Elderly persons is shown in the Fig. 1.

The robotic hand can be operated in Grasp mode. For the grasp mode operation, dynamic control of hand is achieved based on the real time feedback from the FABTAC sensors to prevent slippage of objects grasped. This paper highlights on the work on the development and integration of FABTAC sensors on the custom made 3D printed InMoov Robotic Hand.

The wearable FABTAC sensors are developed as an array of tactile elements(taxels) with the Conductive Fabric touch sensors and Force Senstive Resistor(FSR) placed on the fabric substrate in a two layer architecture. The current version of the array consists of 12 taxels each of dimension 20mm x 20mm with a spatial resolution of 2 mm. The capacitive touch sensors detect the static touch in response to the human finger based on the predetermined threshold level.The FSR placed under the first layer of sensors seperated with the spacer estimates the force applied at the taxels corresponding to the resistance variation. The temperature sensors are sewed to the fabric to perceive the temperature of the human finger at the contact area.

The Fabric tactile sensor array consists of strips of woven conductive fabric, fabricated of Copper and Nickel-plated polyester has been sourced from Adafruit Industries.The tactile sensors are sewed to wearable microcontroller electronic platform -FLORA controller using stainless steel conductive thread which has a fairly low resistivity of 10 ohms per foot. The array structure can be scaled up for the full coverage of  the dorsal and palmar side of hand and the fingers of robotic hand.

FSRs placed below the fabric layer allows to detect physical pressure applied on its sensing region [Adafruit Industries].FSRs changes its resistive value depending on the external pressure applied on it.  The resistance change gives the calculation for the amount of force applied when touched.

NTC Thermistors are also sewed to the fabric substrate to estimate the temperature of the human finger when touched. The tactile data acquired by FABTAC sensors are given to the wearable FLORA microcontroller for further processing and Control action.

## IV. METHODOLOGY

The acquired touch sensor data are processed using a FLORA microcontroller which is a fabric friendly wearable electronic platform with ATMEGA 32u4 microcontroller having 14 sewing pads for electrical connections. The FLORA microcontroller is configured in slave mode and reduces the load of high level processing at the Arduino UNO Master controller. This configuration helps for better scalability when large area coverage of sensors on the robotic body is required.

The slave FLORA microcontroller transmits the touch data wirelessly using the module  nRF24L01 connected through SPI interface with a data rate of 100 Mbps. The nRF24L01 module is suitable for low power applications. At the receiver side, the tactile data is received using the nRF receiver module and fed to an Arduino Uno controller. For the Experimental study the touch response has been demonstrated using an LED display at the destination side. The Robotic hand with the integrated FABTAC sensors can be activated by elderly touch and dynamic control of the hand can be achieved based on reactive control feedback from the sensors in future work.
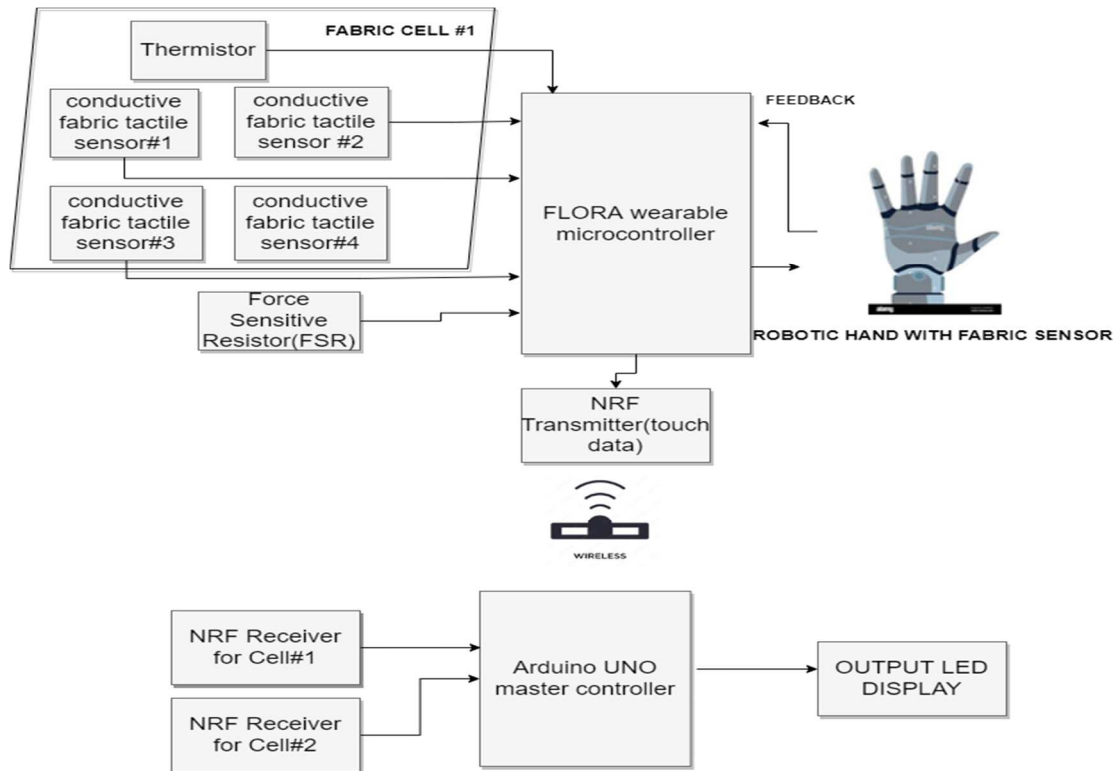
Fig. 1 Hardware Configuration set up of wearable FABTAC sensors for Robotic Hand control

## V. RESULTS AND DISCUSSION

The feasibility study of various flexible, light weight, fabric tactile sensors that can be incorporated to Robotic hand Elderly Assistance System has been conducted in this paper.

### a) Woven Conductive Fabric Touch Sensor

The experimental results show the response of Woven Conductive Fabric sensor to single finger static touch and a plastic pen. The touch detected with the human finger as shown in Fig 2 (a) has high sensitivity. The dielectric constant increases as a result of the finger's interaction with the capacitor's electric field, thereby increasing capacitance. It has also been inferred that the touch response can be obtained with two fingers simultaneously. The touch response of the plastic material with a low dielectric value could not detect the touch as depicted in Fig 2(b).

The Fig. 2(c) demonstrates the capacitive fabric sensors sewed on the cloth substrate using the conductive thread. The tactile data is fed to the digital pins of the sewing pad of FLORA. A simple hand running stitch is used for sewing the sensors and the microcontroller so as to allow the current flow through the conductive thread. The Fig 2(d) shows the response of touch using the neo pixel RGB LED's which are fabric friendly.
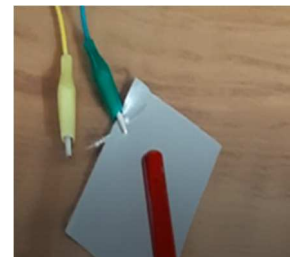


Fig. 2(a)



Fig. 2(b)



Fig. 2(c)



Fig. 2(d)

*Fig. 2(a) Single finger touch on Conductive Fabric sensor (b) Touch using plastic pen on Fabric sensor (c) Fabric sensors sewed to FLORA controller using stainless steel conductive thread (d) Touch response of sensor using neo pixel RGB LED*

### b) Velostat/ Pressure Sensitive sheet Sensor

The study of Velostat sensor was conducted to demonstrate a dynamic touch like vibration on the surface as shown in Fig. 3(a). Velostat is carbon impregnated polyethylene film which can be vibrated and a change in resistance corresponding to vibration was observed.

### c) Thermistor

The experimental study of interfacing NTC 10K thermistor with FLORA was conducted. The thermistor was sewed to the cloth substrate and the observations are obtained as in Table 1. Observations are made at Room temperature, soldering iron and a prolonged contact with single finger. It has been observed that the resistance decreases with the increase in temperature and a prolonged contact of finger on the thermistor recorded values as shown in the table. The equivalent temperature T is calculated using Stein Hart Equation as in (1)

$$\frac{1}{T} = \frac{1}{T0} + \frac{1}{B}\ln(\frac{R}{R0}) \qquad (1)$$

T0 is the Room temperature, B is Coefficient of thermistor, R0 is Resistance at Room temperature and R is unknown resistance calculated.

### d) Force Sensitive Resistor(FSR) Sensor

The Fig. 3 (b) shows experimental set up of FSR with a 38 mm square sensing region and the change in resistance when force applied at the touch point can be calculated. The resistance variation is converted to analog voltage with a base resistance of 10K. The figure 5 (a) shows the variation of Voltage and Resistance and it can be observed that the resistance decreases with the increase in voltage which corresponds to increase in force applied on the sensing region. The Fig 5(b) shows the Force vs Voltage variation and Fig 5 (c) demonstrates the change in Force vs Resistance. The various types of touch based on Force in Newtons has been indicated. The types of touch observed are Light touch with less than 1 N is recorded, Light Squeeze on the sensing square region showed up the Force between 2 N and 4 N, Medium Touch (5 -9 N) and Big Touch( 10- 66 N).
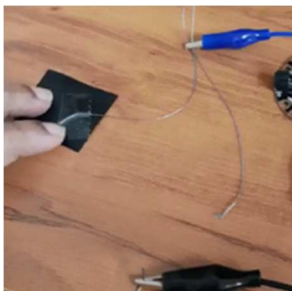
### e) Integration of FABTAC sensors on Robotic Hand

The hardware consists of custom - made 3D printed robotic arm InMoov with 2 DOF controlled using MG996R servos. The developed wearable FABTAC sensors are integrated on to the robotic hand and the response of robotic hand when activated by human touch was demonstrated. The Fig 5(a) shows the 3D printed Robotic hand (without tactile sensors) and Fig 5(b) Hand with Wearable FABTAC sensors

TABLE I: TEMPERATURE vs RESISTANCE VARIATION

| Temperature (°C) | Resistance (KΩ) | |
|---|---|---|
| 27.44 | 8.979 | Room temperature |
| 27.53 | 8.94 | |
| 28.09 | 8.72 | Soldering iron used |
| 28.81 | 8.45 | |
| 29.82 | 8.09 | |
| 31.79 | 7.44 | Prolonged Contact with single finger |
| 32.02 | 7.34 | |
| 32.55 | 7.21 | |
| 31.79 | 7.445 | |
| 32.41 | 7.251 | |
| 32.64 | 7.181 | |
| 32.60 | 7.193 | |
| 32.51 | 7.222 | |
| 32.41 | 7.251 | |



Fig. 3 (a)Dynamic Touch on Velostat sensor (b) Experimental set up of FSR Interfacing with controller



Fig 4 (a) 3D Printed InMoov Robotic Hand (b)Robotic Hand with wearable FABTAC Sensors
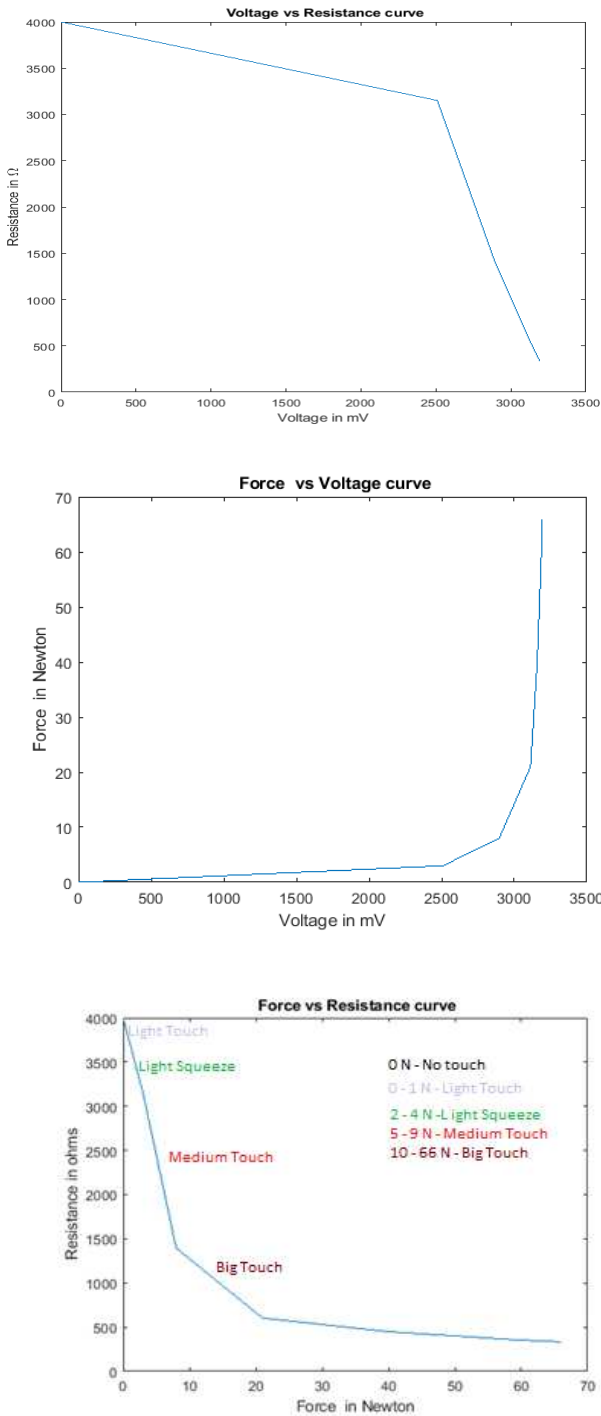
*Fig 5(a) Voltage vs Resistance Curve (b) Force vs Voltage Curve (c) Force vs Resistance and classification of touch based on Force applied at the contact area.*

## VI. CONCLUSION

The work presented in this paper demonstrates the feasibility study of fabric tactile sensors that can be worn by the robots in an environment where human beings and robots co-exist. The growing demand of robotic platforms in the field of nursing and assistive care emphasize the importance of tactile sensors which are cost effective, scalable and conformable. The tactile sensors and the wearable controller chosen for this work are light weight and flexible thereby providing an advantage of smaller size tactile sensing skin suitable for robotic platforms. The work can be extended in

future to provide tactile feedback based on FABTAC sensors for dynamic control of the robotic hand in Elderly assistance.

## REFERENCES

[1]   Dahiya, R. S., Metta, G., Valle, M., & Sandini, G. (2010). Tactile Sensing.Pdf. IEEE Transactions on Robotics, 26(1), 1–20.

[2]   Silvera-Tawil, D., Rye, D., & Velonaki, M. (2015). Artificial skin and tactile sensing for socially interactive robots: A review. *Robotics and Autonomous Systems*, *63*(P3), 230–243. https://doi.org/10.1016/j.robot.2014.09.008

[3]   M. H. Lee and H. R. Nicholls, "Review Article Tactile Sensing for Mechatronics—A State of the Art Survey," Mechatronics, Vol. 9, No. 1, 1999, pp. 1-31. doi:10.1016/S0957 4158(98)00045-2

[4]   P. A. Schmidt, E. Mael, and R. P. Wurtz, "A sensor for dynamic tactile information with applications in human-robot interaction & object exploration," Robot. Auto. Syst., vol. 54, no. 12, pp. 1005–1014, Dec. 2006

[5]   Dahiya, R. S., Mittendorfer, P., Valle, M., Cheng, G., & Lumelsky, V. J. (2013). Directions toward effective utilization of tactile skin: A review. IEEE Sensors Journal, 13(11), 4121–4138. https://doi.org/10.1109/JSEN.2013.2279056

[6]   H.-K. Lee, S.-I. Change, and E. Yoon, "A flexible polymer tactile sensor: Fabrication and modular expandability for large area deployment," J. Mircoelectromech. Sys., vol. 15, no. 6, pp. 1681–1686, Dec. 2006.

[7]   M. Maggiali, G. Cannata, P. Maiolino, G. Metta, M. Randazzao, and G. Sandini, "Embedded tactile sensor modules," in Proc. 11th Mechatron. Forum Biennial Int. Conf., 2008, pp. 1–5.

[8]   P. A. Schmidt, E. Mael, and R. P. Wurtz, "A sensor for dynamic tactile information with applications in human-robot inter- action & object exploration," Robot. Auto. Syst., vol. 54, no. 12, pp. 1005–1014, Dec. 2006

[9]   Dai, Y., & Gao, S. (2021). A Flexible Multi-Functional Smart Skin for Force, Touch Position, Proximity, and Humidity Sensing for Humanoid Robots. IEEE Sensors Journal, 21(23), 26355–26363. https://doi.org/10.1109/JSEN.2021.3055035

[10]   C. Domenici and D. De Rossi, "A stress-component-selective tactile sensor array," Sens. Actuators A, Phys., vol. 13, nos. 1–3, pp. 97–100, Mar. 1992.

[11]   M. Ohka, H. Kobayashi, J. Takata, and Y. Mitsuya, "Sensing precision of an optical three-axis tactile sensor for a robotic finger," in Proc. 15th Int. Symp. Robot Human Interact. Commun., Sep. 2006, pp. 214–219.

[12]   B. Ward-Cherrier, N. Pestell, L. Cramphorn, B. Winstone, M. E. Giannaccini, J. Rossiter, and N. F. Lepora, "The TacTip Family: Soft Optical Tactile Sensors with 3D-Printed Biomimetic Morphologies," Soft Robotics, 2018

[13]   Mukai, T., Onishi, M., Odashima, T., Hirano, S., & Luo, Z. (2008). Development of the tactile sensor system of a human-interactive robot "RI-MAN." IEEE Transactions on Robotics, 24(2), 505–512. https://doi.org/10.1109/TRO.2008.917006

[14]   Inaba, M., Hoshino, Y., Nagasaka, K., Ninomiya, T., Kagami, S., & Inoue, H. (1996). Full-body tactile sensor suit using electrically conductive fabric and strings. IEEE International Conference on Intelligent Robots and Systems,2,450–457. https://doi.org/10.1109/iros.1996.570816

[15]   Sundaram, S., Kellnhofer, P., Li, Y., Zhu, J. Y., Torralba, A., & Matusik, W. (2019). Learning the signatures of the human grasp using a scalable tactile glove. Nature, 569(7758), 698–702. https://doi.org/10.1038/s41586-019-1234-z

[16]   Wade, J., Bhattacharjee, T., Williams, R. D., & Kemp, C. C. (2017). A force and thermal sensing skin for robots in human environments. Robotics and Autonomous Systems, 96, 1–14. https://doi.org/10.1016/j.robot.2017.06.008